

สารยับยั้งแอลฟาไกลูโคซิเดสจากใบมะรุม *Moringa oleifera* และ ใบชมพู *Syzygium samarangense*

นางสาวภัทรวดี โตปรางกอบสิน

วิทยานิพนธ์นี้เป็นส่วนหนึ่งของการศึกษาตามหลักสูตรปริญญาวิทยาศาสตรมหาบัณฑิต
สาขาวิชาเคมี ภาควิชาเคมี
คณะวิทยาศาสตร์ จุฬาลงกรณ์มหาวิทยาลัย
ปีการศึกษา 2555
ลิขสิทธิ์ของจุฬาลงกรณ์มหาวิทยาลัย

บทคัดย่อและแฟ้มข้อมูลฉบับเต็มของวิทยานิพนธ์ตั้งแต่ปีการศึกษา 2554 ที่ให้บริการในคลังปัญญาจุฬาฯ (CUIR)
เป็นแฟ้มข้อมูลของนิสิตเจ้าของวิทยานิพนธ์ที่ส่งผ่านทางบัณฑิตวิทยาลัย

The abstract and full text of theses from the academic year 2011 in Chulalongkorn University Intellectual Repository(CUIR)
are the thesis authors' files submitted through the Graduate School.

α -GLUCOSIDASE INHIBITORS FROM LEAVES OF *Moringa oleifera* AND
Syzygium samarangense

Miss Patrawadee Toprangkobsin

A Thesis Submitted in Partial Fulfillment of the Requirements
for the Degree of Master of Science Program in Chemistry

Department of Chemistry

Faculty of Science

Chulalongkorn University

Academic Year 2012

Copyright of Chulalongkorn University

ภัทรวดี โตปรากฏอบสิน : สารยับยั้งแอลฟาไกลูโคซิเดสจากใบมะรุม *Moringa oleifera*
และ ใบชมพู *Syzygium samarangense*. (α -GLUCOSIDASE INHIBITORS FROM
LEAVES OF *Moringa oleifera* AND *Syzygium samarangense*) อ. ที่ปรึกษา
วิทยานิพนธ์หลัก: ผศ. ดร. ปรีชา ภูวไพริศรศาล, 79 หน้า

สารยับยั้งแอลฟาไกลูโคซิเดส เป็นยากลุ่มหนึ่งที่มีประสิทธิภาพในการรักษาโรคเบาหวานชนิดที่ 2 ได้
เป็นอย่างดี ในงานวิจัยนี้ได้ศึกษาสารยับยั้งแอลฟาไกลูโคซิเดสจากสมุนไพรไทย 2 ชนิด คือ ใบมะรุม และใบ
ชมพู โดยอาศัยเทคนิคทางโครมาโทกราฟีร่วมกับการ ขึ้นนำของทดสอบฤทธิ์ยับยั้งแอลฟาไกลูโคซิเดส การแยก
สารสกัดเมทานอลจากใบมะรุม ได้สารกลุ่มฟลาโวนอยด์ 2 ชนิด คือ kaempferol และ kaempferyl-3-O- β -
glucopyranoside และสารในกลุ่มอะโรมาติกแรมโนไซด์ 2 ชนิดคือ *p*-hydroxybenzaldehyde-O- α -L-
rhamnopyranoside และ 1-O-(4-hydroxymethylphenyl)- α -L-rhamnopyranoside ในบรรดาสารที่แยกได้ นี้
kaempferol ออกฤทธิ์ดีที่สุด ($IC_{50} = 46.46 \mu M$) โดยยับยั้งแอลฟาไกลูโคซิเดสจากยีสต์ได้ดีกว่า acarbose ถึง
10 เท่า ในขณะที่สารกลุ่มอะโรมาติกแรมโนไซด์ ไม่พบการออกฤทธิ์ การแยกสารสกัดเอทิลอะซิเตทของ ใบชมพู
ได้สารทั้งหมด 13 ชนิด โดยแบ่งออกเป็น 4 กลุ่ม คือ ฟลาโวนอล (kaempferol, quercetin, myricetin และ
myricitrin), ฟลาโวนิน (5-hydroxy-7-methoxy-6-methyl flavanone, pinostrobin, demethoxymatteucinol,
7-hydroxy-5-methoxy-6, 8-dimethyl flavanone, strobopinin และ pinocembrin), ซาลิโคน (2', 4'-
dihydroxy-6'-methoxy-3', 5'-dimethylchalcone และ aurentiacin) และ gallic acid จากการทดสอบฤทธิ์
ยับยั้งแอลฟาไกลูโคซิเดส พบว่า ฟลาโวนอลมีฤทธิ์ยับยั้งที่ดีและช่วงความเข้มข้นที่ กว้าง (IC_{50} 3.71- 94.33 μM)
นอกจากนี้ยังพบว่า 2', 4'-dihydroxy-6'-methoxy-3', 5'-dimethylchalcone และ strobopinin ซึ่งมีหมู่เมทิล
ใน ring A เป็นสารที่พบเฉพาะสกุล *Syzygium* มีฤทธิ์ยับยั้งดีเช่นกัน 2', 4'-dihydroxy-6'-methoxy-3', 5'-
dimethylchalcone ยับยั้ง มอลเทสและซูเครสด้วยค่า IC_{50} 94 and 83 μM ตามลำดับ ในขณะที่ strobopinin
ยับยั้งเอนไซม์ทั้งสองชนิดด้วยค่า IC_{50} 175 and 84 μM ตามลำดับ 2', 4'-dihydroxy-6'-methoxy-3', 5'-
dimethylchalcone แสดงการยับยั้ง มอลเทสและซูเครส แบบ mixed-type โดยมีค่าคงที่การสลาย พันธะ K_i
เท่ากับ 3.92 และ 2.32 mM และ K_i' เท่ากับ 18 และ 6.67 mM ตามลำดับ ในส่วนของ strobopinin แสดงการ
ยับยั้งมอลเทสและซูเครส แบบ mixed-type ด้วยค่า K_i เท่ากับ 1.84 และ 1.95 mM และ K_i' เท่ากับ 6.13 และ
9.09 mM ตามลำดับ นอกจากนี้งานวิจัยนี้เป็นรายงานฉบับแรกที่แสดง กลไกการยับยั้งของ 2', 4'-dihydroxy-
6'-methoxy-3', 5'-dimethylchalcone และ strobopinin

ภาควิชา.....เคมี.....

ลายมือชื่อนิสิต.....

สาขาวิชา.....เคมี.....

ลายมือชื่อ อ.ที่ปรึกษาวิทยานิพนธ์หลัก.....

ปีการศึกษา...2555.....

5372399023: MAJOR CHEMISTRY

KEYWORDS: α -GLUCOSIDASE INHIBITORS / *Moringa oleifera* / *Syzygium samarangense* / Diabetes

PATTRAWADEE TOPRANGKOB SIN: α -GLUCOSIDASE INHIBITORS FROM LEAVES OF *Moringa oleifera* AND *Syzygium samarangense*.
ADVISOR: ASST. PROF. PREECHA PHUWAPRAISAN, 79 pp.

α -Glucosidase inhibitors are effective drugs in type 2 diabetes therapy. This research aimed to investigate α -glucosidase inhibitors from two Thai medicinal plants, leaves of *Moringa oleifera* and *Syzygium samarangense*, using chromatographic technique and bioassay guidance. Isolation of methanolic extract of *M. oleifera* leaves yielded two flavonoids named keampferol and kaempferyl-3-*O*- β -glucopyranoside together with two aromatic rhamnosides named *p*-hydroxybenzaldehyde-*O*- α -L-rhamnopyranoside and 1-*O*-(4-hydroxymethylphenyl)- α -L-rhamnopyranoside. Of compounds isolated, keampferol exhibited the most promising inhibition (IC₅₀ 46.46 μ M) against baker's yeast α -glucosidase, which was 10 times more potent than antidiabetic drug acarbose, whereas inhibitory effect of aromatic rhamnosides was not observed. Isolation of ethylacetate extract of *S. samarangense* leaves yielded 13 compounds, classified into four groups: flavonols (kaempferol, quercetin, myricetin and myricitrin), flavanones (5-hydroxy-7-methoxy-6-methyl flavanone, pinostrobin, demethoxymatteucinol, 7-hydroxy-5-methoxy-6, 8-dimethyl flavanone, strobopinin and pinocembrin), chalcones (2', 4'-dihydroxy-6'-methoxy-3', 5'-dimethylchalcone and aurentiacin) and gallic acid. The results indicated flavonols showed broad and potent inhibition (IC₅₀ 3.71- 94.33 μ M). More interestingly, 2', 4'-Dihydroxy-6'-methoxy-3', 5'-dimethylchalcone and strobopinin containing methyl group (s) in ring A, which are common to genus *Syzygium*, also displayed promising inhibition. 2', 4'-Dihydroxy-6'-methoxy-3', 5'-dimethylchalcone inhibited maltase and sucrase with IC₅₀ values of 94 and 83 μ M, respectively, whereas strobopinin inhibited these enzymes which IC₅₀ values of 175 and 84 μ M, respectively. 2', 4'-dihydroxy-6'-methoxy-3', 5'-dimethylchalcone inhibited maltase and sucrase by mixed-type manner: $K_i = 3.92, 2.32$ mM and $K_i' = 18$ and 6.67 mM, respectively. Strobopinin inhibited maltase and sucrase by mixed-type manner: $K_i = 1.84, 1.95$ mM and $K_i' = 6.13$ and 9.09 mM, respectively. Notably, the inhibition mechanism of 2', 4'-dihydroxy-6'-methoxy-3', 5'-dimethylchalcone and strobopinin are first reported herein.

Department : Chemistry

Student's Signature :

Field of Study : Chemistry

Advisor's Signature :

Academic Year : 2012

ACKNOWLEDGEMENTS

I would like to express my deepest appreciation to my advisor, Assistant Professor Preecha Phuwapraisirisan, encouragement and supporting at all time of this research.

I would like to gratefully acknowledge the members of the thesis committees, Assistant Professor Dr. Warinthorn Chavasiri, Assistant Professor Dr. Pattara Sawasdee and Assistant Professor Dr. Wimolpun Rungprom for discussion, guidance and extending cooperation over my presentation.

I would also like to express my appreciation to my family. Furthermore, my specially thank to Miss. Wisuttaya Worawalai, Mr. Nattanan Surapinit, Mr. Thanakon Damsud and Mr. Jirapast Sichaem, for their technical assistance. On the other hand, I would like to thank all of my friends in the laboratory for their friendships and help during the course of my graduate research.

Finally, I would like to express my gratitude to Natural Products Research Unit, Department of Chemistry, Faculty of Science, Chulalongkorn University for supporting of chemicals and laboratory facilities throughout the course of study and Program of Biotechnology, Faculty of Science, Chulalongkorn University for giving me a chance to study here.

CONTENTS

	Page
ABSTRACT IN THAI	Iv
ABSTRACT IN ENGLISH	V
ACKNOWLEDGEMENTS	Vi
CONTENTS	Vii
LIST OF TABLES	Ix
LIST OF FIGURES	X
LIST OF SCHEMES	Xiv
LIST OF ABBREVIATIONS	Xv
CHAPTER I	
INTRODUCTION	1
CHAPTER II	
α-GLUCOSIDASE INHIBITOR FROM THE LEAVES OF <i>Moringa oleifera</i>	8
2.1 Introduction	8
2.1.1 Botanical aspect and distribution of <i>Moringa oleifera</i>	8
2.1.3 Pharmacological investigation of <i>Moringa oleifera</i>	9
2.2 Isolation	12
2.3 Structure elucidation of isolated compounds 1-4	14
2.3.1 Flavonols (2 and 3).....	14
2.3.2 1, 4-disubstituted aromatic group (1 and 4).....	15
2.4 α-Glucosidase inhibitory activity of the isolated compounds	16
2.4 Experiment section	18
2.5.1 General experiment procedures.....	18
2.5.2 Plant material.....	18
2.5.3 Extraction and isolation.....	19
2.5.4 α -Glucosidase inhibitory assay.....	20
2.5.4.1 Chemical and equipment.....	20
2.5.4.2 Assay for determining inhibitory effect against α - glucosidase from baker's yeast.....	20

	Page
2.5.4.3 Rat intestinal α -glucosidase inhibitory activity.....	21
 CHAPTER III	
α-GLUCOSIDASE INHIBITOR FROM THE LEAVES OF <i>Syzygium</i>	
<i>samarangense</i>	27
3.1 Introduction	27
3.1.1 Botanical aspect and distribution of <i>Syzygium samarangense</i>	27
3.1.2 Pharmacological investigation of <i>Syzygium samarangense</i>	28
3.2 Isolation	30
3.3 Structure elucidation of isolated compound 5-16	32
3.3.1 Flavanones (6, 7, 9 10, 11 and 12).....	34
3.3.2 Chalcones (5 and 8).....	35
3.3.3 Flavonols (2, 13, 14 and 16).....	36
3.3.4 Gallic acid (15).....	37
3.4 α-Glucosidase inhibitory activity of the isolated compounds	38
3.5 α-Glucosidase inhibitory mechanism of chalcone 5	42
3.6 α-Glucosidase inhibitory mechanism of flavanone 11	47
3.7 Experiment section	51
3.7.1 General experiment procedures.....	51
3.7.2 Plant material.....	52
3.7.3 Extraction and isolation.....	52
3.7.4 α -Glucosidase inhibitory assay.....	55
3.7.5 Measurement of kinetic constant.....	56
 CHAPTER IV	
CONCLUSION	69
REFERENCES	72
VITA	79

LIST OF TABLES

Table		Page
1.1	Anti-diabetic plant extracts using α -glucosidase inhibitors as positive control.....	7
2.1	Some common medicinal uses of different parts of <i>Moringa oleifera</i> ..	10
2.2	α -Glucosidase (baker's yeast) inhibitory activity of isolated compounds from <i>Moringa Oleifera</i> leaves.....	16
2.3	α -Glucosidase (maltase) inhibitory activity of isolated compounds from <i>Moringa Oleifera</i> leaves.....	17
2.4	α -Glucosidase (sucrase) inhibitory activity of isolated compounds from <i>Moringa Oleifera</i> leaves.....	18
3.1	α -Glucosidase inhibitory activity of isolated compounds from <i>Syzygium samarangense</i> leaves.....	39
3.2	Types of Lineweaver-Burk plot for inhibition mechanism.....	43
3.3	The values from kinetic analyses of 2', 4'-dihydroxy-6'-methoxy-3', 5'-dimethylchalcone (5) in maltase.....	46
3.4	The values from kinetic analyses of strobopinin (11).....	52

LIST OF FIGURES

Figure		Page
1.1	Worldwide prevalence of diabetes in 2000 and estimates for the year 2030 in millions	1
1.2	Defective insulin secretion for type I and II diabete.....	2
1.3	In normal digestion, oligosaccharides are hydrolyzed by α -glucosidase located in the intestinal brush border to monosaccharides, which are then absorbed.....	4
1.4	Hydrolysis of polysaccharides with α -glucosidase enzyme.....	5
1.5	Selected structure flavonoids from <i>Machilus philippinense</i> Merr...	6
2.1	<i>Moringa oleifera</i> : (a) Leaves, (b) flower and (c) Fruit.....	8
2.2	Isolated compounds of <i>M. Oleifera</i> leaves.....	14
2.3	Hydrolysis of baker's yeast α -glucosidase.....	21
2.4	The reaction principle of α -glucosidase from rat small intestine	22
3.1	<i>Syzygium samarangense</i> : (a) Leaves, (b) Fruit and (c) flower.....	28
3.2	Selected isolated compounds from <i>Syzygium samarangense</i> leaves.....	30
3.3	Isolated compounds from <i>S. samarangense</i> leaves	33
3.4	Biosynthetic pathways of chalcone, flavanone and flavonol	34
3.5	Inhibition trends of active compounds (11 , 12 and 9), the present of hydroxy group on aromatic ring against rat intestine	42
3.6	The Lineweaver-Burk plot, $1/v$ against $1/[\text{maltose}]$ of 2', 4'-dihydroxy-6'-methoxy-3', 5'-dimethylchalcone in maltase.....	44
3.7	Dixon plot of slope vs. concentrations of compound 5 from a primary Lineweaver-Burk plot for the determination of K_i	45
3.8	Secondary replot plot slope vs. concentrations of compound 5 from a primary Lineweaver-Burk plot for the determination of K_i'	45

Figure	Page
3.9 The Lineweaver-Burk plot, $1/v$ against $1/[\text{sucrose}]$ of 2', 4'-dihydroxy-6'-methoxy-3', 5'-dimethylchalcone in sucrase.....	47
3.10 Dixon plot of slope vs. concentration of compound 5 from a primary Lineweaver-Burk plot for the determination of K_i	47
3.11 Secondary replot plot slope vs. concentration of compound 5 from a primary Lineweaver-Burk plot for the determination of K_i'	48
3.12 The Lineweaver-Burk plot, $1/v$ against $1/[\text{maltose}]$ of strobopinin in maltase.....	49
3.13 Dixon plot of slope vs. concentration of compound 11 from a primary Lineweaver-Burk plot for the determination of K_i	49
3.14 Secondary replot plot slope vs. concentration of compound 11 from a primary Lineweaver-Burk plot for the determination of K_i'	50
3.15 The Lineweaver-Burk plot, $1/v$ against $1/[\text{sucrose}]$ of strobopinin in sucrase.....	51
3.16 Dixon plot of slope vs. concentration of compound 11 from a primary Lineweaver-Burk plot for the determination of K_i	51
3.17 Secondary replot plot slope vs. concentration of compound 11 from a primary Lineweaver-Burk plot for the determination of K_i'	52
S-2.1 The ^1H NMR (acetone- d_6) spectrum of <i>p</i> -hydroxybenzaldehyde- <i>O</i> - α -L-rhamnopyranoside (1).....	24
S-2.2 The ^{13}C NMR (acetone- d_6) spectrum of <i>p</i> -hydroxybenzaldehyde- <i>O</i> - α -L-rhamnopyranoside (1).....	24
S-2.3 The ^1H NMR (CD_3OD) spectrum of keampferol (2).....	25

Figure	Page
S-2.4 The ¹ H NMR (CD ₃ OD) spectrum of kaempferol-3- <i>O</i> -β-glucopyranoside (3).....	25
S-2.5 The ¹³ C NMR (CD ₃ OD) spectrum of kaempferol-3- <i>O</i> -β-glucopyranoside (3).....	26
S-2.5 The ¹ H NMR (CD ₃ OD) spectrum of 1- <i>O</i> -(4-hydroxymethylphenyl)-α-L-rhamnopyranoside (4).....	26
S-2.6 The ¹³ C NMR (CD ₃ OD) spectrum of 1- <i>O</i> -(4-Hydroxymethylphenyl)-α-L-rhamnopyranoside (4).....	27
S-3.1 The ¹³ H NMR (CDCl ₃) spectrum of 2', 4'-dihydroxy-6'-methoxy-3', 5'-dimethylchalcone (5).....	59
S-3.2 The ¹³ C NMR (CDCl ₃) spectrum of 2', 4'-dihydroxy-6'-methoxy-3', 5'-dimethylchalcone (5).....	59
S-3.3 The ¹ H NMR (CDCl ₃) spectrum of 5-hydroxy-7-methoxy-6-methyl flavanone (6).....	60
S-3.4 The ¹³ C NMR (CDCl ₃) spectrum of 5-hydroxy-7-methoxy-6-methyl flavanone (6).....	60
S-3.5 The ¹ H NMR (CDCl ₃) spectrum of pinostrobin (7).....	61
S-3.6 The ¹³ C NMR (CDCl ₃) spectrum of pinostrobin (7).....	61
S-3.7 The ¹ H NMR (CDCl ₃) spectrum of aurentiacin (8).....	62
S-3.8 The ¹³ C NMR (CDCl ₃) spectrum of aurentiacin (8).....	62
S-3.9 The ¹ H NMR (CDCl ₃) spectrum of demethoxymatteucinol (9).....	63
S-3.10 The ¹³ C NMR (CDCl ₃) spectrum of demethoxymatteucinol (9).....	63
S-3.11 The ¹ H NMR (CDCl ₃) spectrum of 7-hydroxy-5-methoxy-6, 8-dimethyl flavanone (10).....	64
S-3.12 The ¹³ C NMR (CDCl ₃) spectrum of 7-hydroxy-5-methoxy-6, 8-dimethyl flavanone (10).....	64
S-3.13 The ¹ H NMR (CDCl ₃) spectrum of strobopinin (11).....	65

Figure		Page
S-3.15	The ¹ H NMR (CD ₃ OD) spectrum of pinocembrin (12).....	66
S-3.16	The ¹³ C NMR (CD ₃ OD) spectrum of pinocembrin (12).....	66
S-3.17	The ¹ H NMR (CD ₃ OD) spectrum of kaempforal (2).....	67
S-3.18	The ¹ H NMR (CD ₃ OD) spectrum of quercetin (13).....	67
S-3.19	The ¹ H NMR (CD ₃ OD) spectrum of myricetin (14).....	67
S-3.20	The ¹ H NMR (CD ₃ OD) spectrum of gallic acid (15).....	68
S-3.21	The ¹³ C NMR (CD ₃ OD) spectrum of gallic acid (15).....	68
S-3.22	The ¹ H NMR (CD ₃ OD) spectrum of myricitrin (16).....	69
S-3.23	The ¹³ C NMR (CD ₃ OD) spectrum of myricitrin (16).....	69
4.1	The structure of isolated compounds from <i>M. oleifera</i>	71
4.2	The structure of isolated compounds from <i>S. samarangense</i>	72

LIST OF SCHEMES

Scheme		Page
2.1	Isolation procedure of <i>M. Oleifera</i> leaves.....	13
3.1	Isolation procedure of <i>S. samarangense</i> leaves.....	32
3.2	Inhibition mechanism of compounds 5 and 11 against rat intestine...	43

LIST OF ABBREVIATIONS

^{13}C NMR	carbon 13 nuclear magnetic resonance
^1H NMR	proton nuclear magnetic resonance
d	doublet (NMR)
dd	doublet of doublet (NMR)
g	gram (s)
Hz	Hertz
IC ₅₀	concentration that is required for 50% inhibition <i>in vitro</i>
<i>J</i>	coupling constant
m	multiplet (NMR)
M	Molar
MeOH	methanol
mg	milligram (s)
MHz	megahertz
min	minute
mL	milliliter (s)
NMR	nuclear magnetic resonance
s	singlet (NMR)
UV	ultraviolet
VLC	vacuum liquid chromatography
δ	chemical shift
δ_{C}	chemical shift of carbon
δ_{H}	chemical shift of proton
μ	micro

CHAPTER I

Introduction

Diabetes mellitus (DM), commonly referred to as diabetes, is a group of metabolic syndromes characterized by elevated blood glucose levels that stem from defects in pancreatic insulin secretion with or without concurrent impairment of insulin action. DM are increasingly being acknowledged and other chronic conditions as major public health problems. According to the World Health Organization (WHO, 2006), the worldwide evaluation of the disease around 2030 will be more than double from that of 2005, which accounts for an increase of 144% over the next 30 years (Gershell, 2005).

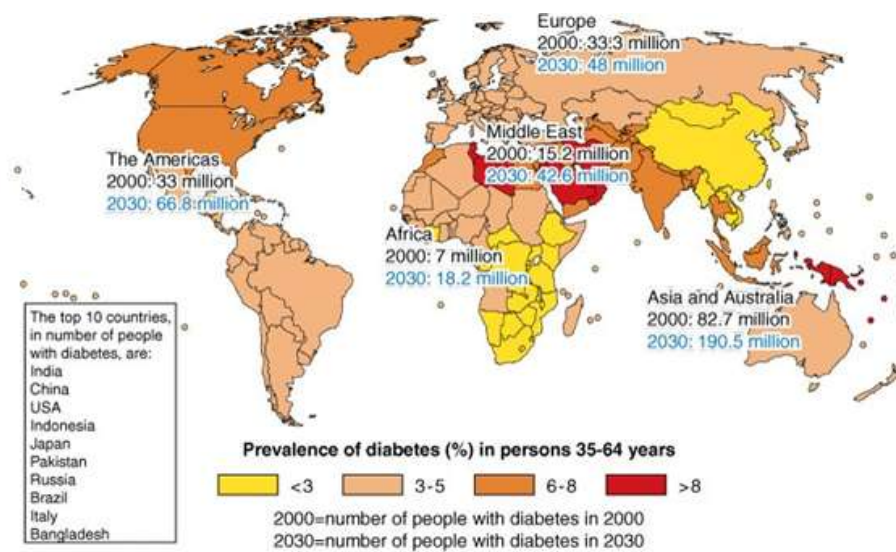


Figure 1.1 Worldwide prevalence of diabetes in 2000 and estimates for the year 2030 in millions (www.myhealthywaist.org/the-concept-of-cmr/the-obesity-and-type-2-diabetes-epidemics/the-epidemiological-evidence)

1.1 Diabetes mellitus: Classifications, causes and its complication

There are several forms of diabetes. Scientists are still defining and categorizing some of these variations and establishing their prevalence in the population. DM can be classified into two groups (Figure 1.2):

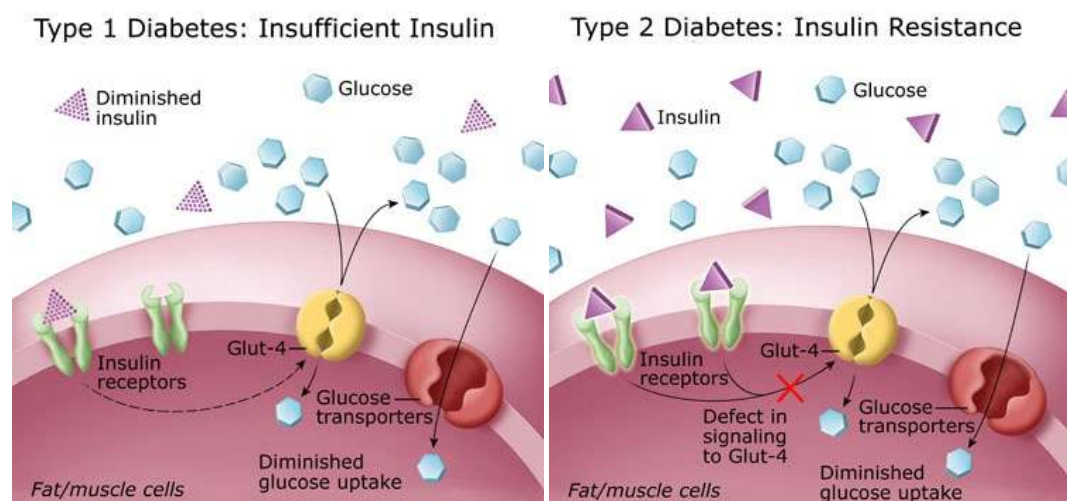


Figure 1.2 Defective insulin secretion for type I and II diabetes

(www.uscf.mightyminnow.com/images/charts)

Type 1 diabetes is defined as an autoimmune disease in which the immune system mistakenly impairs the insulin-making beta cells of the pancreas. It typically develops more quickly than other forms of diabetes. Type 1 DM is usually diagnosed in children and adolescents, and sometimes in young adults. To survive, patients must administer insulin medication regularly. Type 1: diabetes used to be called juvenile diabetes and insulin-dependent diabetes mellitus (IDDM). A variation of type 1 that develops later in life, usually after age 30, is called latent autoimmune diabetes of adulthood (LADA). Sometimes patients with autoimmune diabetes develop insulin resistance because of weight gain or genetic factors. This condition is commonly known as double diabetes (Samreen, 2009).

Type 2 diabetes is defined as a disorder of metabolism, usually involving excess body weight and insulin resistance. In these Type 2 DM patients pancreas initially secrete insulin, but the body has trouble utilizing this glucose-controlling hormone. Eventually, the pancreas cannot produce enough insulin to respond to the

body requirement. Type 2 diabetes is by far the most common form of diabetes, accounting for 85 to 95% of cases in developed nations and an even higher percentage in developing nations, according to the International Diabetes Federation. Type 2 diabetes used to be called adult-onset diabetes and non-insulin-dependent diabetes mellitus (NIDDM) (Samreen, 2009).

There are currently over 3 million people with diabetes in Thailand and there are more than half a million people with diabetes who have the condition and do not know it. About 80 percent of those with type 2 diabetes are overweight. It is more common among people who are older, sedentary or obese, or have a family history of the disease. It may reappear in women who had gestational diabetes. It is more common among people of Asian, Hispanic, African or Native American ancestry.

Type 2 DM is a progressive disease that results in significant, severe complications such as heart disease, kidney disease, blindness and loss of limbs through amputation. Treatment differs at various stages of the condition. In its early stages, many people with type 2 diabetes can control their blood glucose levels by losing weight, eating properly and exercising. Many may subsequently need oral medication, and some people with type 2 diabetes may eventually need insulin shots to control their diabetes and avoid the disease's serious complications. Even though there is no cure for diabetes, proper treatment and glucose control enable people with type 2 diabetes to have normal and productive lives (Loutfi, 2003).

1.2 α -Glucosidase inhibitors

A potential therapeutic approach is to suppress the postprandial hyperglycaemia by retarding absorption of glucose through inhibition of carbohydrate-hydrolysing enzymes, α -glucosidase (sucrase, maltase and isomaltase) in the digestive trace of the small intestine (Figure 1.3).

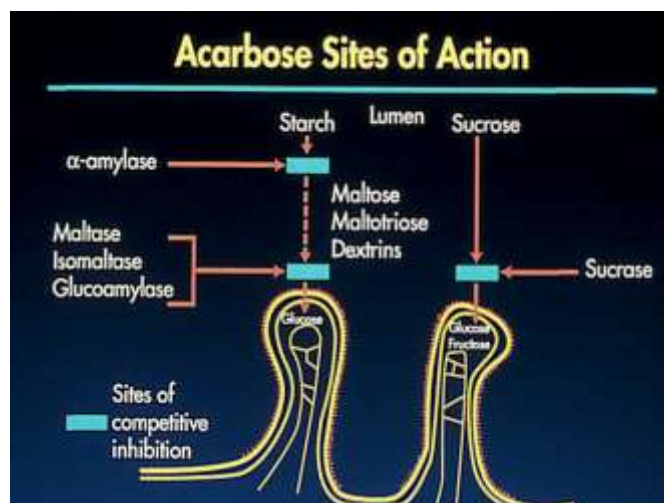


Figure 1.3 In normal digestion, oligosaccharides are hydrolyzed by α -glucosidase located in the intestinal brush border to monosaccharides, which are then absorbed.

α -Glucosidase catalyzes the hydrolysis of α -glucosidic bond from the non reducing end of a chain, together with α -glucosidic bond of free disaccharides. The enzyme, which belongs to glycoside hydrolases family 13, has common specific structural features such as the catalytic (β/α)₈-barrel domain, which acts specifically on α -1,4-O-glucosidic linkages (Figure 1.4) (Heng, 2010). Inhibitors of these enzyme delay carbohydrate digestion and prolong overall carbohydrate digestion time, causing a decline in the rate of glucose absorption and consequently blunting the postprandial plasma glucose level (Rhabasa-Lhoret, 2004). Currently, the α -glucosidase inhibitors are used orally as anti-diabetes including acarbose (Precose[®] or Glucobay[®]), miglitol (Glyset[®]) and voglibose (Basen[®]) (Melo, 2006). In general, these drugs suppress glucose levels without risk for weight gain or hypoglycemia. Unfortunately, these drugs have gastrointestinal side effects that often limit their acceptance.

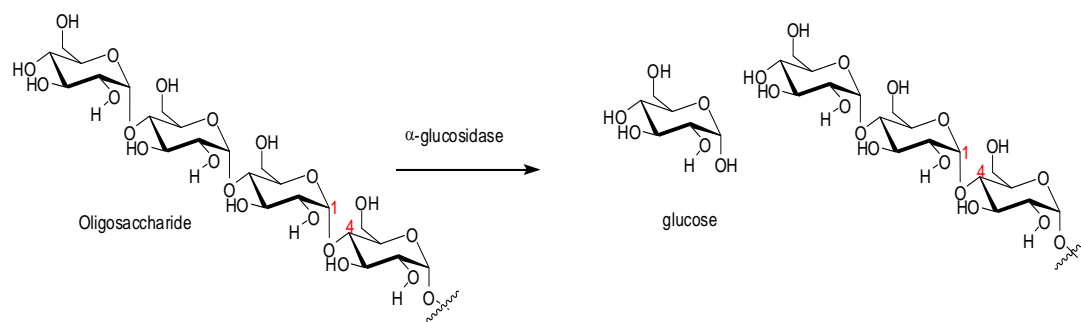


Figure 1.4 Hydrolysis of oligosaccharides with α -glucosidase.

1.3 Antidiabetes drugs from medicinal plants

In many developing countries, the use of herbal medicine by patients suffered from chronic disease is encouraged because there is concern of the adverse effects from chemical drugs (Bhattarai, 1993; Manandham, 1995; Shrestha and Joshi, 1993). Herbal drugs are prescribed widely because of their effectiveness, fewer side effects and relatively low cost. To this end, research has launched to embrace traditional medicines from various cultures, as scientists search for clues to discover new therapeutic drugs for diabetes (Li, 2004). Traditional Indian and Chinese medicines have long used plant and herbal extracts as anti-diabetic agents (Chen, 2001; Grover, 2002). Therefore, investigation on such agents from traditional medicinal plants has become more important and researches are competing to discover novel new effective and safe therapeutic agents for the treatment of diabetes.

A recent review of hyperglycaemia compounds mentions the following isolated pure plant natural products such as lignans, flavonoids and terpenoids. Flavonoids were more interesting than other groups because they have various beneficial effects associated with diabetic therapy such as sulfonylureas, biguanides, α -glucosidase inhibitors, thiazolidinedione (TZD) and insulin.

Prominent examples of flavanoids having α -glucosidase inhibition included two acylated kaempferol-3-*O*- α -L-rhamnopyranosides (**A** and **B**) isolated from *Machilus philippinensis* Merr. (Lauraceae). They inhibited α -glucosidase type II

(from *Bacillus stearothermophilus*) with IC_{50} values of 6.10 and 1.0 μ M, respectively (Lee, 2008).

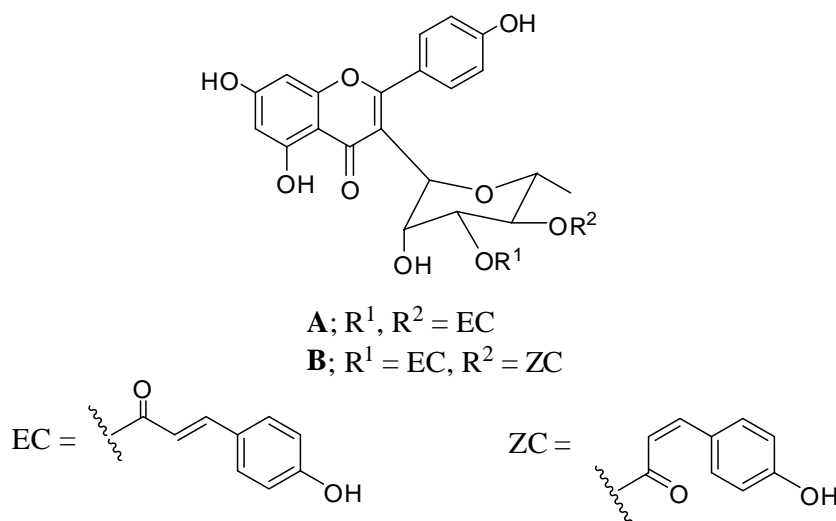


Figure 1.5 Selected structure flavonoids from *Machilus philippinense*

Moreover, several natural product extracts were newly discovered to show anti-diabetic activity through α -glucosidase inhibition, and they are summarized in Table 1.1 (Hung, 2012).

Thai ethnopharmacology, the knowledge of medicinal plants is abundant within the Thai Traditional Medicine. Thai Traditional Medicine was long-term mainstream medical system, which has benefit of the healthcare system. In addition, there are many reports showed increasing use of medicinal plants as anti-diabetic drugs, which studied both in subject and animal models. Therefore, Thai medicinal plants have potentially antidiabetic. In this study, criterion of selecting Thai medicinal plants as summarized as follow.

1. Reducing blood sugar levels and no toxic in long-term administration
2. Commercially or readily available and use less time in production
3. No report on the use as α -glucosidase inhibitors

In this research, α -glucosidase inhibitors from the leaves of *Moringa oleifera* Lam. and *Syzygium samarangense* will be investigated as well as inhibitory mechanism underlying the activity.

Table 1.1 Anti-diabetic plant extracts using α -glucosidase inhibitors as positive control

Plant species	Family	Animal model	Extracts teased	Positive control	Reference
Effects/Constituent/Possible mechanisms					
Voi, <i>Cleistocalyx operculatus</i> (Roxb.) Merr and Perry, <i>Eugenia operculata</i> Roxb.	Myrtaceae	<i>In vitro</i> , α -glucosidase; <i>in vivo</i> , STZ rats (<i>p.o.</i>)	Aqueous extract	Acarbose (25 mg/kg): Guava leaf extract (500 mg/kg)	Mai, 2007
<i>In vitro</i>: inhibited rat-intestinal maltase and sucrase; <i>in vivo</i>: reduced BG (500 mg/kg)					
<i>Syzygium cumini</i> seed kernel	Myrtaceae	<i>In vitro</i> , α -glucosidase; <i>in vivo</i> , Goto-Kakizki (GK) (<i>p.o.</i>)	Acetone extract	Acarbose (<i>in vitro</i>); N/A (<i>in vivo</i>)	Shinde, 2008
<i>In vitro</i>: inhibition by the extracts is better than inhibition by acarbose. <i>In vivo</i>: inhibited α-glucosidase hydrolysis of maltose (250 mg/kg bw)					
<i>Rosa damascena</i> Mill.	Rosaceae	<i>In vitro</i> , α -glucosidase; <i>in vivo</i> , STZ rats (<i>p.o.</i>)	Methanol extract	Acarbose (50 mg/kg)	Gholamhoseinia n, 2009
<i>In vitro</i>: inhibited α-glucosidase (2, 5 μg/ mL); <i>in vivo</i>: dose-dependent decrease of PG after maltose loading in normal and diabetic rats (100-1000 mg/kg)					
Tronadora, <i>Tecomastans</i> (L.) Juss. ex Kunth	Bignoniaceae	<i>In vitro</i> , α -glucosidase; <i>in vivo</i> , STZ rats (<i>p.o.</i>)	Aqueous extract	Acarbose (50 mg/kg) Tolbutamide (60 mg/kg)	Ramirez, 2009
<i>In vitro</i>: dose-dependent inhibition of glucose release from starch; <i>in vivo</i>: improved lipid profile and decreased postprandial hyper-glycemic peak, but had no effect on FPG (500 mg/kg)					

CHAPTER II

α -GLUCOSIDASE INHIBITORS FROM *Moringa oleifera*

2.1 Introduction

2.1.1 Botanical aspect and distribution

Moringa oleifera (Figure 2.1) is one of the best known and most widely distributed and naturalized species of a monogeneric family *Moringaceae* (Nadkarni, 1976; Ramachandran, 1980). The tree ranges in height from 5 to 10 m (Morton, 1991). It is found wild and cultivated throughout the plains, especially in hedges and in house yards, thrives best under the tropical insular climate, and is plentiful near the sandy beds of rivers and streams (The Wealth of India, 1962; Qaiser, 1973). It can grow well in the humid tropics or hot dry lands, can survive destitute soils, and is little affected by drought (Morton, 1991). It tolerates a wide range of rainfall with minimum annual rainfall requirements estimated at 250 mm and maximum at over 3000 mm and a pH of 5.0–9.0 (Palada, 2003).

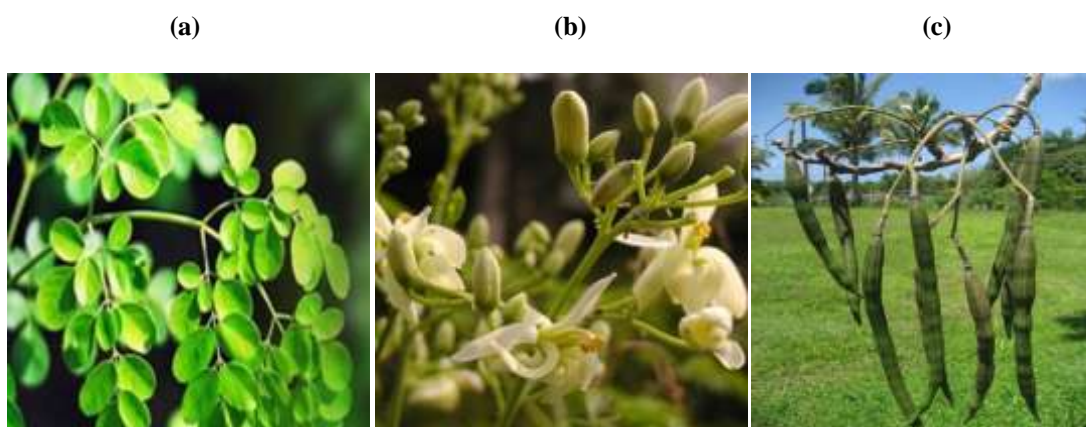


Figure 2.1 *Moringa oleifera*: (a) leaf, (b) flower and (c) fruit

2.1.2 Pharmacological investigation

Moringa oleifera is a short, slender and perennial tree belonging to the Moringaceae family. It is widely cultivated and naturalized in tropical India, Africa, tropical America, Sri Lanka, Mexico, Malaysia and the Phillipine Islands (Sabale, 2008). The plant has been used widely as antispasmodic, stimulant, expectorant, diuretics and also for the treatment of hiccough, influenza and internal abscess in Indian traditional medicines (Mishra, 2000). Moreover, leaves, fruit flowers and immature pods of this plant are used as a highly nutritive vegetable in many countries such as India, Pakistan, Hawaii and many parts of Africa (Sabale, 2008). In Thailand it is commonly known as “Marum” and immature fruits or pods of this plant have long been used as vegetable or as food ingredient (Wutythamawech, 1997). The leaves were proven to be a prolific source of β -carotene, protein, vitamin C, calcium, potassium and antioxidant compounds such as ascorbic acid, flavonoids, carotenoids, phenolics (Sabale, 2008) and various amino acids (Mishra, 2000).

For pharmacological properties and medicinal uses, *M. oleifera* is very important for its medicinal value. Various parts of this plant act as cardiac and circulatory stimulants and several benefit activities such as antitumor, antipyretic, anti-inflammatory, antiepileptic, hepatoprotective, antioxidant, antihypertensive, cholesterol lowering and anti-diabetic. In addition, medicinal properties have been arbitrated to diverse parts of this highly regarded tree (Table 2.1) and reviewed by Anwar, 2007.

Table 2.1 Some common medicinal uses of different parts of *Moringa oleifera*

Plant part	Medicinal Uses	Reference
Root	Anti-inflammatory, antilithic, rubefacient, vesicant, antifertility, carminative, treating rheumatism, articular pains, constipation and car minative.	Padmarao, 1996; Dahot, 1988; Ruckmani, 1998.
Leave	Purgative, used for fever, piles, sore throat, eye and ear infection, applied to reduce glandular and treatment of diabetes mellitus.	Dahot, 1988; Makonnen, 1997.
Stem bark	Rubefacient, prevent enlargement of the spleen and formation of tuberculous glands of the neck, to destroy tumors and anti-tubercular activity.	Bhatnagar, 1961; Siddhuraju, 2003.
Flower	Treated inflammation, muscle disease, tumors, lower serum cholesterol, phospholipid, triglyceride, decrease lipid profile of liver, heart and aorta in hypercholesterolaemic rabbits.	Bhattacharya, 1982; Dahot, 1998; Siaddhuraju, 2003; Mehta, 2003.
Seed	Decreasing liver lipid peroxides, antihypertensive compounds thiocarbamate and isothiocyanate glycosides have been isolated from the acetate phase of the ethanolic extract of Moringa pods	Faizi, 1998; Lalas, 2002.

From the Table 2.1, we found that leaves of *M. oleifera* possess several interesting biological activities including anti-diabetic activity.

Jaiswal and coworker (2009) studied the effect of leave aqueous extract on blood glucose levels of normal and hyperglycemic rats. The extract reduced the blood glucose level in normal rat and normalized high blood glucose levels in sub, mild and

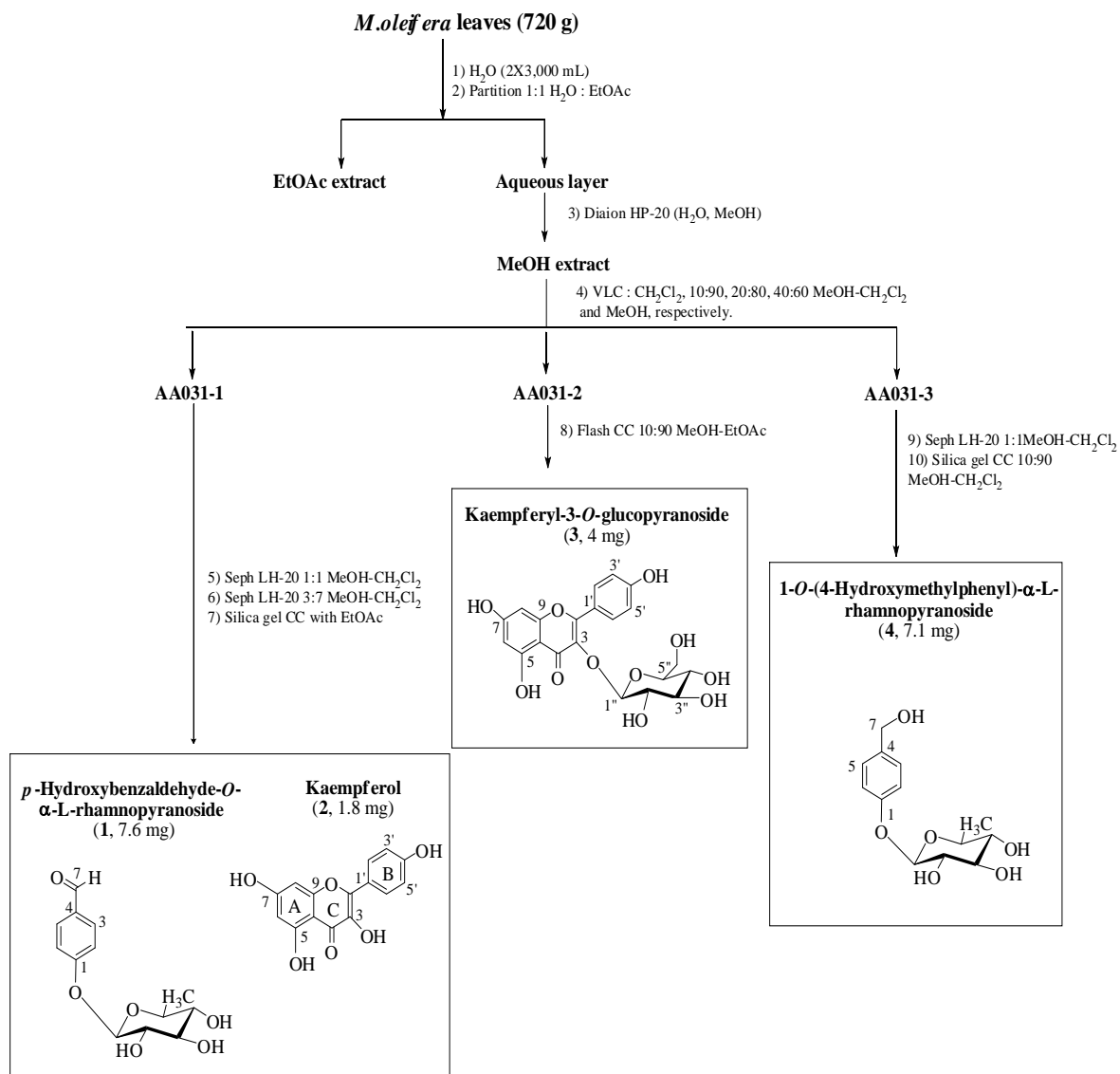
severely diabetic rats within 3 h. In addition, it improved glucose tolerance both in normal and hyperglycemic rat more effectively than reference drug Glipizide (Jaiswal, 2009).

Tende *et al.* studied the effect of ethanolic leaves extract of *Moringa oleifera* on blood glucose levels of streptozocin-induced diabetics and normoglycemic Wistar rats. This study was undertaken to determine the hypoglycemic effect of *Moringa oleifera* ethanolic extract in normal (normoglycemic) and STZ induced diabetic Wistar rats. In one set of experiment, graded doses of the leaves extract (250 and 500 mg/kg i.p.) were separately administered to groups of fasted normal and fasted STZ diabetic rats. The hypoglycemic effect of the ethanolic leaves extract was compared with that of insulin 6 i.u/kg in fasted normal and STZ diabetic rats. Following treatment, relatively moderate to high doses of *Moringa oleifera* (250 and 500 mg/kg i.p.) produced a dose-dependent, significant reduction ($p < 0.05$) in blood glucose levels of fasted STZ diabetic rats only. A significant decrease in the blood glucose levels after 1-7 h of administration with the doses of 250 and 500 mg/kg was observed in the STZ diabetic group when compared to control. As regards to the dose of 250 and 500 mg/kg for the fasted normal rats, there was significant increase in the blood glucose levels when compared to control. In conclusion the ethanolic extract of the leaves of *Moringa oleifera* possesses hypoglycemic activity in STZ induced diabetic Wistar rats only (Tende, 2011).

From aforementioned reports, concluded that *M. oleifera* leaves possess hypoglycemic effect possibly through α -glucosidase inhibition. Therefore, this research is aimed at identifying active components responsible for inhibiting α -glucosidase function.

2.2 Isolation

Dried leaves of *M. oleifera* (720 g) were boiled in water. The aqueous extract was partitioned with EtOAc. Then we choose aqueous extract to isolate because aqueous extract have been reported for antidiabetes (Dolly, 2009) and bioassay guide, which aqueous extract was more potent inhibition than ethylacetate extract. The aqueous extract was subjected to diaion HP-20 and eluted with H₂O and MeOH, respectively. The MeOH layer was subjected to vacuum liquid column chromatography (VLC) using silica gel as adsorbent and eluted with CH₂Cl₂, 10:90, 20:80 and 40:60 MeOH-CH₂Cl₂ and MeOH, respectively. The eluents were pooled into three major fractions (AA031-1 to AA031-3), based on TLC analysis. Fraction AA031-1 was isolated using sephadex LH-20 CC with 1:1 and 3:7 MeOH-CH₂Cl₂. Further purification was performed by silica gel CC and eluted with EtOAc to afford *p*-hydroxybenzaldehyde-*O*- α -L-rhamnopyranoside (**1**) and keampferol (**2**). Fraction AA031-2 was purified by flash CC with 10:90 MeOH-EtOAc, yielding kaempferyl-3-*O*- β -glucopyranoside (**3**). Fraction AA031-3 was purified by sephadex LH-20 with 1:1 MeOH-CH₂Cl₂ and followed by silica gel CC with 10:90 MeOH-CH₂Cl₂, yielding 1-*O*-(4-hydroxymethylphenyl)- α -L-rhamnopyranoside (**4**). The isolation is summarized in Scheme 2.1.



Scheme 2.1 Isolation procedure of *M. oleifera* leaves

2.3 Structure elucidation of isolated compounds 1-4

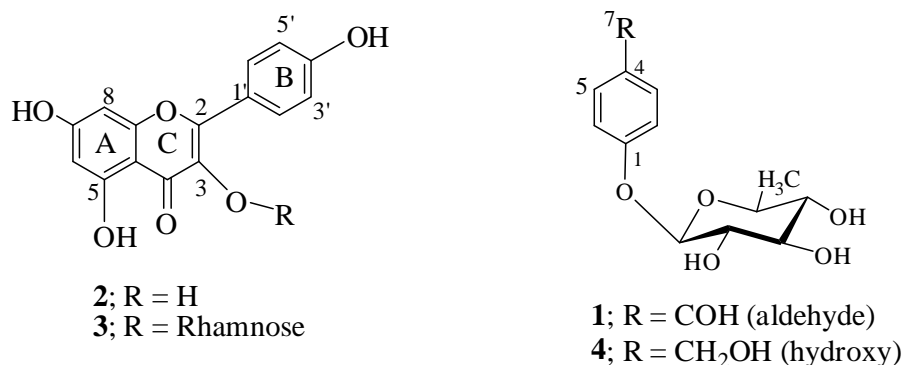


Figure 2.2 Isolated compounds of *M. oleifera* leaves

Isolated compound from *Moringa oleifera* was divided into two groups. They are flavonols group and 1, 4-disubstituted aromatic group.

2.3.1 Flavonols (2 and 3)

Flavonol is a flavanoid characterized by the presence of olifinic carbon in 2, 3-position and 3-position was replaced by hydroxyl group. The ¹H NMR spectrum showed signals of aromatic on ring A at δ_{H} 6.31-6.40 ppm in 8-position and δ_{H} 6.11-6.18 ppm in 6-position. The similar characteristic signal of isolated compounds showed one hydroxyl group on ring B so, we found proton signal in 2', 6'-position and 3', 5'-position, which displayed two doublet signals, at δ_{H} 7.96-8.09 ppm and 6.79-6.90 ppm, respectively. Above data showed characteristic structure of keampferol. However, each isolated compound was showed the different signal of R group.

Compound **2** was obtained as yellow solids. The ¹H NMR spectrum showed characteristic signals as same as the above data. Therefore, the structure of compound **2** was identified as keampferol (Lin, 2009) (Figure 2.3).

Compound **3** was obtained as yellow solids. The ^1H NMR spectrum showed similar characteristic signals of kaempferol except the replacing of sugar moieties in R group. The sugar unit, suggested to be an 3-*O*-glucopyranosyl moiety were revealed by the corresponding anomeric proton at δ_{H} 5.17 (d, $J = 2$ Hz). Therefore, compound **3** was identified as kaempferol-3-*O*- β -glucopyranoside (Lin, 2009) (Figure 2.4 and 2.5).

2.3.2 1, 4-Disubstituted aromatic group (1 and 4)

1, 4-Disubstituted aromatic group showed signal proton at δ_{H} 7.16-7.78 ppm (d, $J = 8$ Hz, H-2 and H-6) and δ_{H} 6.90-7.14 ppm (d, $J = 8$ Hz, H-3 and H-5), which are characteristic signal of *para*-disubstituted aromatic ring. The ^1H NMR spectrum showed similar characteristic signals of sugar moiety at δ_{H} 3.12-3.90 ppm. The sugar unit, suggest to be a α -L-rhamnopyranosyl moiety was revealed anomeric and secondary methyl protons at δ_{H} 5.53 and 1.07 (3H, showed doublet signals), respectively. However, each isolated compound was showed the different signal of R group.

Compound **1** was obtained as yellow oil. From above data, the ^1H NMR spectrum showed characteristic signal as same as the above data but substituted group (R) was replaced by aldehyde group, showed signals at δ_{H} 9.79 ppm in 7-position and confirmed ^{13}C NMR signals of aldehyde group at δ_{C} 190.9 ppm. In addition, structure of compound **1** was confirmed with 2D NMR spectroscopic methods. Therefore, compound **1** was identified as *p*-hydroxybenzaldehyde-*O*- α -L-rhamnopyranoside (Michael, 1998) (Figure 2.1 and 2.2).

Compound **4** was obtained as yellow oil. The ^1H NMR showed similar characteristic signal of *p*-hydroxybenzaldehyde-*O*- α -L-rhamnopyranoside, but the carbon in 7-position was reduced to alcohol form. The ^{13}C NMR of alcohol form in 7-position showed signal at δ_{C} 64.3 ppm. Therefore, compound **4** was identified as 1-*O*-(4-hydroxymethylphenyl)- α -L-rhamnopyranoside (Grond, 2002) (Figure 2.6 and 2.7).

2.4 α -Glucosidase inhibitory activity of the isolated compounds

The α -glucosidase inhibitory activity of compounds **1-4** isolated from *M. oleifera* leaves was evaluated by colorimetric method and the results are shown in Tables 2.2, 2.3 and 2.4, respectively.

Table 2.2 α -Glucosidase (baker's yeast) inhibitory activity of isolated compounds from *M. oleifera* leaves

Compound	%Inhibition concentration of compounds (mg/mL)				IC ₅₀ (μ M) ^a
	0.01	0.1	1	5	
1	9.9 \pm 3.9	10.0 \pm 1.3	1.1 \pm 2.6	NA	NI ^b
2	29.5 \pm 1.5	40.5 \pm 0.9	85.9 \pm 1.1	NA	46.4
3	NA	6.6 \pm 1.1	28.2 \pm 0.5	62.7 \pm 0.7	523.0
4	4.8 \pm 3.1	-3.6 \pm 2.3	-2.8 \pm 3.5	NA	NI ^b
Acarbose[®]	-				480.0

^aThe IC₅₀ value is defined as the inhibitor concentration to inhibit 50% of enzyme activity.

^bNo inhibition, less than 50% inhibition at 5 mg/ml. and NA is not measuring in that concentration

From Table 2.2, the isolated compounds were evaluated for α -glucosidase inhibitory effect using baker's yeast α -glucosidase as a model. The results showed that keampferol (**2**) exhibited the most effective activity with IC₅₀ value of 46.46 μ M, which is more potent than kaempferyl-3-*O*- β -glucopyranoside (**3**) with IC₅₀ value of 523 μ M. Therefore, we concluded that the sugar moiety of compound **3** decrease activity inhibit α -glucosidase for baker's yeast. However, compound **3** was equipotent to standard drug, acarbose while compounds **1** and **4** were not active because the present of percent inhibition was reduced at a high concentration.

Table 2.3 α -Glucosidase (maltase) inhibitory activity of isolated compounds from *M. oleifera* leaves

Compound	%Inhibition				IC ₅₀ (μ M) ^a
	Concentration of inhibitor (mg/mL)				
	0.01	0.1	1	5	
1	10.2 \pm 1.7	19.2 \pm 7.1	13.5 \pm 2.7	NA	NI ^b
2	10.6 \pm 0.7	29.6 \pm 1.8	57.9 \pm 2.0	NA	94.3
3	NA	40.2 \pm 2.1	94.0 \pm 1.8	96.0 \pm 0.6	77.0
4	13.5 \pm 2.1	5.4 \pm 0.4	4.6 \pm 1.6	NA	NI ^b
Acarbose[®]	-				1.5

^aThe IC₅₀ value is defined as the inhibitor concentration to inhibit 50% of enzyme activity.

^bNo inhibition, less than 50% inhibition at 5 mg/ml. and NA is not measuring in that concentration

From Table 2.3, the isolated compounds were evaluated for α -glucosidase inhibitory effect using rat intestine α -glucosidase of maltase as a model. The results showed that kaempferyl-3-*O*- β -glucopyranoside (**3**) exhibited the most effective activity with IC₅₀ value of 77 μ M, which is equipotent to kaempferol (**2**), while compounds **1** and **4** were not active. However, the active compounds have the inhibitory activity lower than standard drug, acarbose.

Table 2.4 α -Glucosidase (sucrase) inhibitory activity of isolated compounds from *M. oleifera* leaves

Compound	%Inhibition				IC ₅₀ (μ M) ^a
	Concentration of inhibitor (mg/mL)				
	0.01	0.1	1	5	
1	11.9 \pm 1.9	11.6 \pm 1.5	11.7 \pm 0.2	NA	NI ^b
2	22.2 \pm 1.2	44.6 \pm 2.1	79.7 \pm 0.4	NA	30.1
3	NA	26.3 \pm 1.7	45.8 \pm 1.1	75.4 \pm 0.5	359.0
4	12.2 \pm 1.6	13.3 \pm 0.7	16.3 \pm 1.4	NA	NI ^b
Acarbose[®]	-				2.3

^aThe IC₅₀ value is defined as the inhibitor concentration to inhibit 50% of enzyme activity.

^bNo inhibition, less than 50% inhibition at 5 mg/ml. and NA is not measuring in that concentration

From Table 2.4, the isolated compounds were evaluated for α -glucosidase inhibitory effect using rat intestine α -glucosidase of sucrase as a model. The results showed that kaempferol (**2**) exhibited the most effective activity with IC₅₀ value of 30.04 μ M, while compounds **1** and **4** were not active. However, the active compounds have the inhibitory activity lower than standard drug, acarbose.

We concluded that the active compounds of isolated *M. oleifera* leaves are kaempferol (**2**) and kaempferyl-3-*O*- β -glucopyranoside (**3**), while isolated compound of 1, 4-disubstituted aromatic group were not active for α -glucosidase inhibitory effect. From data, compound **2** was more potent than compound **3**. Therefore, sugar moiety didn't support to inhibit α -glucosidase activity.

2.5 Experiment section

2.5.1 General experiment procedures

The ¹H and ¹³C NMR spectra (in CDCl₃, CD₃OD and acetone-*d*₆) were determined with a nuclear magnetic resonance spectrometer of Varian model

Mercury+ 400. The chemical shift in δ (ppm) was assigned with reference to the signal from the residual protons in deuterated solvents and using TMS as an internal standard in some cases. Diaion HP-20, sephadex LH-20 and silica gel 60 Merck cat. No. 7734 and 7729 were used for flash column chromatography. Thin layer chromatography (TLC) was performed on precoated Merck silica gel 60 F₂₅₄ plates (0.25 mm thick layer).

2.5.2 Plant material

The leaves of *M.oleifera* (voucher specimen number: BCU 013507) were collected in Lampang, Thailand in January 2010. Plant authentication was performed by Miss Parinyanoot Klinratana, and the specimen has been deposited in Botanical Herbarium, Department of Botany, Faculty of Science, Chulalongkorn University.

2.5.3 Extraction and isolation

Dried leaves of *M. Oleifera* (720 g) were boiled in water at 80°C (2×3,000 mL) for 3 hours. The aqueous extract was partitioned with EtOAc. The aqueous extract was subjected to diaion HP-20 and eluted with H₂O and MeOH to afford MeOH extracts. The MeOH layer was subjected to vacuum liquid column chromatography (VLC) using silica gel as adsorbent and eluted with dichloromethane (CH₂Cl₂), 10:90, 20:80 and 40:60 MeOH-CH₂Cl₂ and MeOH, respectively. The eluents were pooled into three major fractions (AA031-1 to AA031-3), based on TLC analysis. Fraction AA031-1 was isolated using sephadex LH-20 with 1:1 MeOH-CH₂Cl₂ to yield three fractions (AA032-1 to AA032-3). Fraction AA032-1 was purified by sephadex LH-20 column using 3:7 MeOH-CH₂Cl₂, after which adsorbed onto silica gel and eluted with EtOAc to afford *p*-hydroxybenzaldehyde-*O*- α -L-rhamnopyranoside (**1**). Fraction AA032-3 afforded keampferol (**2**). Fraction AA031-2 was purified by flash CC with 10:90 MeOH-EtOAc, yielding kaempferyl-3-*O*- β -glucopyranoside (**3**). Fraction AA031-3 was purified by sephadex LH-20 with 1:1 MeOH-CH₂Cl₂ and followed silica gel CC with 10:90 MeOH-CH₂Cl₂, yielding 1-*O*-(4-hydroxymethylphenyl)- α -L-rhamnopyranoside (**4**).

***p*-Hydroxybenzaldehyde-*O*- α -L-rhamnopyranoside (1):** yellow oil; ^1H NMR (acetone- d_6 , 400 MHz) δ_{H} 9.79 (1H, s, H-7), 7.78 (2H, d, $J = 8$ Hz, H-2 and H-6), 7.14 (2H, d, $J = 8$ Hz, H-3 and H-5), 5.53 (1H, s, H-1'), 3.12-3.64 (sugar moiety); ^{13}C NMR (acetone- d_6 , 400 MHz) δ_{C} 190.9 (C-7), 160.8 (C-1), 131.5 (C-3 and C-5), 129.3 (C-4), 116.9 (C-2 and C-6), 98.2 (C-1'), 72.3-70.4 (C-2'-C-5') and 17.5 (CH₃-6') (Michael, 1998).

Keampferol (2): yellow solid; ^1H NMR (CD₃OD, 400 MHz) δ_{H} 8.09 (2H, d, $J = 8.8$ Hz, H-2' and H-6'), 6.90 (2H, d, $J = 8.8$ Hz, H-3' and H-5'), 6.40 (1H, d, $J = 2$ Hz, H-8), 6.18 (1H, d, $J = 2$ Hz, H-6) (Lin, 2009).

Keampferol-3-*O*- β -glucopyranoside (3): yellow solid; ^1H NMR (CD₃OD, 400 MHz) δ_{H} 7.96 (2H, d, $J = 8.8$ Hz, H-2' and H-6'), 6.79 (2H, d, $J = 8.8$ Hz, H-3' and H-5'), 6.31 (1H, d, $J = 2$ Hz, H-8), 6.11 (1H, d, $J = 2$ Hz, H-6), 5.17 (1H, d, $J = 2$ Hz, H-1"), 3.61-3.10 (sugar moiety). ^{13}C NMR (CD₃OD, 400 MHz) δ_{C} 177.4 (C-4), 164.1 (C-7), 161.1 (C-5), 159.9 (C-4'), 156.3 (C-2), 156.2 (C-9), 133.1 (C-3), 130.8 (C-2' and C-6'), 120.8 (C-1'), 115.1 (C-3' and C-5'), 103.9 (C-10), 100.8 (C-1''), 98.6 (C-6), 93.6 (C-8), 60.8-77.4 (C-2''-C-6'') (Lin, 2009).

1-*O*-(4-Hydroxymethylphenyl)- α -L-rhamnopyranoside (4): yellow oil; ^1H NMR (acetone- d_6 , 400 MHz) δ_{H} 7.16 (2H, d, $J = 8$ Hz, H-2 and H-6), 6.90 (2H, d, $J = 12$ Hz, H-3 and H-5), 5.33 (1H, s, H-1'), 4.42-4.40 (2H, m, H-7), 3.36-3.90 (sugar moiety); ^{13}C NMR (acetone- d_6 , 400 MHz) δ_{C} 156.5 (C-1), 128.9 (C-3 and C-5), 117.2 (C-2 and C-6), 136.9 (C-4), 99.5 (C-1'), 64.3-70.5 (C-2'-C-5'), 41.1 (C-7), 18.2 (CH₃-6') (Grond, 2002).

2.5.4 α -Glucosidase inhibitory assay

2.5.4.1 Chemical and equipment

Sucrose, maltose, baker's yeast α -glucosidase, rat intestinal acetone powder, and *p*-nitrophenyl- α -D-glucopyranoside were purchased from Sigma-Aldrich (St. Louis, MO, USA). Glucose assay kit was purchased from Human Gesellschaft für

Biochemica und Diagnostica mbH (Germany). Acarbose was obtained from Bayer (Germany).

2.5.4.2 Assay for determining inhibitory effect against α -glucosidase from baker's yeast

The α -glucosidase inhibition assay was performed according to the slightly modified method by Hwang *et al.* The α -glucosidase (0.1 U/mL) and substrate (1 mM *p*-nitrophenyl- α -D-glucopyranoside) were dissolved in 0.1 M phosphate buffer, pH 6.9. Ten μ L of isolated compounds (0.1, 1, 10 mg/mL in DMSO) was pre-incubated with 40 μ L of α -glucosidase at 37°C for 10 min. A 50 μ L substrate solution was then added to the reaction mixture and incubated at 37°C for 20 min, and terminated by adding 100 μ L of 1 M Na₂CO₃. The enzymatic hydrolysis of the *p*NPG was monitored based on the amount of *p*-nitrophenol released into the reaction mixture (Figure 2.3) by Bio-Rad microplate reader model 3550 UV at 405 nm. The percentage inhibition of activity was calculated by %inhibition = [(A₀-A₁)/A₀] \times 100, where A₀ is the absorbance without the sample, A₁ is the absorbance with the sample. The IC₅₀ value was determined from a plot of percentage inhibition versus sample concentration. Acarbose[®] was used as standard control and the experiment was performed in duplicate.

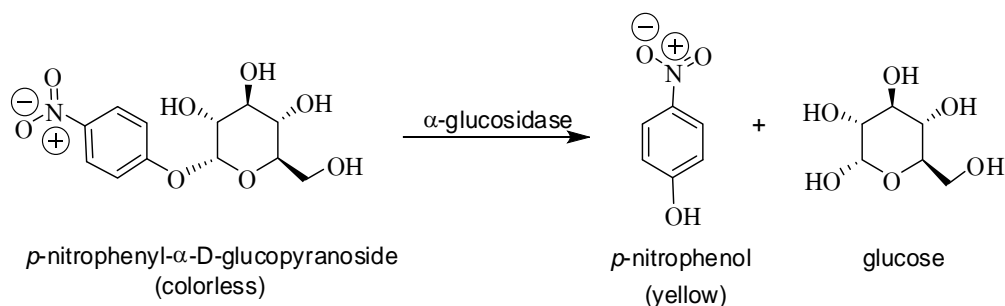


Figure 2.3 Hydrolysis of baker's yeast α -glucosidase

2.5.4.3 Rat intestinal α -glucosidase inhibitory activity

Rat intestinal α -glucosidase inhibitory activity was determined according to the method of Adisakwattana *et al.* with slight modification. The crude enzyme solution prepared from rat intestinal acetone powder was used as a source of maltase and sucrase. Rat intestinal acetone powder (1 g) was homogenized in 30 mL of 0.9% NaCl solution. After centrifugation ($12,000g \times 30$ min), the aliquot was subjected to assay. A 10 μ L of isolated compounds (1 mg/mL in DMSO) was added with 30 μ L of the 0.1 M phosphate buffer (pH 6.9), 20 μ L of the substrate solution (maltose: 10 mM; sucrose: 100 mM) in 0.1 M phosphate buffer, 80 μ L of glucose assay kit, which showed the mechanism reaction in this assay (Figure 2.4), and 20 μ L of the crude enzyme solution. The reaction mixture was then incubated at 37 $^{\circ}$ C for 10 min (for maltose) and 40 min (for sucrose). The percentage inhibition was calculated by $[(A_0 - A_1)/A_0] \times 100$, where A_0 is the absorbance without the sample, and A_1 is the absorbance with the sample. The IC_{50} value was determined from a plot of percentage inhibition versus sample concentration. Acarbose[®] was used as standard control and the experiment was performed in duplicate.

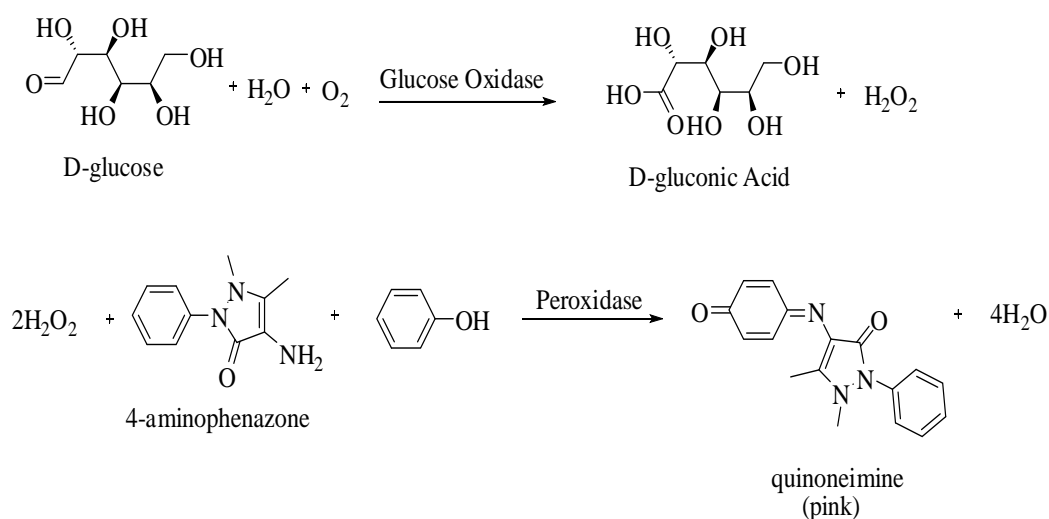


Figure 2.4 The reaction principle of α -glucosidase from rat small intestine

Supporting information

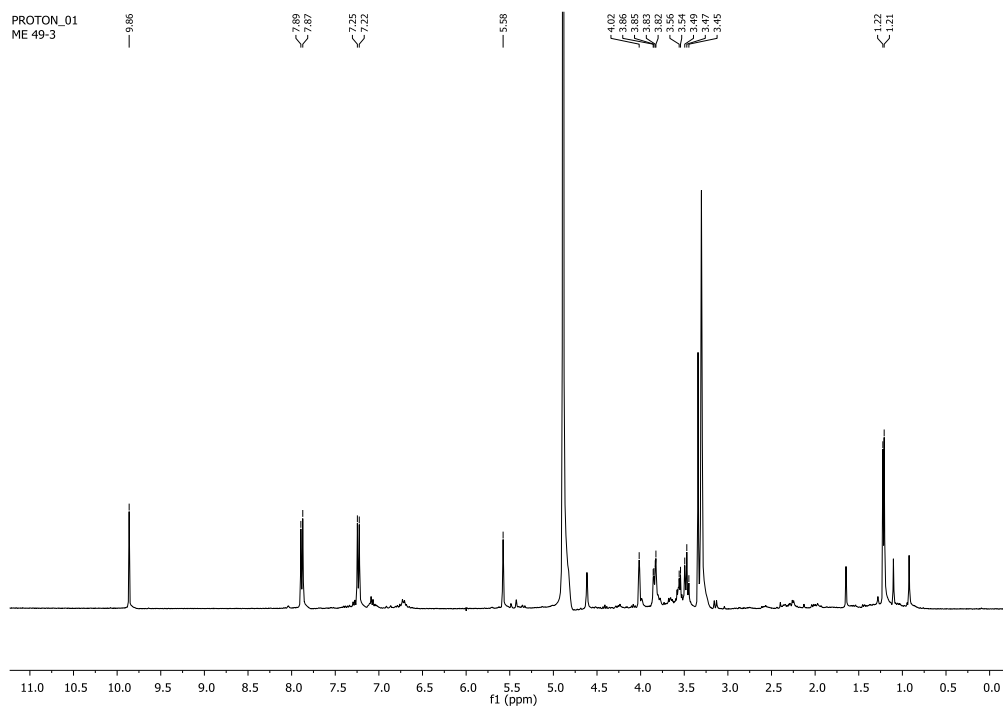


Figure S-2.1 The ^1H NMR (acetone- d_6) spectrum of *p*-hydroxybenzaldehyde-*O*- α -L-rhamnopyranoside (**1**)

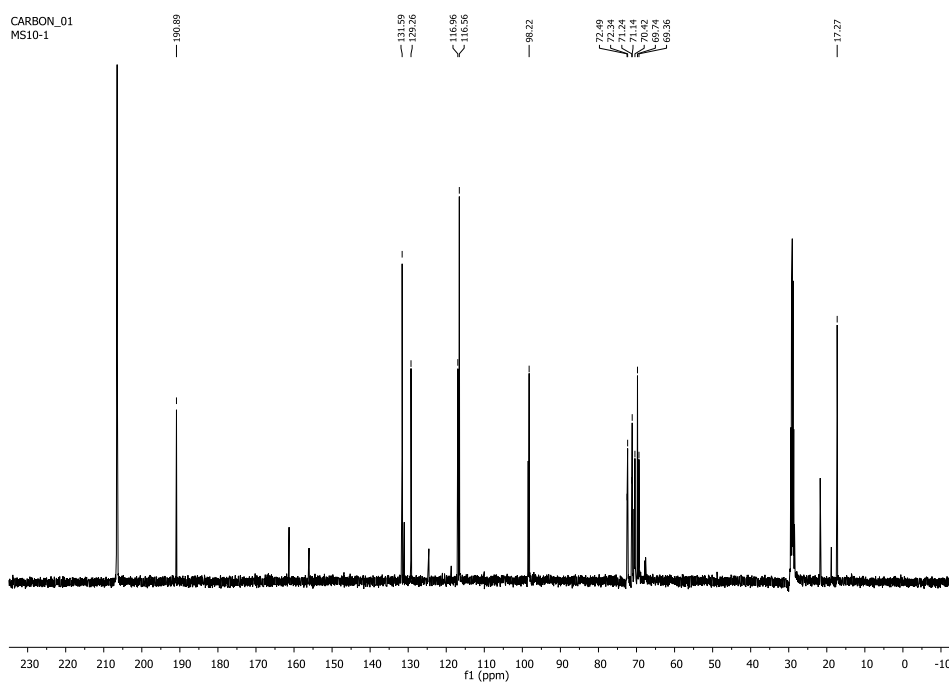


Figure S-2.2 The ^{13}C NMR (acetone- d_6) spectrum of *p*-hydroxybenzaldehyde-*O*- α -L-rhamnopyranoside (**1**)

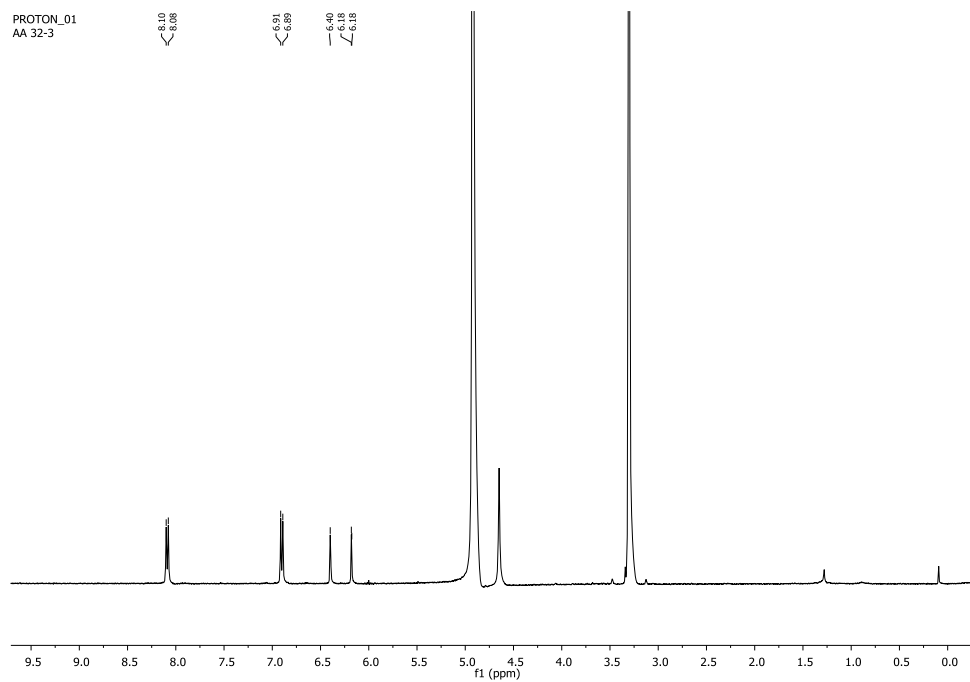


Figure S-2.3 The ^1H NMR (CD_3OD) spectrum of keampferol (**2**)

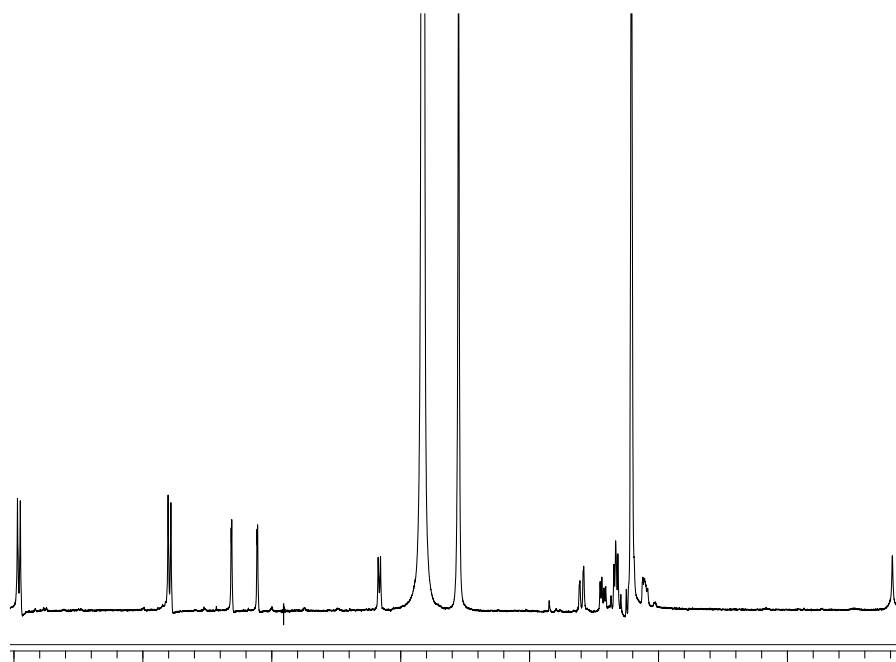


Figure S-2.4 The ^1H NMR (CD_3OD) spectrum of kaempferyl-3- O - β -glucopyranoside (**3**)

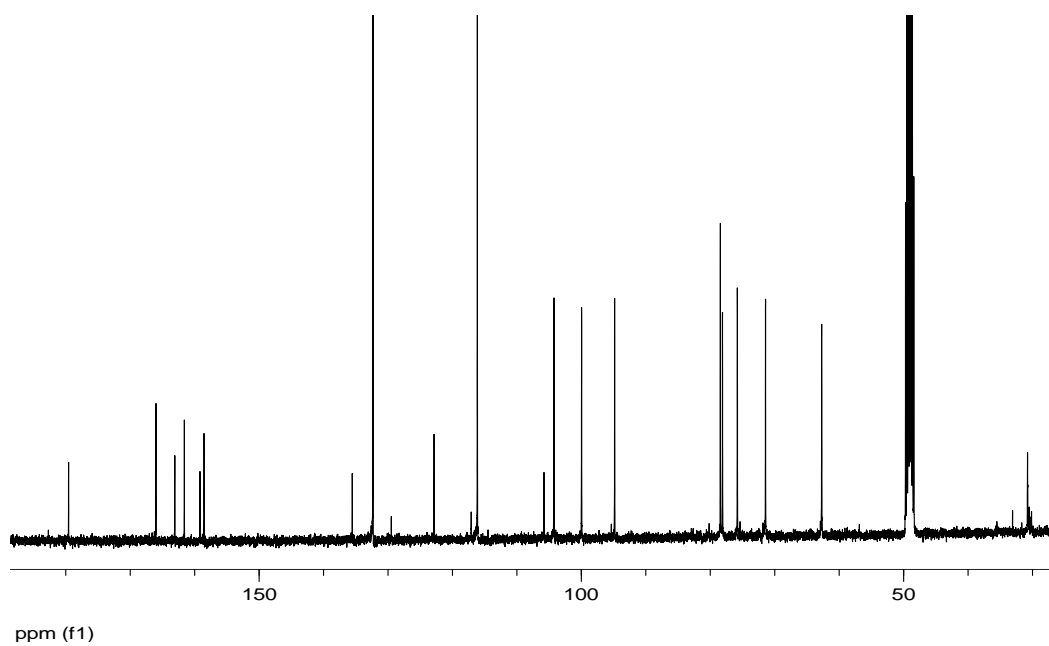


Figure S-2.5 The ^{13}C NMR (CD_3OD) spectrum of kaempferyl-3-*O*- β -glucopyranoside (**3**)

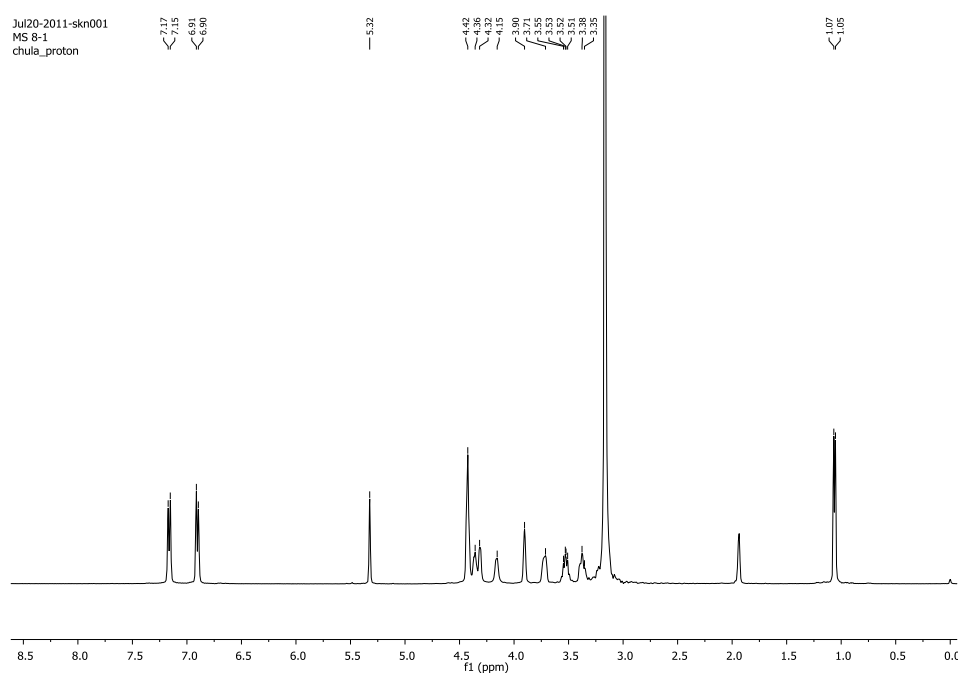


Figure S-2.6 The ^1H NMR (CD_3OD) spectrum of 1-*O*-(4-hydroxymethylphenyl)- α -L-rhamnopyranoside (**4**)

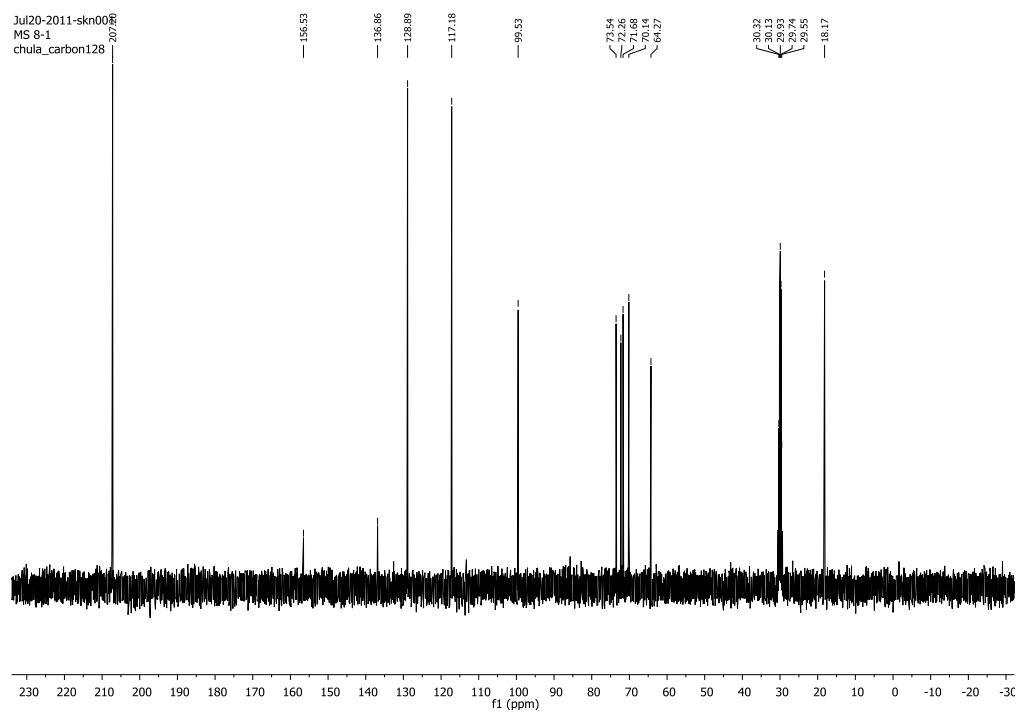


Figure S-2.7 The ^{13}C NMR (CD_3OD) spectrum of 1-*O*-(4-Hydroxymethylphenyl)- α -L-rhamnopyranoside (**4**)

CHAPTER III

α -GLUCOSIDASE INHIBITORS FROM *Syzygium samarangense* Leaves

3.1 Introduction

3.1.1 Botanical aspect and distribution

Syzygium samarangense (Syn. *Eugenia javanica*, Figure 3.1) belongs to the family Myrtaceae, which is native to the tropics, particularly in tropical America and Australia. It is commonly known as wax apple, in addition to vernacular names wax jambu, water apple and java apple. It is a small tree with pretty, top-shaped, pink edible fruit. The yellow to dark bluish green leaves, 12-20 cm long, are opposite, elliptical with very short stalks and are aromatic when crushed. The tree can produce abundant fruits and has two fruiting seasons annually, May to September and November to March. Fruit are are pear-shaped, 1.5-2 inches long, skin is smooth, waxy, come in varying colors ranging from white, pale green, green, pink, rose red and crimson. *Syzygium samarangense* needs adequate rainfall, some humidity and fertile soil for best growth, and is hardy to around freezing, possibly a few degrees below (Simirgiotis, 2008).

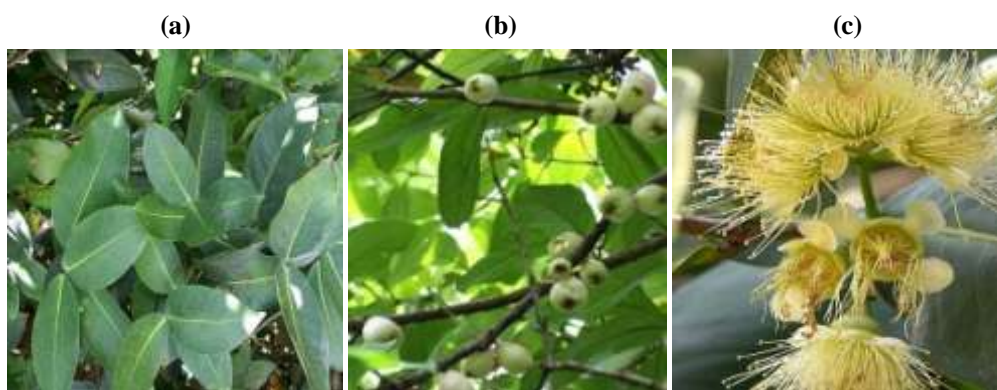


Figure 3.1 *Syzygium samarangense*: (a) leaves, (b) fruit and (c) flower

3.1.2 Pharmacological investigation

In Malaysia, the green fruits of wax apple are eaten raw with salt or cooked as a sauce. The flowers, which contain tannins, desmethoxymatteucinol, 5-*O*-methyl-4-*O*-desmethoxymatteucinol, oleanic acid, and β -sitosterol, are used in Taiwan to treat fever and halt diarrhea (Morton, 1987).

Previous phytochemical studies of the leaves of *S. samarangense* have shown the presence of ellagitannins (Nonaka, 1992), flavanones, flavonol glycosides (Kuo, 2004), proanthocyanidins (Nonaka, 1992), anthocyanidins (Kuo, 2004; Nonaka, 1992), triterpenoids (Srivastava, 1995), chalcones and volatile terpenoids (Wong, 1996).

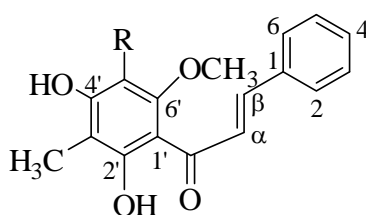
Ethanol leaf extract exhibited immunostimulant activity (Srivastava, 1995). The hexane extract was found to relax the hypermotility of the gut (Ghayur, 2006), while the alcoholic extract of the stem bark showed antibacterial activity (Chattopadhyay, 1998).

The immunomodulatory (Kuo, 2004), antihyperglycaemic (Resurreccion-Magno, 2005), spasmolytic, and prolyl endopeptidase inhibitory effects of chalcones and 5-*O*-methyl-4-desmethoxymatteucinol isolated from the leaves have also been reported (Amor, 2005).

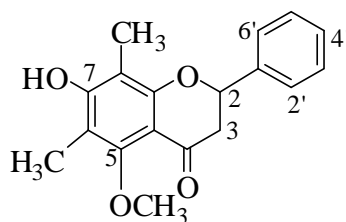
Chalcones are a group of plant-derived polyphenolic compounds that are intermediates in the biosynthesis of flavonoids and are associated with several biological activities, including antiviral (Kiat, 2006), antifungal (Svetaz, 2004) anti-inflammatory (Lespagnol, 1972), antioxidant (Han, 2006), anticancer and cytotoxic activities (Liu, 2005).

Chalcones also displayed *in vivo* antihyperglycemic effect in 2005, 2', 4'-dihydroxy-3', 5'-dimethyl-6'-methoxychalcone, its isomeric flavanone 5-*O*-methyl-4'-desmethoxymatteucinol and 2', 4'-dihydroxy-6'-methoxy-3'-methylchalcone were isolated from the leaves of *S. samarangense* using a bioassay-directed scheme. In an oral glucose tolerance test at a dosage of 1.0 mg/20 g mouse, 2', 4'-dihydroxy-3', 5'-dimethyl-6'-methoxychalcone and 5-*O*-methyl-4'-desmethoxymatteucinol significantly ($\alpha = 0.05$) lowered the blood glucose levels (BGLs) in glucose-hyperglycaemic mice when administered 15 min after a glucose load. When co-administered with glucose,

only 2', 4'-dihydroxy-3', 5'-dimethyl-6'-methoxychalcone showed a significant lowering of BGLs 45 min after its oral administration. When administered 15 min before glucose, none of the flavonoids showed a positive effect. Only 2', 4'-dihydroxy-3', 5'-dimethyl-6'-methoxychalcone decreased significantly, at $\alpha = 0.05$, the BGLs of alloxan-diabetic mice at $t = 90-150$ min (Resurreccion-Magno, 2005). Therefore, hypoglycemic effect of *S. samarangense* leaves is likely to be associated with α -glucosidase inhibition.



2',4'-dihydroxy-3',5'-dimethyl-6'-methoxychalcone R = CH₃
 2', 4'-dihydroxy-6'-methoxy-3'-methylchalcone R = H



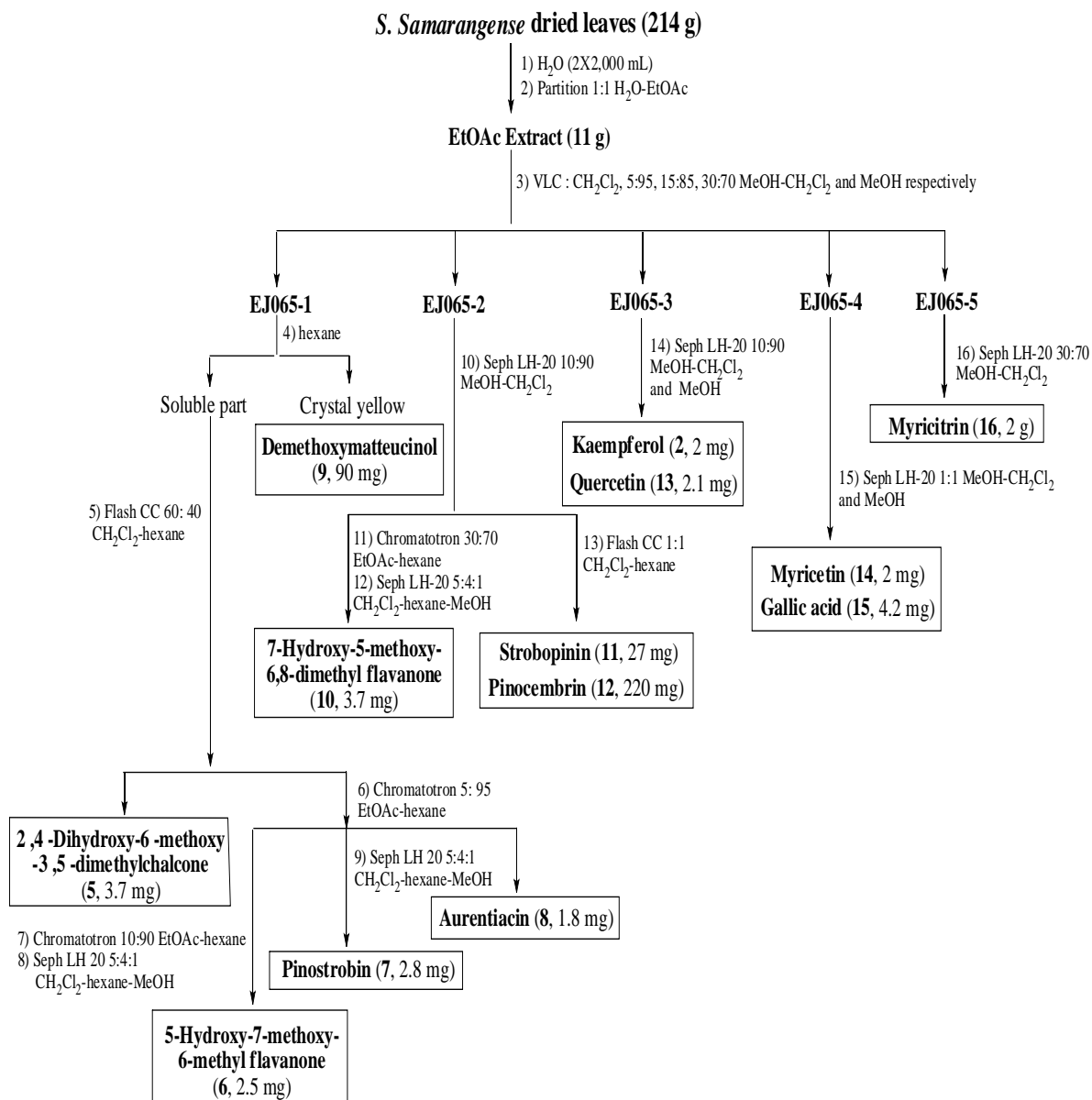
5-*O*-methyl-4'-desmethoxymatteucinol

Figure 3.2 Selected isolated compounds from *Syzygium samarangense* leaves

From aforementioned reports, concluded that *S. samarangense* leaves possess hypoglycemic effect possibly through α -glucosidase inhibition. Therefore, this research is aimed at identifying active components responsible for inhibiting α -glucosidase function.

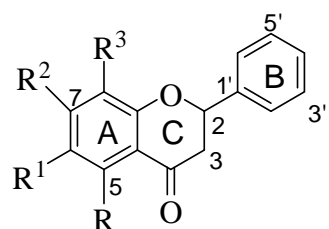
3.2 Isolation

Dried leaves of *S. Samarangense* were boiled in water. The aqueous extract was partitioned with EtOAc to afford EtOAc extract. Then we choose EtOAc extract to isolate because aqueous extract have been reported for antidiabetes (Resurreccion-Magno, 2005) and bioassay guide. The EtOAc extract was subjected to vacuum liquid column chromatography (VLC) using silica gel as adsorbent and eluted with dichloromethane (CH_2Cl_2), MeOH- CH_2Cl_2 (5:95, 15:85 and 30:70) and MeOH, respectively. The eluents were pooled into five major fractions (EJ065-1 to EJ065-5), based on TLC analysis. Fraction EJ065-1 was defatted with hexane, yielding yellow crystals of demethoxymatteucinol (**9**). The hexane soluble part was isolated using flash column chromatography to afford 2', 4'-dihydroxy-6'-methoxy-3', 5'-dimethylchalcone (**5**) and the residue fraction separated through chromatotron with 5:95 EtOAc-hexane, affording three fractions (EJ070-1 to EJ070-3). Fraction EJ070-1 was purified by chromatotron followed by Sephadex LH-20 column to afford 5-hydroxy-7-methoxy-6-methyl flavanone (**6**). Fractions EJ070-2 and EJ070-3 were independently purified by Sephadex LH-20 column to afford pinostrobin (**7**) and aurentiacin (**8**). The fraction EJ065-2 was isolated using Sephadex LH-20 CC with 10:90 MeOH- CH_2Cl_2 that yielded two fractions (EJ068-3 and EJ068-4). Fraction EJ068-3 was purified by chromatotron followed by Sephadex LH-20 column to afford 7-hydroxy-5-methoxy-6, 8-dimethyl flavanone (**10**). Fraction EJ068-4 was purified by flash CC, yielding strobopinin (**11**) and pinocembrin (**12**). Fraction EJ065-3 was purified by Sephadex LH-20 column to afford kaempferol (**2**) and quercetin (**13**). Fraction EJ065-4 was purified by Sephadex LH-20 column to afford myricetin (**14**) and gallic acid (**15**). Fraction EJ065-5 was purified by Sephadex LH-20 column to afford myricitrin (**16**). The isolation is summarized in Scheme 3.1.

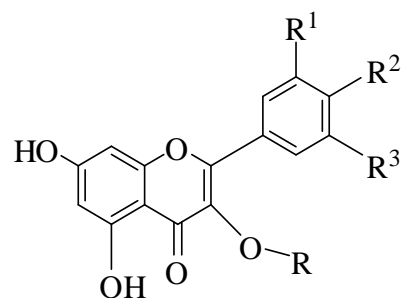


Scheme 3.1 Isolation procedure of *S. samarangense* leaves

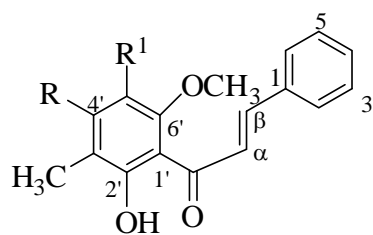
3.3 Structure elucidation of isolated compounds 5-16



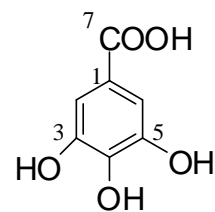
	R	R ¹	R ²	R ³
6	OH	CH ₃	OCH ₃	H
7	OH	H	OCH ₃	H
9	OH	CH ₃	OH	CH ₃
10	OCH ₃	CH ₃	OH	CH ₃
11	OH	CH ₃	OH	H
12	OH	H	OH	H



	R	R ¹	R ²	R ³
2	H	H	OH	H
13	H	OH	OH	H
14	H	OH	OH	OH
16	Rhamnose	OH	OH	OH



	R	R ¹
5	OH	CH ₃
8	OCH ₃	H



15

Figure 3.3 Isolated compounds from *S. samarangense* leaves

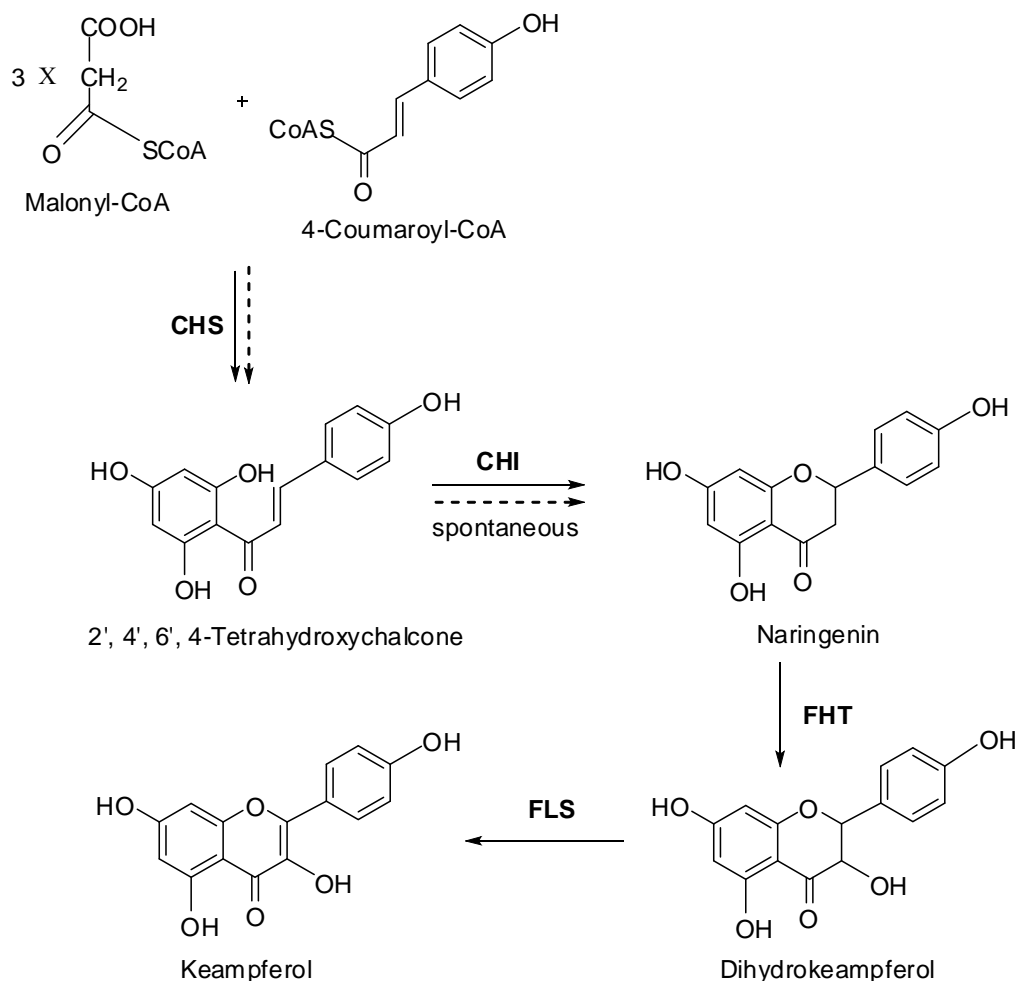


Figure 3.4 Biosynthetic pathways of chalcone, flavanone and flavonol

Isolated compounds from *S. samarangense* could be divided into four groups: flavanones, chalcones, flavonols and gallic acid.

To easily understand structure elucidation of the first three groups in next section, biosynthetic pathway of chalcone, flavanone and flavonol (Figure 3.4) was demonstrated (Harborne, 1986). The key enzyme for the formation of the flavonoid skeleton is chalcone synthase (CHS), which catalyses the stepwise condensation of three acetate units from malonyl-CoA with 4-coumaroyl-CoA to the C₁₅ intermediate 2', 4', 6', 4-tetrahydroxychalcone, is the typical chalcone skeleton. The stereo-specific cyclization of the chalcone, catalysed by chalcone isomerase (CHI), provides naringenin, is the typical flavanone skeleton. Flavanones can be hydroxylated in position 3 to dihydroflavonols (e.g. dihydrokempferol). This reaction is catalysed by

flavanone 3-hydroxylase (FHT). Dihydroflavonols are the direct substrates for the abundant class of flavonols. Flavonols (e.g. keampferol) are formed from dihydroflavonols by introduction of double bond between C-2 and C-3. The reaction is catalysed by flavonol synthase (FLS).

3.3.1 Flavanones (6, 7, 9, 10, 11 and 12)

Flavanone is a flavanoid characterized by the presence of methylene (H₂-3) and chiral oxygenated methylene (H-2), which resonate around 2.70-2.85 (H-3a), 2.96-3.10 (H-3b) and 5.30-5.45 (H-2) ppm respectively. In addition, the ¹H NMR spectra of all isolated flavanones (**6-8**, **9-12**) showed similar characteristic signals of monosubstituted aromatic ring B at 7.31-7.48 ppm (5H). However, each flavanone showed the different signal of substituents at ring A.

Compound **6** was obtained as a yellowish gum. The ¹H NMR spectrum showed a down field shift (δ_{H} 12.06 ppm) of hydroxy group at C-5 forming hydrogen bonding with C-4 carbonyl. Compound **6** showed methoxyl signal at δ_{H} 3.83 ppm on ring A. According to biosynthetic pathway (Figure 3.4), methoxyl group was deposited at C-7. In addition, substituent group showed methyl signal at δ_{H} 2.01 ppm at C-6. The ¹³C NMR spectra showed 17 carbon signals. Methyl carbon at δ_{C} 6.9 ppm and methoxyl carbon at δ_{C} 55.8 ppm were assigned at in C-6 and C-7 position, respectively. Thus, the structure of compound **6** was identified as 5-hydroxy-7-methoxy-6-methyl flavanone (Mustafa, 2003) (Figure 3.3 and 3.4).

Compound **7** was obtained as colorless solid. The ¹H NMR spectrum of compound **7** showed similar characteristic signal with compound **6** but methyl signal at 6-position that was replaced by hydrogen proton. The aromatic protons (2H) showed at δ_{H} 6.08 ppm for H-6 and H-8. The ¹³C NMR spectrum showed 16 carbon signals. Methoxyl carbon at δ_{C} 55.8 ppm was assigned at C-7. Thus, the structure of compound **7** was identified as pinostrobin (Sukari, 2007) (Figure 3.5 and 3.6).

Compound **9** was obtained as yellow crystal. The ¹H NMR spectrum showed hydroxyl signals at δ_{H} 12.06 and 5.49 ppm that were deposited in C-5 and C-7, respectively. In addition, compound **9** displayed each methyl signal at δ_{H} 2.07 and

2.08 ppm at C-6 and C-8, respectively. The ^{13}C NMR spectrum showed 17 carbon signals. Methyl carbons at δ_c 7.6 and 6.8 ppm were assigned at C-6 and C-8, respectively. Thus, the structure of compound **9** was identified as demethoxymatteucinol (Hufford, 1982) (Figure 3.9 and 3.10).

Compound **10** was obtained as yellow crystal. The ^1H NMR spectrum of compound **10** showed similar characteristic methyl signals with compound **9**. In addition, we found no hydroxyl proton resonating at high field. So, we concluded that the hydroxyl proton at C-5 of compound **9** was replaced by methoxyl proton at δ_H 3.81 ppm. The ^{13}C NMR spectrum showed 18 carbon signals. The carbon of methoxyl group displayed signal at δ_c 61.3 ppm. Thus, the structure of compound **10** was identified as 7-hydroxy-5-methoxy-6, 8-dimethyl flavanone (Kou, 2004) (Figure 3.11 and 3.12).

Compound **11** was obtained as yellow crystal. The ^1H NMR spectrum of compound **11** showed similar characteristic signal with compound **9**, except for number of methyl group. Compound **11** displayed one methyl signal at δ_H 1.94 ppm at C-6. The ^{13}C NMR spectrum showed 16 carbon signals. Methyl carbon at δ_c 6.7 ppm was signed at C-6. Thus, the structure of compound **11** was identified as strobopin (Solladić, 1999) (Figure 3.13 and 3.14).

Compound **12** was obtained as white crystal. The ^1H NMR spectrum of compound **12** showed similar characteristic signal with compound **9**. However, compound **12** showed no methyl signal because they were replaced by aromatic proton at δ_H 5.90 ppm (2H) at C-6 and C-8. The ^{13}C NMR spectrum showed 15 carbon signals. Thus, the structure of compound **12** was identified as pinocembrin (Sukari, 2007) (Figure 3.15 and 3.16).

3.3.2 Chalcones (5 and 8)

Chalcone is a flavanoid characterized by presence of olefinic protons at α , β -position. These signals appeared around δ_H 7.77-7.93 ppm. In addition, the ^1H NMR spectrum of two isolated chalcone showed similar characteristic signal of monosubstituted aromatic ring at 7.34-7.58 ppm.

Chalcones **5** and **8** showed one strongly hydrogen-bonded signals at δ_{H} 13.55 and 14.06 ppm, respectively, indicating the presence of 2'-OH. The ^1H NMR spectrum of two chalcones showed similar characteristic signal of methyl and methoxy protons. Methyl protons appeared at δ_{H} 2.05 ppm in 3'-position and methoxy protons appeared at δ_{H} 3.92 ppm in 6'-position. However, each chalcone were showed the different signal of substituents.

Compound **5** was obtained as orange solid. The ^1H NMR spectrum showed hydroxyl proton at δ_{H} 5.31 ppm in 4'-position and showed methyl signal at δ_{H} 2.09 ppm in 5'-position. The ^{13}C NMR spectrum showed 18 carbon signals. Methyl carbons at δ_{C} 8.2 and 7.5 ppm were assigned at C-3' and C-6' positions, respectively. Methoxyl carbon at δ_{C} 62.3 ppm was assigned at C-6'. Thus, the structure of compound **5** was identified as 2', 4'-dihydroxy-6'-methoxy-3', 5'-dimethylchalcone (Amor, 2005) (Figure 3.1 and 3.2).

Compound **8** was obtained as yellow solid. The ^1H NMR spectrum of compound **8** showed similar characteristic signal with compound **5**. However, the hydroxyl proton at C-4' of compound **5** was replaced by methoxyl proton that showed signals at δ_{H} 3.96 ppm. The methyl proton at C-5' of compound **5** was replaced by hydrogen proton that showed signals at δ_{H} 6.01 ppm. The ^{13}C NMR spectrum showed 18 carbon signals. Methyl carbon at δ_{C} 7.3 ppm was assigned at C-3' and methoxyl carbons at δ_{C} 55.5 and 55.9 ppm were assigned at C-4' and C-6', respectively. Thus, the structure of compound **8** was identified as aurentiacin (Mustafa, 2005; Adityachaudhury, 1976) (Figure 3.7 and 3.8).

3.3.3 Flavonols (2, 13, 14 and 16)

Flavonol is a flavanoid that showed similar characteristic proton with flavanone. However, H-2 and H-3 were replaced by unsaturation and the presence of OR group at C-3. Therefore, the proton signals observed in ^1H NMR spectrum of flavonol are derived from ring A or B. In addition, the ^1H NMR spectra of all flavonol showed similar characteristic signals of aromatic on ring A at δ_{H} 6.34-6.82 ppm (H-8)

and δ_{H} 6.34-6.82 ppm (H-6). The different proton signals of aromatic ring B can indicate characteristic of each flavonol.

Compound **2** was obtained as brown solids. The ^1H NMR spectrum showed aromatic signals of ring B, in addition to two signals of H-6 and H-8 early mentioned. The proton signals resonated around δ_{H} 7.74 (2H) and 6.91 ppm (2H) with coupling constant each 8.4 Hz of H-2'/ H-6' and H-3'/ H-5', respectively. Thus, the structure of compound **2** was identified as kaempferal (Eldahshan, 2010) (Figure 3.17).

Compound **13** was obtained as brown solids. The ^1H NMR spectrum showed three proton signals on aromatic ring B. The proton signals resonated around at δ_{H} 7.76, 7.54 and 6.82 ppm belonged to H-2', H-6' and H-5', respectively. Thus, the structure of compound **13** was identified as quercetin (Eldahshan, 2010) (Figure 3.18).

Compound **14** was obtained as brown solids. The ^1H NMR spectrum showed singlet signal of two protons on aromatic ring B. The proton signals resonated around δ_{H} 6.95 ppm (2H) belonged to H-2' and H-6'. Thus, the structure of compound **14** was identified as myricetin (Shen, 2009) (Figure 3.19).

Compound **16** was obtained as brown solids. The ^1H NMR spectrum showed similar characteristic signals of myricetin aglycone. In addition, there were signals of sugar moiety, which was suggest to be an rhamnopyranosyl moiety due to anomeric and secondary methyl protons at δ_{H} 5.30 and 0.96 ppm, respectively. The α -oriented rhamnose linked to aglycone was suggested by a small coupling constant of 1.5 Hz (H-1''). Thus, the structure of compound **16** was identified as myricitrin (Shimizu, 2006), whose name is nearly closed to its aglycone, myricetin (Figure 3.22 and 3.23).

3.3.4 Gallic acid (15)

Compound **15** was obtained light brown solid. The ^1H NMR spectrum showed only one proton signal at δ_{H} 6.91 ppm. However, the ^{13}C NMR spectra showed 7 carbon signals. Carbonyl carbon signal displayed signals at δ_{C} 168.0 ppm, which was assigned as C-7. Thus, the structure of compound **15** was identified as gallic acid (Eldahshan, 2010) (Figure 3.20 and 3.21).

3.4 α -Glucosidase inhibitory activity of the isolated compounds

The α -glucosidase inhibitory activity of compounds **5-16** isolated from *Syzygium samarangense* leaves was evaluated by colorimetric method and the results are shown in Table 3.1.

Table 3.1 α -Glucosidase inhibitory activity of isolated compounds from *Syzygium samarangense* leaves.

compounds	α -glucosidase inhibitory activity (IC ₅₀ , μ M) ^a		
	baker's yeast	rat intestine	
		maltase	Sucrose
5	34.0	94.0	83.0
6	47.8	NI ^b	NI ^b
7	68.5	NI ^b	NI ^b
8	87.8	795.0	526.0
9	109.4	400.0	202.0
10	72.0	NI ^c	NI ^c
11	98.8	175.0	84.0
12	142.4	1,145.0	538.0
2	46.5	94.3	30.0
13	62.8	12.3	31.7
14	3.7	79.5	28.5
15	67.6	232.2	29.3
16	35.9	76.2	72.1
Acarbose[®]	480.0	1.5	2.3

^aThe IC₅₀ value is defined as the inhibitor concentration to inhibit 50% of enzyme activity.

^b No inhibition, less than 50% inhibition at 1 mg/ml. ^c No inhibition, less than 50% inhibition at 5 mg/ml.

From Table 3.1, all isolated compounds of *Syzygium samarangense* leaves were evaluated for α -glucosidase inhibitory effect using α -glucosidase from baker's yeast and rat intestine. Using baker's yeast α -glucosidase as a model, the results showed that all isolated compounds were more potent than the standard drug, acarbose while using rat intestine α -glucosidase as a model, all isolated compounds were less potent than acarbose.

The α -glucosidase inhibitory effect was dependent on typical structure of compound. The results showed that isolated flavonols exhibited the most effective activity with lower IC_{50} value. The following structures enhanced the inhibitory activity: the unsaturated C ring, 3-OH and 4-CO (Kenjiro, 2005).

Isolated compounds of flavonols (**2**, **13**, **14** and **16**) showed a broad inhibition because they displayed α -glucosidase inhibitory activity in the same trend. Compounds **2**, **13** and **14** displayed different characterized structure at ring B. We found that compound **14** is exhibited the most effective activity with the IC_{50} value of 3.71 μ M, using baker's yeast α -glucosidase as a model. However, using rat intestine α -glucosidase as a model, compound **13** is the most potent activity with IC_{50} value of 12.32 μ M toward maltase, while compounds **2**, **13** and **14** were equipotent toward sucrase. Therefore, α -glucosidase inhibitory activity was dependent on the 3-position of hydroxy group at aromatic ring B, enhanced the inhibitory activity (Kenjiro, 2005).

Myricetin (**14**) is aglycone part of myricitrin (**16**). The results showed that myricetin displayed the higher α -glucosidase inhibitory activity than myricitrin because of sugar moieties led to decrease in inhibitory activity. We assumed that the flavonoid aglycone is critical for binding to active site of enzyme. However, we found that both compound were equipotent, using rat intestine α -glucosidase from maltase as a model.

Gallic acid showed similar characteristic structure with myricetin at ring B, that is, gallic acid didn't appear aromatic on ring A and C. The results showed that gallic acid (**15**) was less potent than myricetin (**14**). Therefore, aromatic on ring A and C of myricetin affected to potent α -glucosidase inhibitory activity.

Typical chalcones, found that 2', 4'-dihydroxy-6'-methoxy-3', 5'-dimethylchalcone (**5**) was more potent than aurentiacin (**8**) because the presence of a

methoxy group can reduce the inhibitory effect, indicated that loss of hydroxyls from aromatic on ring A significantly reduced the activity (Eduardo, 2006) while methyl group (3-CH₃) on aromatic ring can increase the inhibitory effect. However, chalcones was cyclized to flavanone, that showed different α -glucosidase inhibitory activity. We found that chalcones (**5** and **8**) were more potent than flavanones (**6** and **9**), using α -glucosidase from rat intestine. Therefore, chalcones were more appropriate structure than flavanones for binding α -glucosidase because of double bond at 2 and 3 positions (Kenjiro, 2005).

Flavanones can be separated to two groups for discussion. Two groups were the present of methoxy (**6**, **7** and **10**) and hydroxy groups (**9**, **11** and **12**) on aromatic rings. The results showed that the presence of methoxy group on aromatic ring showed selectively inhibition toward α -glucosidase from baker's yeast and also they were more potent than the present of hydroxy group on aromatic ring. Moreover, compound **6** was more potent than compound **7** because the presence of methyl group on the aromatic ring increased the inhibitory effect (Eduardo, 2006).

Flavanones, the presence of hydroxy group on aromatic ring (**9**, **11** and **12**) were discussed by number of methyl groups on the core structure (Figure 3.5). The results showed that pinocembrin (**12**) displayed no methyl group so value of α -glucosidase inhibitory activity, was less potent than compounds possessing methyl groups on structure. Therefore, the present of methyl groups on aromatic ring at 6 or 8 positions increased the inhibitory effect. However, the presence of only one methyl group at 6-position, strobopinin (**11**), exhibited the most effective α -glucosidase inhibitory activity. Demethoxymatteucinol (**9**) appeared two methyl groups at 6 and 8 positions, reduced the inhibitory effect but showed the higher activity than pinocembrin. As showed in Figure 3.5.

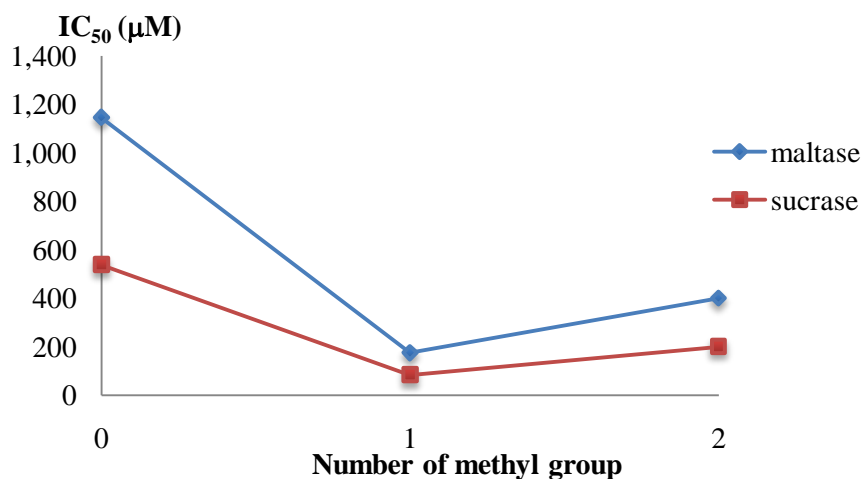
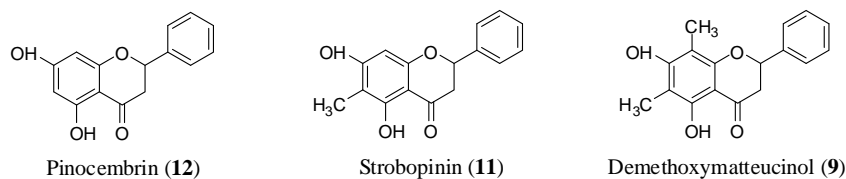


Figure 3.5 Inhibition trends of active compounds (**11**, **12** and **9**), the presence of hydroxy group on aromatic ring against.

From the results, we found that series flavonols exhibited more effective activity than other series. They were not advertent for kinetic study because they have been reported for antidiabetic activity widely (Kenjiro, 2005; Escandón-Rivera, 2012). Thus, we interested in the isolated compound of flavanones and chalcones series that responsible for hyperglycemic effect, using α -glucosidase from rat intestine.

2',4'-Dihydroxy-6'-methoxy-3',5'-dimethylchalcone (**5**), typical chalcones exhibited the most effective activity with IC₅₀ values of 94 and 83 μ M toward maltase and sucrase, respectively, which is equipotent to a typical flavanone, strobopinin (**11**). Therefore, we concluded that compounds **5** and **11** were active components responsible for hyperglycemic effect in *S. samarangense*. Moreover, 2', 4'-dihydroxy-6'-methoxy-3', 5'-dimethylchalcone (**5**) has been reported that it exhibited antidiabetic activity in both NIDDM and IDDM-simulated conditions, using glipizide as a standard drug (Resurreccion-Magno, 2005). Thus, compounds **5** and **11** were studied

the modes of α -glucosidase inhibition from rat intestine because α -glucosidase in human brush border and rat are categorized into the same group.

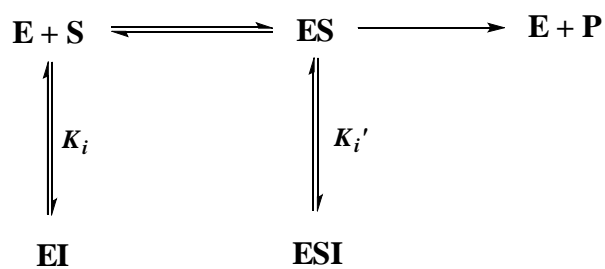
3.5 α -Glucosidase inhibitory mechanism of chalcone 5

Herein, it is the first time for kinetic study of 2', 4'-dihydroxy-6'-methoxy-3', 5'-dimethylchalcone (**5**). Kinetic analysis of inhibitor was calculated by using Lineweaver-Burk plot (Adisakwattana, 2009). In this work, we used α -glucosidase from rat intestine as model, which maltase and sucrase are substrate. The results showed that the Lineweaver-Burk plot of different concentrations of compound **5** produced series of straight lines, all of which intersected in the second quadrant. The analysis showed that K_m increased with decreased V_{max} values (Table 3.2). Therefore, Figures 3.6 and 3.9, indicating that 2', 4'-dihydroxy-6'-methoxy-3', 5'-dimethylchalcone possesses mixed-type inhibition towards both maltase and sucrase.

Table 3.2 Types of Lineweaver-Burk plot for inhibition mechanism

Type of inhibition	K_m	V_{max}	Intersection
Competitive	increase	unchanged	Y axis, $Y > 0$
Non-competitive	unchange	decrease	X axis, $X < 0$
Uncompetitive	decrease	decrease	no intersection
Mixed	increase	decrease	second quadrant

The possible binding mode of 2', 4'-dihydroxy-6'-methoxy-3', 5'-dimethylchalcone was presumed that one inhibitor can bind either to active site of free enzyme (**E**) in competitive manner (K_i) or to the enzyme-substrate complex (**ES**) in noncompetitive manner (K_i'). To gain insight into binding affinity of inhibitor (**I**) to free enzyme and ES complex, dissociation constants K_i and K_i' were further determined.



Scheme 3.2 Inhibition mechanism of compounds **5** and **11** towards rat intestine

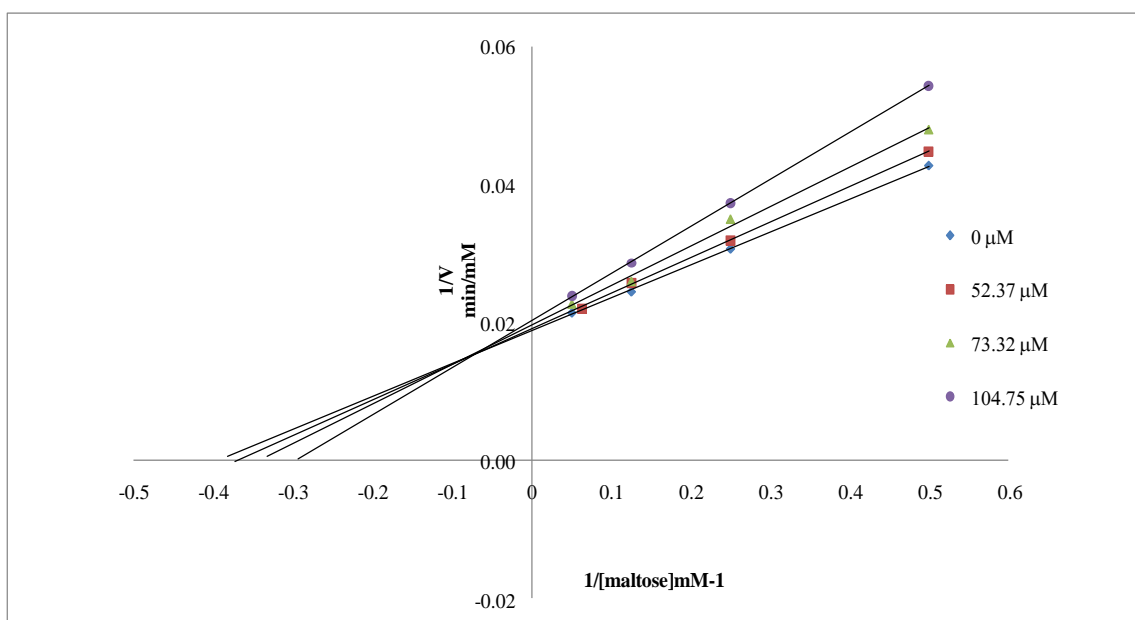


Figure 3.6 The Lineweaver-Burk plot, $1/v$ against $1/[\text{maltose}]$ of 2', 4'-dihydroxy-6'-methoxy-3', 5'-dimethylchalcone.

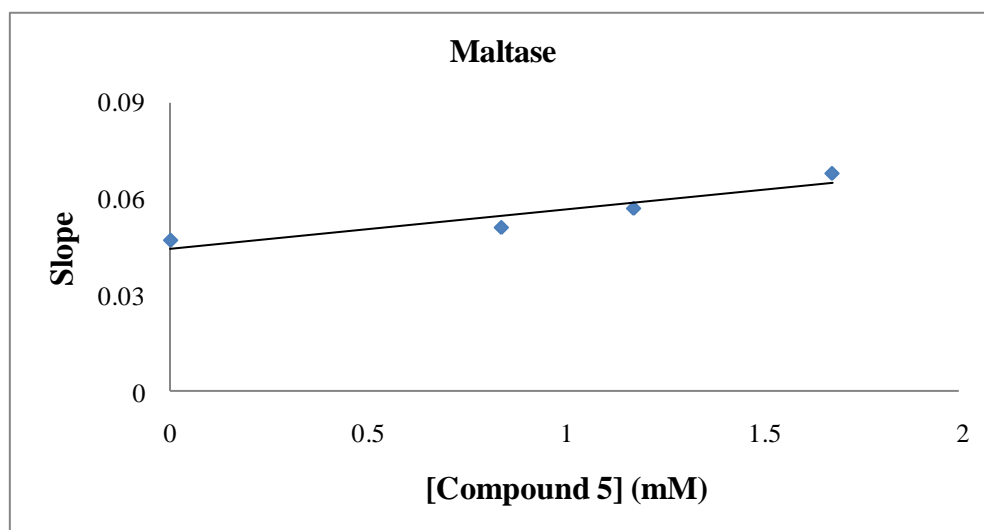


Figure 3.7 Dixon plot of slope vs. concentrations of compound **5** from a primary Lineweaver-Burk plot for the determination of K_i (2', 4'-dihydroxy-6'-methoxy-3', 5'-dimethylchalcone).

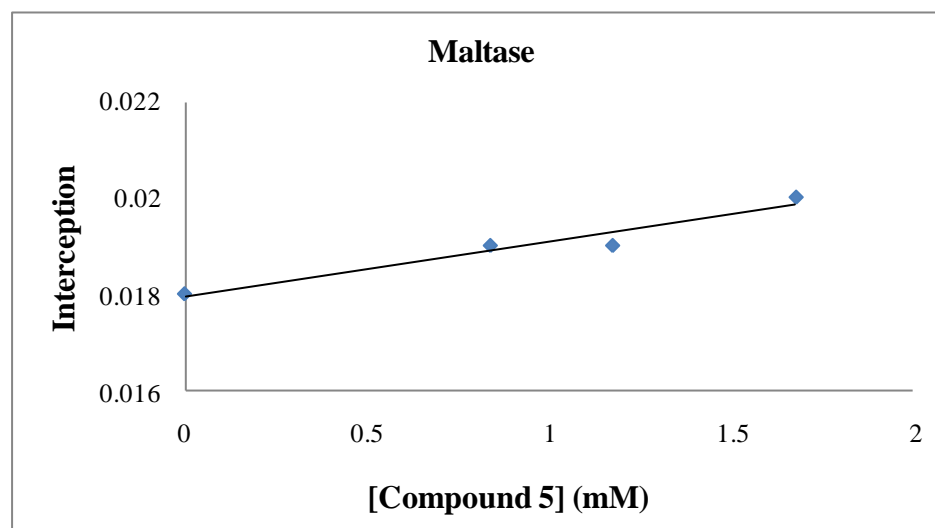


Figure 3.8 Secondary plot interception vs. concentrations of compound **5** from a primary Lineweaver-Burk plot for the determination of K_i' (2', 4'-dihydroxy-6'-methoxy-3', 5'-dimethylchalcone).

Dixon plot (Fig 3.7) showed the dissociation constant of EI complex with K_i value of 3.92 mM, whereas secondary plot (Fig 3.8) showed the dissociation constant of ESI complex with K_i' value of 18 mM toward maltase.

Apparently, K_i value of 2', 4'-dihydroxy-6'-methoxy-3', 5'-dimethylchalcone was approximately five times less than K_i' value (Table 3.3), indicating that binding of 2', 4'-dihydroxy-6'-methoxy-3', 5'-dimethylchalcone to the ES complex was weaker than that of 2', 4'-dihydroxy-6'-methoxy-3', 5'-dimethylchalcone to free enzyme. In addition, the data implied that 2', 4'-dihydroxy-6'-methoxy-3', 5'-dimethylchalcone is dominant in competitive inhibition toward maltose.

Similar in maltase the inhibitory mechanisms of sucrase shown mixed type inhibition (Fig 3.9). Dixon plot (Fig 3.10) showed the dissociation constant of EI complex with K_i value of 2.32 mM, whereas secondary replot (Fig 3.11) showed the dissociation constant of ESI complex with K_i' value of 6.67 mM toward sucrase.

Apparently, K_i value of 2', 4'-dihydroxy-6'-methoxy-3', 5'-dimethylchalcone was approximately three times less than K_i' value (Table 3.3), indicating that binding of 2', 4'-dihydroxy-6'-methoxy-3', 5'-dimethylchalcone to the ES complex was weaker than that of 2', 4'-dihydroxy-6'-methoxy-3', 5'-dimethylchalcone to free enzyme. In addition, the data implied that 2', 4'-dihydroxy-6'-methoxy-3', 5'-dimethylchalcone is dominant in competitive inhibition toward sucrase.

Table 3.3 The values from kinetic analyses of 2', 4'-dihydroxy-6'-methoxy-3', 5'-dimethylchalcone (5)

dissociation constant (mM)	maltase	sucrase
K_i	3.92	2.32
K_i'	18	6.67

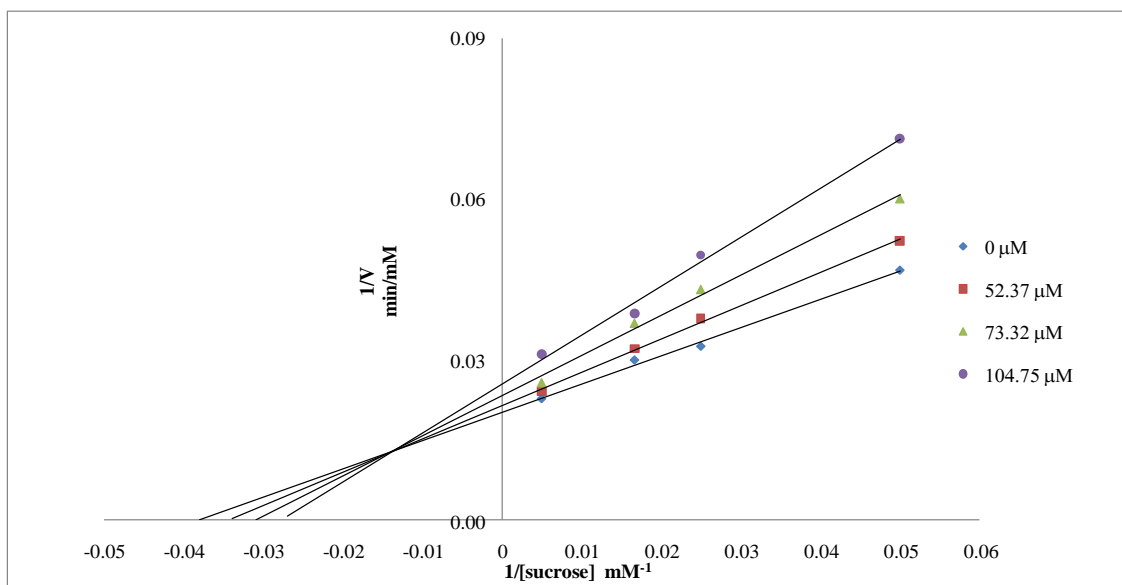


Figure 3.9 The Lineweaver-Burk plot, $1/v$ against $1/[sucrose]$ of 2', 4'-dihydroxy-6'-methoxy-3', 5'-dimethylchalcone.

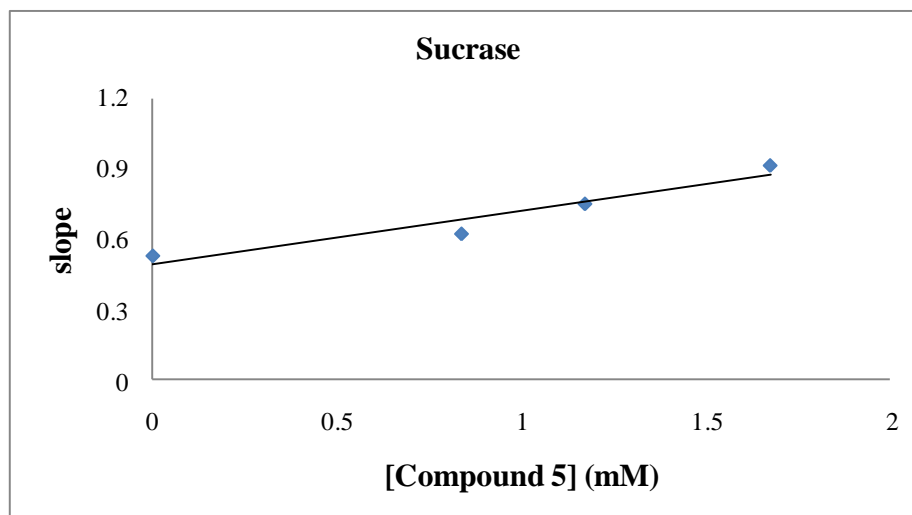


Figure 3.10 Dixon plot of slope vs. concentrations of compound 5 from a primary Lineweaver-Burk plot for the determination of K_i (2', 4'-dihydroxy-6'-methoxy-3', 5'-dimethylchalcone).

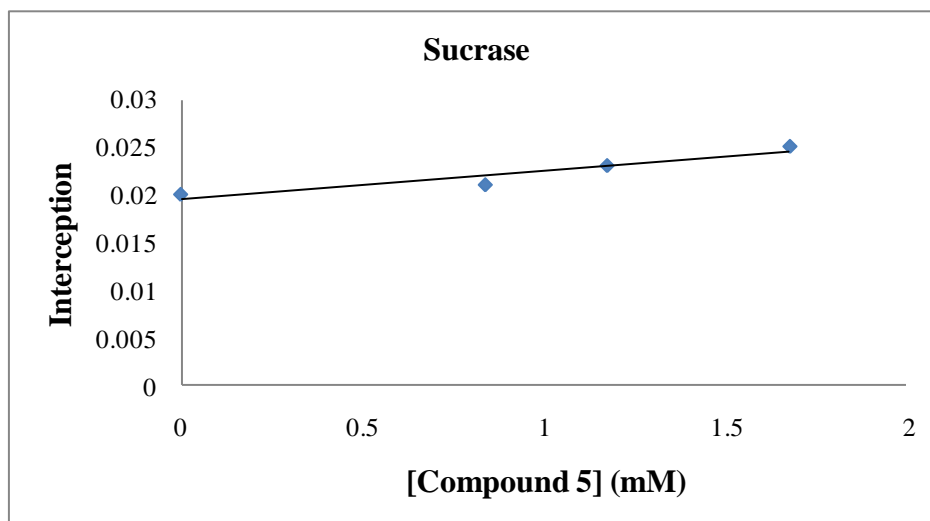


Figure 3.11 Secondary plot interception vs. concentrations of compound **5** from a primary Lineweaver-Burk plot for the determination of K_i' (2', 4'-dihydroxy-6'-methoxy-3', 5'-dimethylchalcone).

3.6 α -Glucosidase inhibitory mechanism of flavanone **11**

Herein, it is first time for kinetic study of strobopinin (**11**). The analysis showed that K_m increased with decreased V_{max} values (Table 3.2). Therefore, Figure 3.12 and 3.15, indicating that strobopinin possesses mixed-type inhibition towards both maltase and sucrase.

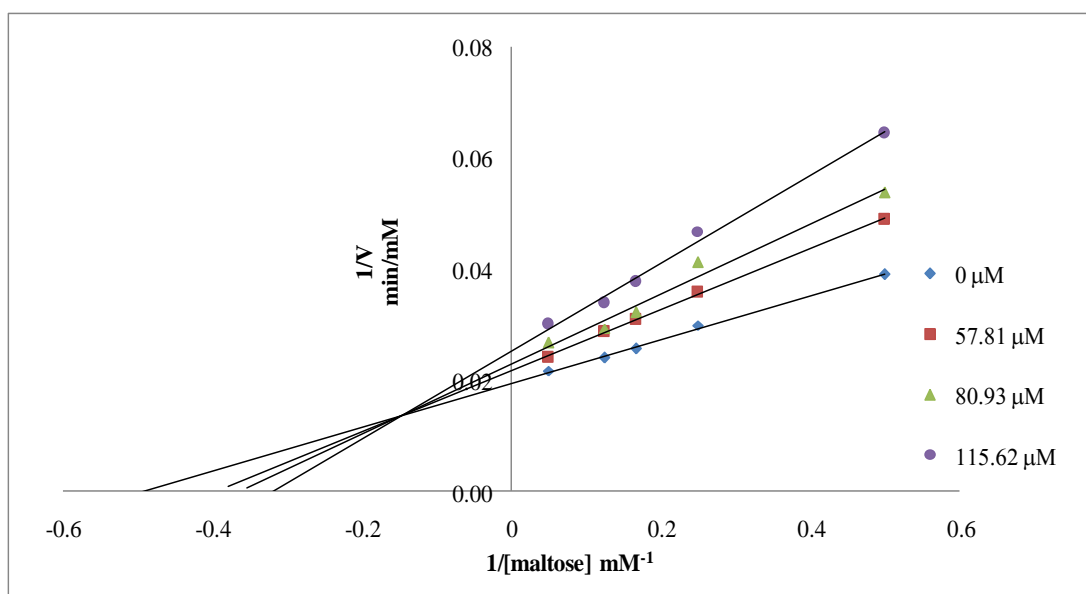


Figure 3.12 The Lineweaver-Burk plot, $1/v$ against $1/[maltose]$ of strobopinin.

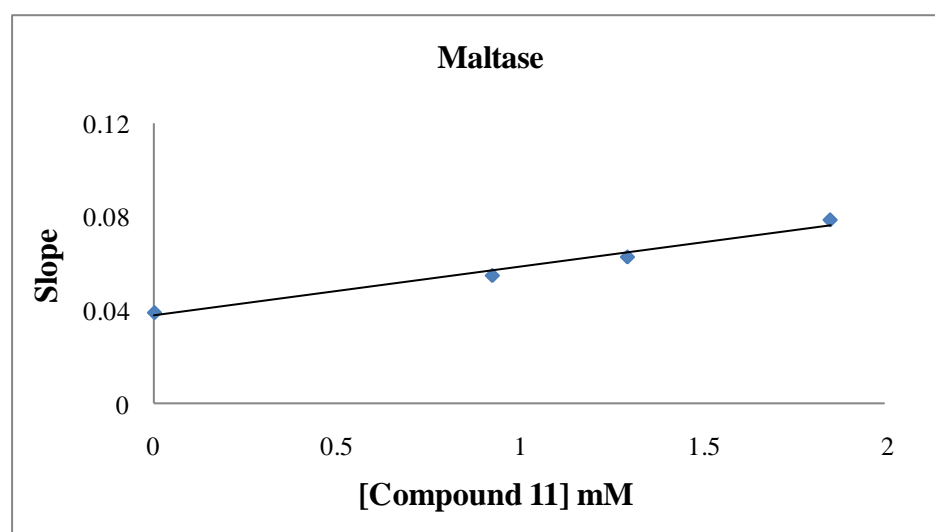


Figure 3.13 Dixon plot of slope vs. concentrations of compound **11** from a primary Lineweaver-Burk plot for the determination of K_i (strobopinin).

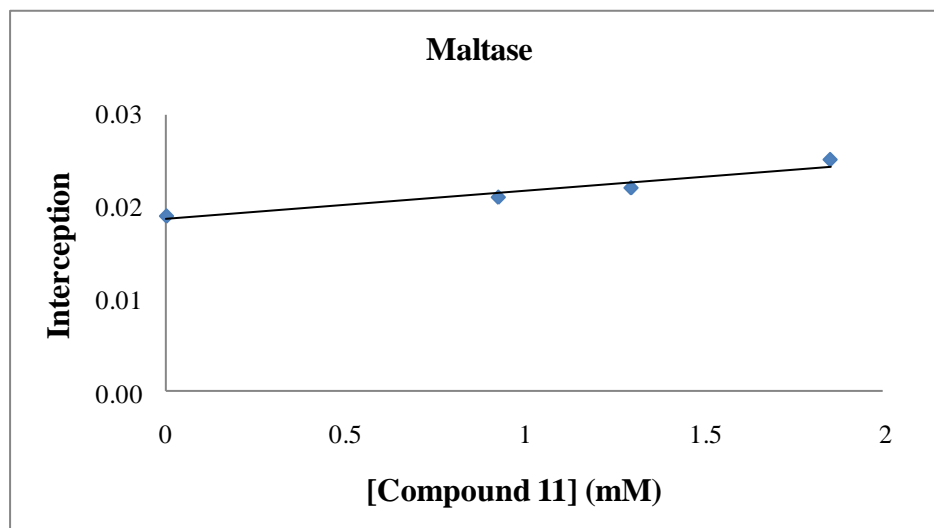


Figure 3.14 Secondary plot interception vs. concentrations of compound **11** from a primary Lineweaver-Burk plot for the determination of K_i' (strobopinin).

Dixon plot (Fig 3.13) showed the dissociation constant of EI complex with K_i value of 1.84 mM, whereas secondary plot (Fig 3.14) showed the dissociation constant of ESI complex with K_i' value of 6.13 mM toward maltase.

Apparently, K_i value of strobopinin was approximately 3 times less than K_i' value (Table 3.4), indicating that binding of strobopinin to the ES complex was weaker than that of strobopinin to free enzyme toward maltase. In addition, the data implied that strobopinin is dominant in competitive inhibition.

Similar in maltase the inhibitory mechanisms of sucrase shown mixed type inhibition (Fig 3.15). Dixon plot (Fig 3.16) showed the dissociation constant of EI complex with K_i value of 1.95 mM, whereas secondary plot (Fig 3.17) showed the dissociation constant of ESI complex with K_i' value of 9.09mM toward sucrase.

Apparently, K_i value of strobopinin was approximately five times less than K_i' value (Table 3.4), indicating that binding of strobopinin to the ES complex was weaker than that of strobopinin to free enzyme. In addition, the data implied that strobopinin is dominant in competitive inhibition toward sucrase.

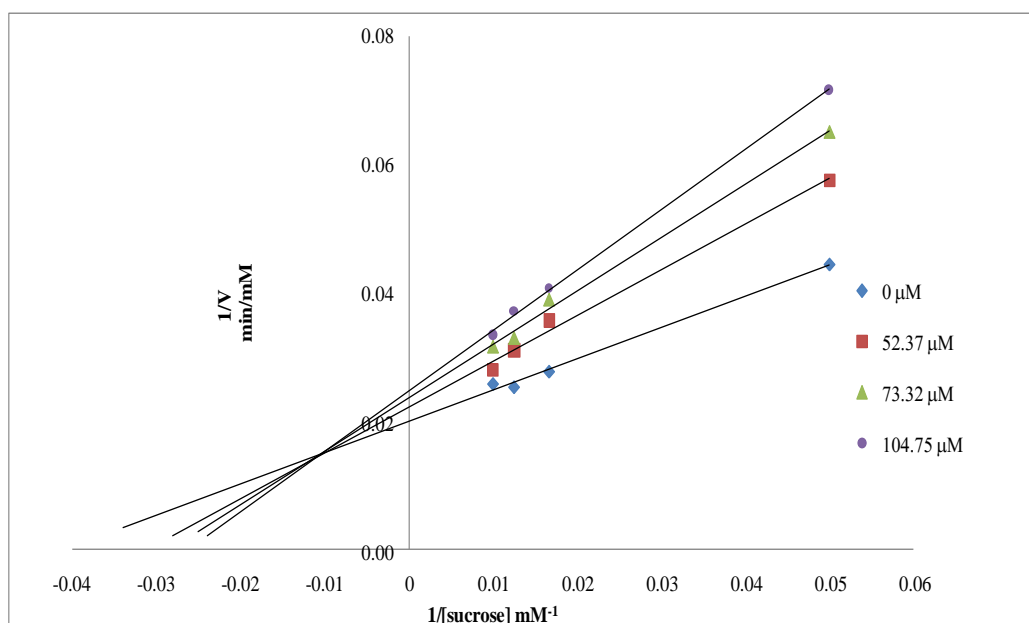


Figure 3.15 The Lineweaver-Burk plot, $1/v$ against $1/[sucrose]$ of strobopinin

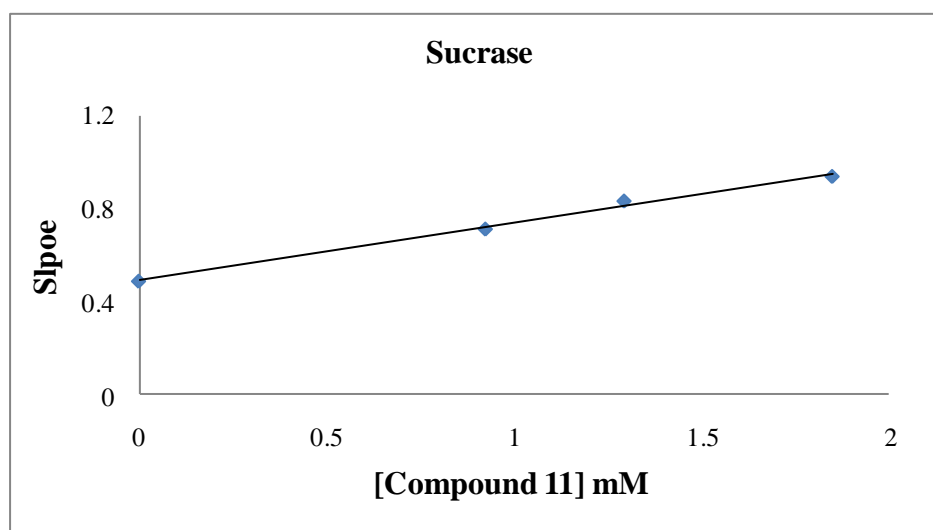


Figure 3.16 Dixon plot of slope vs. concentrations of compound **11** from a primary Lineweaver-Burk plot for the determination of K_i (strobopinin).

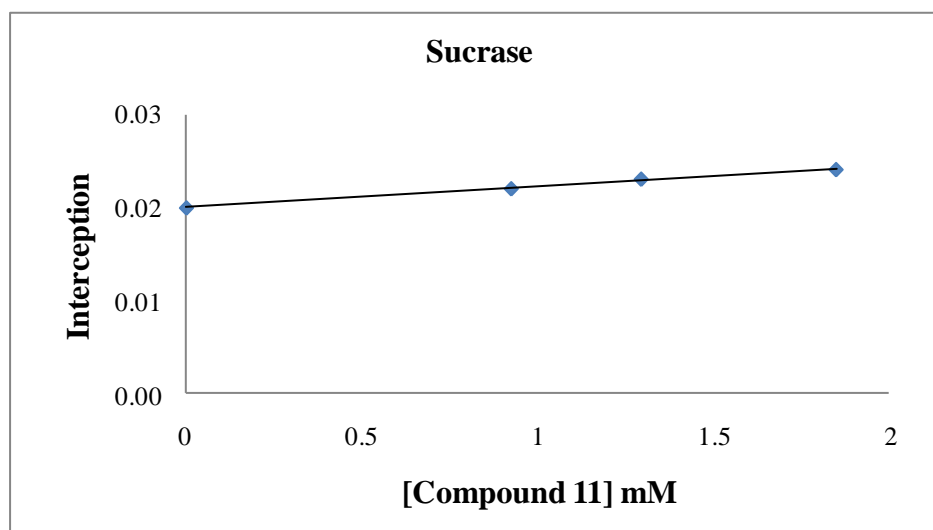


Figure 3.17 Secondary plot interception vs. concentrations of compound **11** from a primary Lineweaver-Burk plot for the determination of K_i' (strobopinin).

Table 3.4 The values from kinetic analyses of strobopinin (**11**)

dissociation constant (mM)	maltase	sucrase
K_i	1.84	1.95
K_i'	6.13	9.09

3.7 Experiment section

3.7.1 General experiment procedures

The ^1H and ^{13}C NMR spectra (in CDCl_3 , CD_3OD and acetone- d_6) were determined with a nuclear magnetic resonance spectrometer of Varian model Mercury+ 400. The chemical shift in δ (ppm) was assigned with reference to the signal from the residual protons in deuterated solvents and using TMS as an internal standard in some cases. Sephadex LH-20 and silica gel 60 Merck cat. No. 7734 and

7729 were used for open column chromatography. Thin layer chromatography (TLC) was performed on precoated Merck silica gel 60 F₂₅₄ plates (0.25 mm thick layer).

3.7.2 Plant material

The leaves of *Syzygium samarangense* (voucher's specimen number: BCU 013588) were collected in Nakhon Ratchasima, Thailand in October 2011. Plant authentication was performed by Miss Parinyanoot Klinratana, and the specimen has been deposited in Botanical Herbarium, Department of Botany, Faculty of Science, Chulalongkorn University.

3.7.3 Extraction and isolation

Dried leaves of *S. samarangense* (214g) were boiled in water at 80°C (2×2,000 mL) for 3 hours. The aqueous extract was partitioned with EtOAc to afford EtOAc extract. The EtOAc extract (11g) was subjected to quick column chromatography (QCC) using silica gel as adsorbent and eluted with dichloromethane (CH₂Cl₂), MeOH-CH₂Cl₂ (5:95, 15:85 and 30:70) and MeOH, respectively. The eluents were pooled into five major fractions (EJ065-1 to EJ065-5), based on TLC analysis. Fraction EJ065-1 was defatted with hexane at 60°C, yielding white crystal demethoxymatteucinol (**9**, 90 mg). The soluble part was isolated using flash column chromatography and eluted with 60:40 CH₂Cl₂-hexane to afford 2',4'-dihydroxy-6'-methoxy-3',5'-dimethylchalcone (**5**, 3.7 mg) and the residue fraction was separated through chromatotron with 5:95 EtOAc-hexane that offer three fractions (EJ070-1 to EJ070-3). Fraction EJ070-1 was purified by chromatotron with 10:90 EtOAc-hexane followed by sephadex LH-20 column with 5:4:1 CH₂Cl₂-hexane-MeOH to afford 5-hydroxy-7-methoxy-6-methyl flavanone (**6**, 2.5 mg). Fractions EJ070-2 and EJ070-3 were independently purified by sephadex LH-20 column with 5:4:1 CH₂Cl₂-hexane-MeOH to afford pinostrobin (**7**, 2.8 mg) and aurentiacin (**8**, 1.8 mg). The EJ065-2 fraction was isolated using sephadex LH-20 with 10:90 MeOH-CH₂Cl₂ to afford two fractions (EJ068-3 and EJ068-4). Fraction EJ068-3 was purified by chromatotron with 30:70 EtOAc-hexane followed by sephadex LH-20 column with 5:4:1 CH₂Cl₂-

hexane-MeOH to afford 7-hydroxy-5-methoxy-6, 8-dimethyl flavanone (**10**, 3.7 mg). Fraction EJ068-4 was purified by flash CC with 50:50 CH₂Cl₂-hexane, yielding strobopinin (**11**, 27 mg) and pinocembrin (**12**, 220 mg). Fraction EJ065-3 was purified by sephadex LH-20 column with 10:90 MeOH-CH₂Cl₂ and MeOH respectively to afford khempferal (**2**, 2 mg) and quercetin (**13**, 2.1 mg). Fraction EJ065-4 was purified by sephadex LH-20 column with 20:80 MeOH-CH₂Cl₂ and MeOH respectively to afford myricetin (**14**, 2 mg) and gallic acid (**15**, 4.2 mg). Fraction EJ065-5 was purified by sephadex LH-20 column with 30:70 MeOH-CH₂Cl₂ to afford myricitrin (**16**, 2 g).

2',4'-dihydroxy-6'-methoxy-3',5'-dimethylchalcone (5): orange solid; ¹H NMR (CDCl₃, 400 MHz) δ_H 13.55 (1H, s, 2'-OH), 7.93 (1H, d, *J* = 15.7 Hz, H-β), 7.77 (1H, d, *J* = 15.7 Hz, H-α), 7.58 (2H, m, Ph), 7.34 (3H, m, Ph), 5.31 (1H, s, 4'-OH), 3.59 (3H, s, 6'-OCH₃), 2.09 and 2.07 (each 3H, s, 3'-CH₃ and 5'-CH₃); ¹³C NMR (CDCl₃, 100 MHz) δ_C 193.4 (C=O), 162.1 (C-2'), 159.1 (C-4'), 158.9 (C-6'), 142.9 (C-β), 135.4 (C-1), 130.2 (C-4), 128.9 (C-3 and C-5), 128.4 (C-2 and C-6), 126.8 (C-α), 109.1 (C-5'), 108.8 (C-3'), 106.5 (C-1'), 62.3 (6'-OCH₃), 8.2 and 7.5 (3'-CH₃ and 5'-CH₃) (Amor, 2005).

5-Hydroxy-7-methoxy-6-methyl flavanone (6): yellowish gum; ¹H NMR (CDCl₃, 400 MHz) δ_H 12.06 (1H, s, 5-OH), 7.41-7.45 (5H, m, Ph), 6.09 (1H, s, H-8), 5.42 (1H, dd, *J* = 12.8, 3.7 Hz, H-2), 3.83 (3H, s, 7-OCH₃), 3.10 (1H, dd, *J* = 17.4, 12.9 Hz, H-3), 2.80 (1H, dd, *J* = 16.9, 3.0 Hz, H-3), 2.01 (3H, s, 6-CH₃); ¹³C NMR (CDCl₃, 100 MHz) δ_C 195.8 (C-4), 165.8 (C-7), 161.2 (C-5), 160.4 (C-9), 138.6 (C-1'), 128.9 (C-3' and C-5'), 128.8 (C-4'), 126.1 (C-2' and C-6'), 106.1 (C-6), 102.8 (C-10), 90.8 (C-8), 79.4 (C-2), 55.8 (7-OCH₃), 43.5 (C-3), 6.9 (6-CH₃) (Mustafa, 2003).

Pinostrobin (7): colorless solid; ¹H NMR (CDCl₃, 400 MHz) δ_H 12.03 (1H, s, 5-OH), 7.39-7.47 (5H, m, Ph), 6.08 (2H, d, *J* = 2.7 Hz, H-6 and H-8), 5.42 (1H, dd, *J* = 12.8, 2.8 Hz, H-2), 3.81 (3H, s, 7-OCH₃), 3.10 (1H, dd, *J* = 15.4, 12.8 Hz, H-3), 2.82 (1H, dd, *J* = 14.7, 2.8 Hz, H-3); ¹³C NMR (CDCl₃, 100 MHz) δ_C 195.6 (C-4), 168.1 (C-7), 164.2 (C-9), 162.8 (C-5), 138.5 (C-1'), 128.8 (C-4'), 126.1 (C-2', C-3',

C-5' and C-6'), 95.2 (C-6), 94.3 (C-8), 79.2 (C-2), 55.6 (7-OCH₃), 43.4 (C-3) (Sukari, 2007).

Aurentiacin (8): yellow solid; ¹H NMR (CDCl₃, 400 MHz) δ_H 14.06 (1H, s, 2'-OH), 7.89 (1H, d, *J* = 15.6 Hz, H-β), 7.78 (1H, d, *J* = 15.6 Hz, H-α), 7.62 (2H, m, Ph), 7.40 (3H, m, Ph), 6.01 (1H, s, H-5'), 3.96 (3H, s, 4'-OCH₃), 3.92 (3H, s, 6'-OCH₃), 2.05 (3H, s, 3'-CH₃); ¹³C NMR (CDCl₃, 100 MHz) δ_C 193.1 (C=O), 164.5 (C-2'), 163.5 (C-4'), 160.9 (C-6'), 141.9 (C-β), 135.5 (C-1), 129.9 (C-α), 128.9 (C-3 and C-5), 128.3 (C-2 and C-6), 128.0 (C-4), 111.7 (C-1'), 106.2 (C-3'), 86.4 (C-5'), 55.9 and 55.5 (4'-OCH₃ and 6'-OCH₃), 7.3 (3'-CH₃) (Mustafa, 2005 ; Adityachaudhury, 1976).

Demethoxymatteucinol (9): yellow crystal; ¹H NMR (CDCl₃, 400 MHz) δ_H 12.28 (1H, s, 5-OH), 7.37-7.48 (5H, m, Ph), 5.49 (1H, s, 7-OH), 5.40 (1H, dd, *J* = 12.8, 3.7 Hz, H-2), 3.06 (1H, dd, *J* = 17.4, 12.9 Hz, H-3), 2.85 (1H, dd, *J* = 16.9, 3.6 Hz, H-3), 2.07 and 2.08 (each 3H, s, 6-CH₃ and 8-CH₃) ; ¹³C NMR (CDCl₃, 100 MHz) δ_C 196.4 (C-4), 163.9 (C-7), 159.4 (C-5), 157.7 (C-9), 140.0 (C-1'), 128.8 (C-3' and C-5'), 128.6 (C-4'), 125.9 (C-2' and C-6'), 103.1 (C-6), 102.9 (C-8), 102.1 (C-10), 78.7 (C-2), 43.4 (C-3), 7.6 and 6.8 (CH₃-8 and CH₃-6) (Hufford, 1982).

7-hydroxy-5-methoxy-6,8-dimethyl flavanone (10): yellow crystal; ¹H NMR (CDCl₃, 400 MHz) δ_H 7.37-7.48 (5H, m, Ph), 5.45 (1H, dd, *J* = 13.0, 3.0 Hz, H-2), 3.81 (3H, s, 5-OCH₃), 2.96 (1H, dd, *J* = 16.5, 13.0 Hz, H-3), 2.83 (1H, dd, *J* = 16.5, 13.0 Hz, H-3), 2.14 and 2.13 (each 3H, s, 6-CH₃ and 8-CH₃) ; ¹³C NMR (CDCl₃, 100 MHz) δ_C 189.7 (C-4), 159.6 (C-7), 158.9 (C-9), 157.7 (C-5), 139.3 (C-1'), 128.7 (C-3' and C-5'), 128.4 (C-4'), 125.8 (C-2' and C-6'), 111.3 (C-6), 109.1 (C-10), 107.0 (C-8), 78.6 (C-2), 61.3 (C-OCH₃), 45.7 (C-3), 8.1 and 7.8 (CH₃-8 and CH₃-6) (Kou, 2004).

Strobopinin (11): yellow crystal; ¹H NMR (CDCl₃, 400 MHz) δ_H 12.18 (1H, s, 5-OH), 9.85 (1H, s, 7-OH), 7.31-7.39 (5H, m, Ph), 5.93 (1H, s, H-8), 5.30 (1H, dd, *J* = 12.8, 3.7 Hz, H-2), 2.98 (1H, dd, *J* = 17.4, 12.9 Hz, H-3), 2.70 (1H, dd, *J* = 16.9, 3.6 Hz, H-3), 1.94 (3H, s, 6-CH₃) ; ¹³C NMR (CDCl₃, 100 MHz) δ_C 195.9 (C-4), 164.3 (C-7), 161.5 (C-5), 160.6 (C-9), 138.6 (C-1'), 128.8 (C-3' and C-5'), 128.8 (C-4'), 126.2 (C-2' and C-6'), 104.8 (C-6), 102.1 (C-10), 94.6 (C-8), 79.1 (C-2), 43.4 (C-3), 6.7 (CH₃-6) (Solladić, 1999).

Pinocembrin (12): white crystal; ^1H NMR (CD_3OD , 400 MHz) δ_{H} 12.04 (1H, s, 5-OH), 7.32-7.47 (5H, m, Ph), 5.90 (2H, d, $J = 1.8$ Hz, H-6 and H-8), 5.41 (1H, dd, $J = 12.8, 3.6$ Hz, H-2), 3.05 (1H, dd, $J = 17.4, 12.8$ Hz, H-3), 2.74 (1H, dd, $J = 16.9, 3.6$ Hz, H-3) ; ^{13}C NMR (CD_3OD , 100 MHz) δ_{C} 197.3 (C-4), 168.4 (C-7), 165.5 (C-5), 164.7 (C-9), 140.4 (C-1'), 129.7 (C-3'andC-5'), 129.7 (C-4'), 127.4 (C-2'andC-6'), 103.4 (C-6), 97.2 (C-8), 96.3 (C-10), 80.5 (C-2), 44.2 (C-3) (Sukari, 2007).

Kaempforal (2): brown solid; ^1H NMR (CD_3OD , 400 MHz) δ_{H} 7.74 (2H, d, $J = 8.4$ Hz, H-2' and H-6'), 6.91(2H, d, $J = 8.4$ Hz, H-3' and H-5'), 6.42 (1H, d, $J = 2.5$ Hz, H-8), 6.21 (1H, d, $J = 2.5$ Hz, H-6). (Eldahshan, 2010).

Quercetin (13): brown solid; ^1H NMR (CD_3OD , 400 MHz) δ_{H} 7.76(1H, d, $J = 2.5$ Hz,H-2'), 7.54 (1H, dd, $J = 8.5$ and 2.5Hz, H-6'), 6.82 (1H, d, $J = 8.5$ Hz, H-5'), 6.82 (1H, d, $J = 2.0$ Hz, H-8), 6.20 (1H, d, $J = 2.0$ Hz, H-6)(Eldahshan, 2010).

Myricetin (14): brown solid; ^1H NMR (CD_3OD , 400 MHz) δ_{H} 6.95 (2H, s. H-2' and H-6'), 6.34 (1H, d, $J = 2.1$ Hz, H-8), 6.18 (1H, d, $J = 2.1$ Hz, H-6). (Shen, 2009).

Gallicacid (15): light brown solid; ^1H NMR (CD_3OD , 400 MHz) δ_{H} 6.91 (1H, s, H-2, and H-6) ; ^{13}C NMR (CD_3OD , 100 MHz) δ_{C} 121.0 (C-1), 109.0 (C-2 and C-6), 145.9 (C-3 and C-5), 138.3 (C-4), 168.0 (C-7) (Eldahshan, 2010).

Myricitrin (16): brown solid; ^1H NMR (CD_3OD , 400 MHz) δ_{H} 6.95 (2H, s. H-2' and H-6'), 6.34 (1H, d, $J = 2.1$ Hz, H-8), 6.18 (1H, d, $J = 2.1$ Hz, H-6), 5.30 (1H, dd, $J = 1.5$ Hz, H-1'), 4.22 (1H, dd, $J = 3.3, 1.5$ Hz, H-2'), 3.79 (1H, dd, $J = 9.5, 3.3$ Hz, H-3'), 3.52 (1H, dd, $J = 9.5, 6.2$ Hz, H-5'), 3.33 (1H, dd, $J = 9.5$ Hz, H-4'), 0.96 (3H, d, $J = 6.2$ Hz, H-6') ; ^{13}C NMR (CD_3OD , 100 MHz) δ_{C} 179.6 (C-4), 165.9 (C-7), 163.1 (C-5), 159.4 (C-2), 158.4 (C-9), 146.8 (C-3'andC-5'), 137.8 (C-4'), 136.3 (C-3), 121.8 (C-1'), 109.2 (C-2'andC-6'), 105.8 (C-10), 103.6 (C-1''), 99.8 (C-6), 94.7 (C-8), 73.3 (C-4''), 72.0 (C-3''), 72.0 (C-5''), 71.8 (C-2''), 17.6 (C-6'') (Shimizu, 2006).

3.7.4 α -Glucosidase inhibitory assay

α -Glucosidase inhibitory assay was performed the same as previously described in Chapter II.

3.7.5 Measurement of kinetic constant

Kinetic analysis of maltase and sucrase were determined using the methods described by Adisakwattana *et al.*, Kandra *et al.* and Lineweaver-Burk *et al.*, with slight modification. Briefly, the active compounds and enzyme were incubated with increasing concentration of maltose and sucrose (2-20 mM). A Lineweaver-Burk plot of substrate concentration ($1/[\text{substrate}]$) on horizontal axis and velocity ($1/V$) on vertical axis was constructed. K_m or substrate constant, which is dissociation constant for the ES and V_{\max} were calculated using the following expression.

Which is;

$$V_{\max} = 1/C \quad \text{where; } C = Y \text{ intercept}$$

$$K_M = \text{slope} \times V_{\max}$$

For calculation of K_i and K_i' values, slopes and interception from a Lineweaver-Burk plot were plotted vs. [active compound] which gave the secondary plot. The general equation for the kinetic analysis is

$$V_0 = \frac{V_{\max} [S]}{K_m(1 + \frac{1}{K_i} [I]) + [S](1 + \frac{1}{K_i'} [I])}$$

Where V_0 is the initial velocity of the inhibitor, V_{\max} is the limiting velocity. [substrate] and [active compound] are the final concentration of substrate and inhibitor, respectively. K_i and K_i' are the dissociation constants of EI and ESI, respectively.

Supporting information

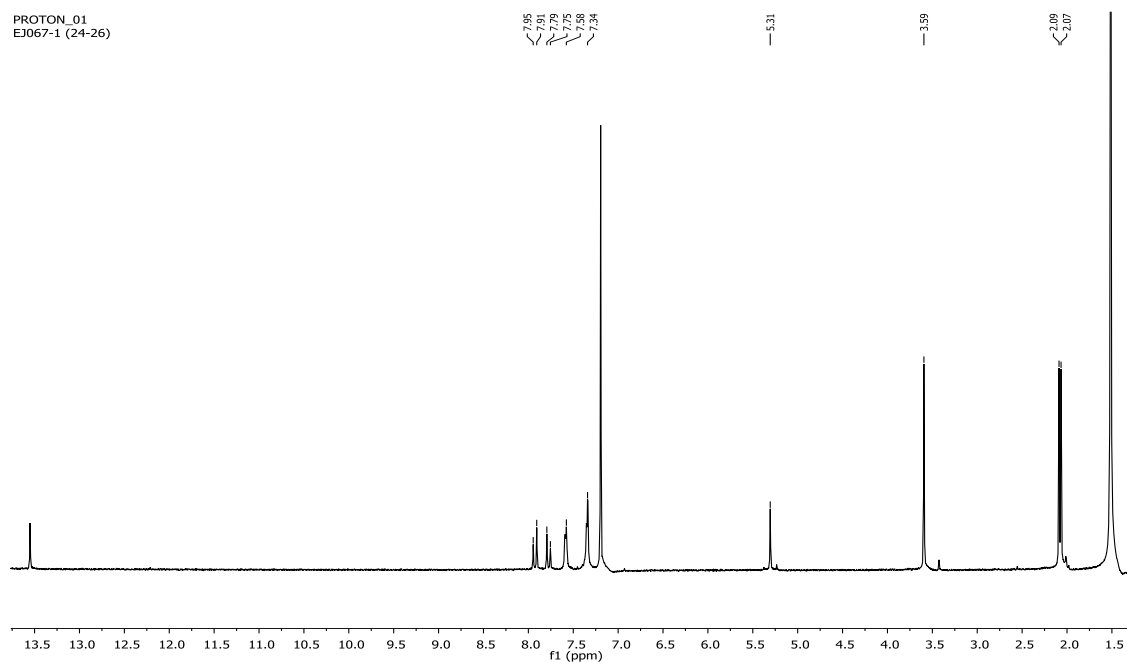


Figure S-3.1 The ^1H NMR (CDCl_3) spectrum of 2', 4'-dihydroxy-6'-methoxy-3', 5'-dimethylchalcone (**5**)

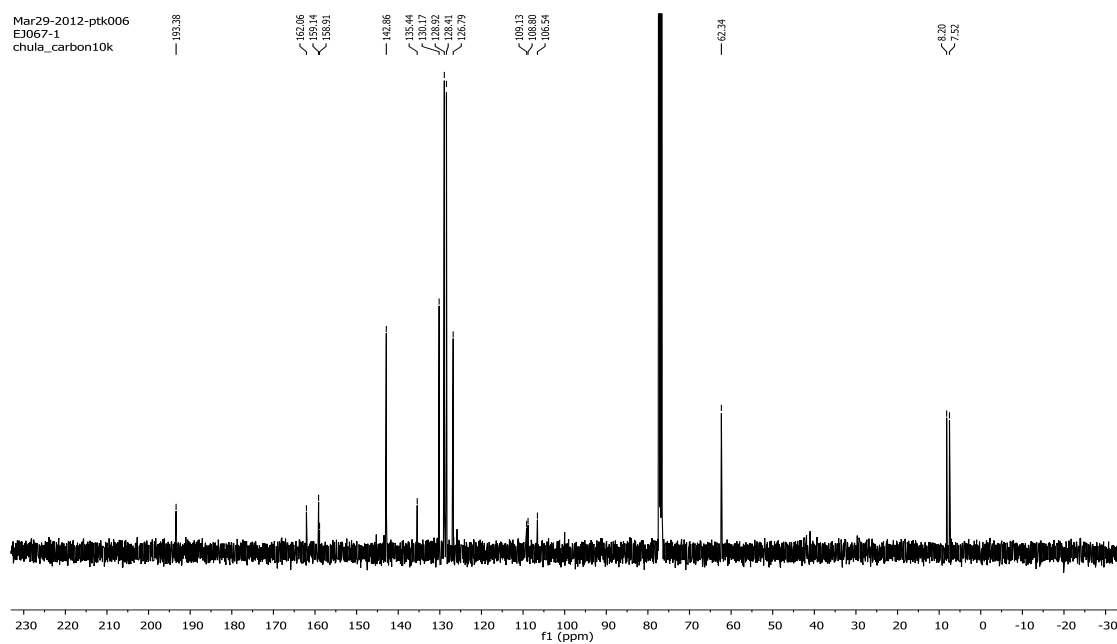


Figure S-3.2 The ^{13}C NMR (CDCl_3) spectrum of 2', 4'-dihydroxy-6'-methoxy-3', 5'-dimethylchalcone (**5**)

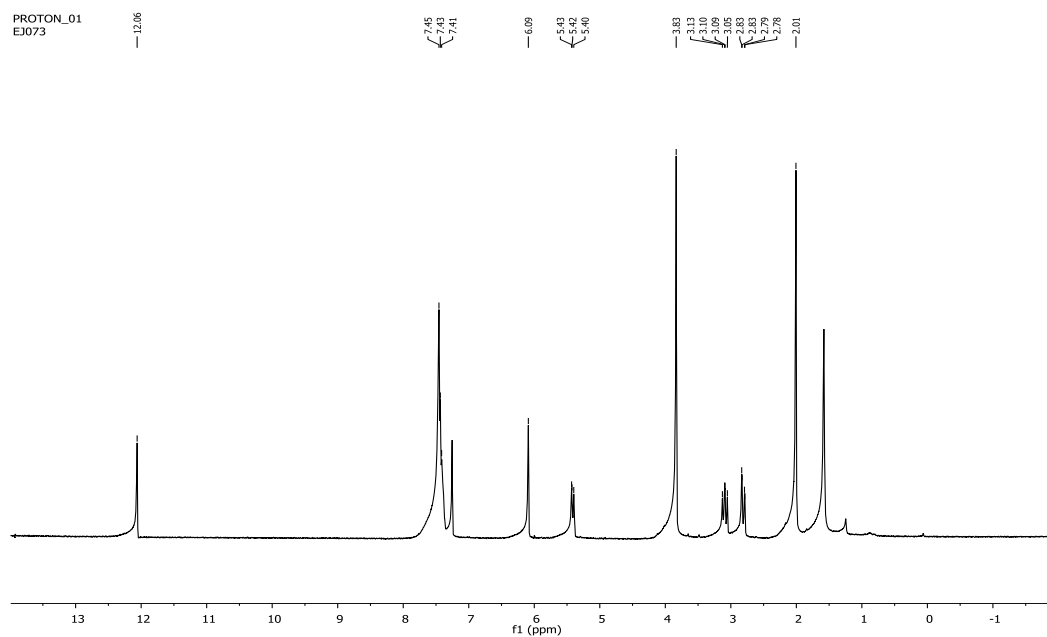


Figure S-3.3 The ^1H NMR (CDCl_3) spectrum of 5-hydroxy-7-methoxy-6-methyl flavanone (**6**)

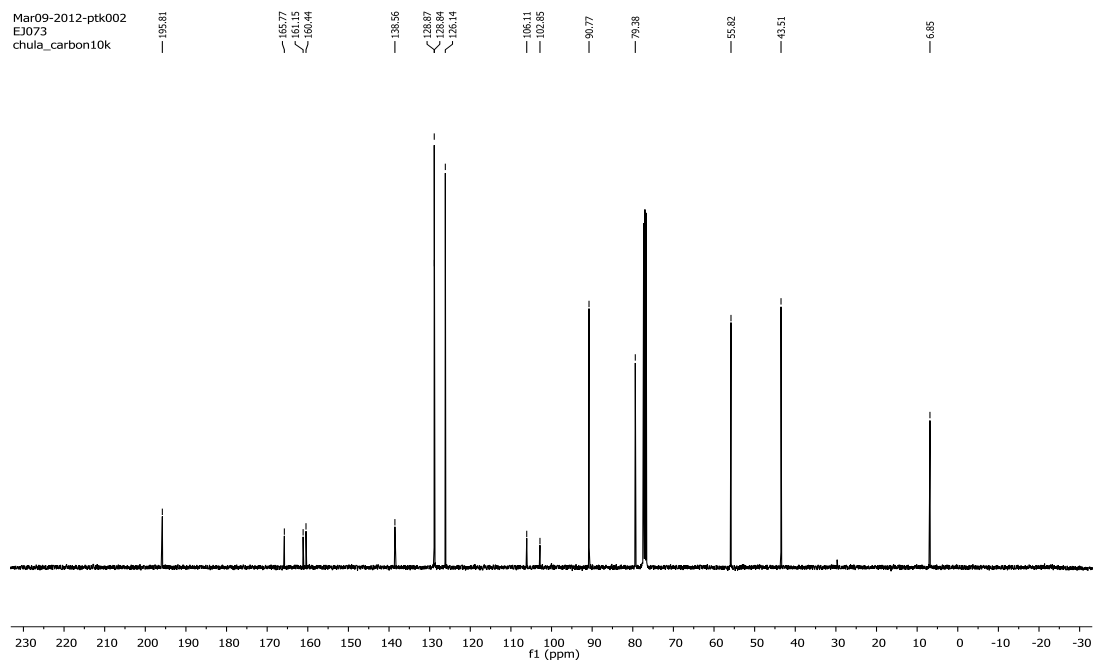


Figure S-3.4 The ^{13}C NMR (CDCl_3) spectrum of 5-hydroxy-7-methoxy-6-methyl flavanone (**6**)

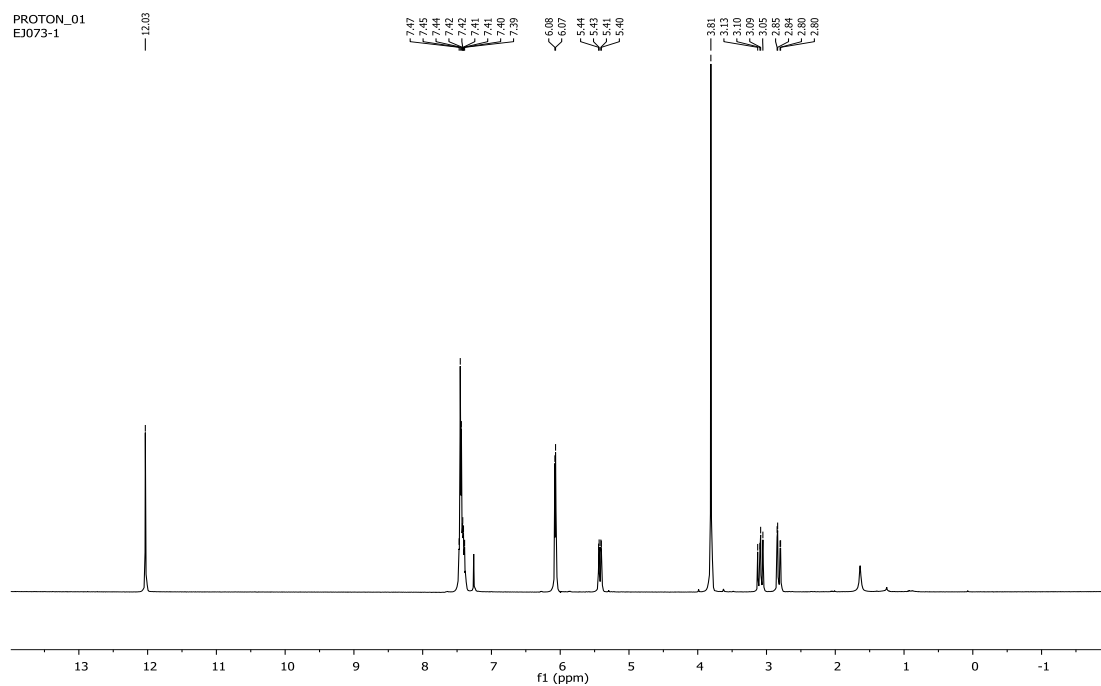


Figure S-3.5 The ^1H NMR (CDCl_3) spectrum of pinostrobin (**7**)

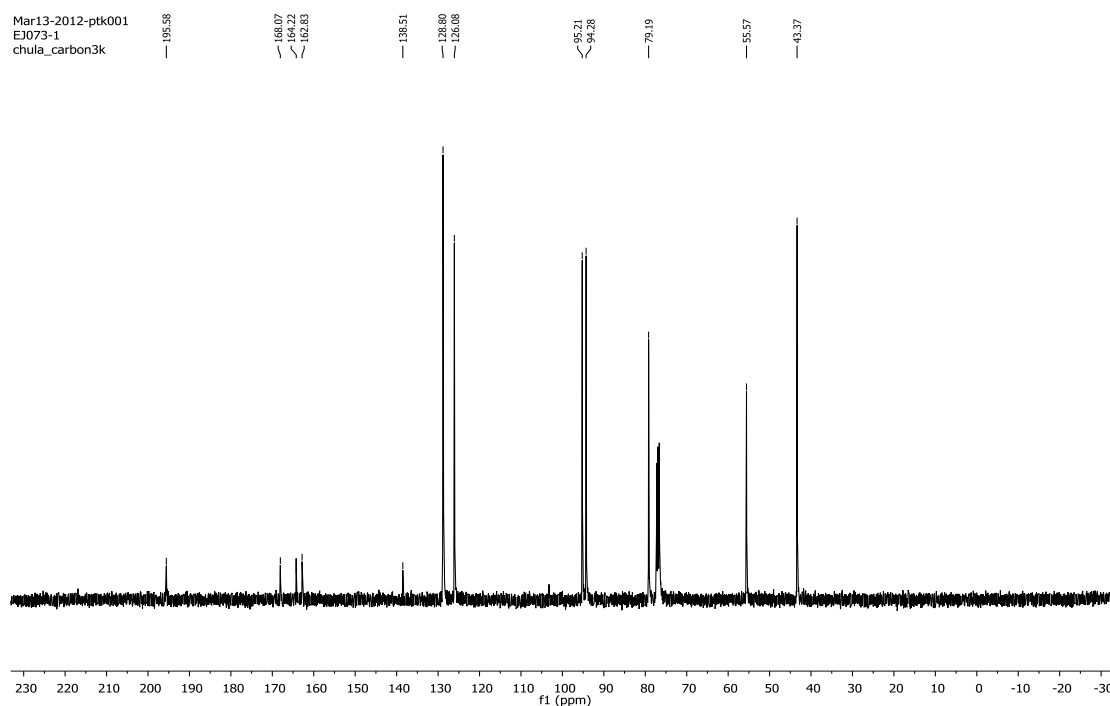


Figure S-3.6 The ^{13}C NMR (CDCl_3) spectrum of pinostrobin (**7**)

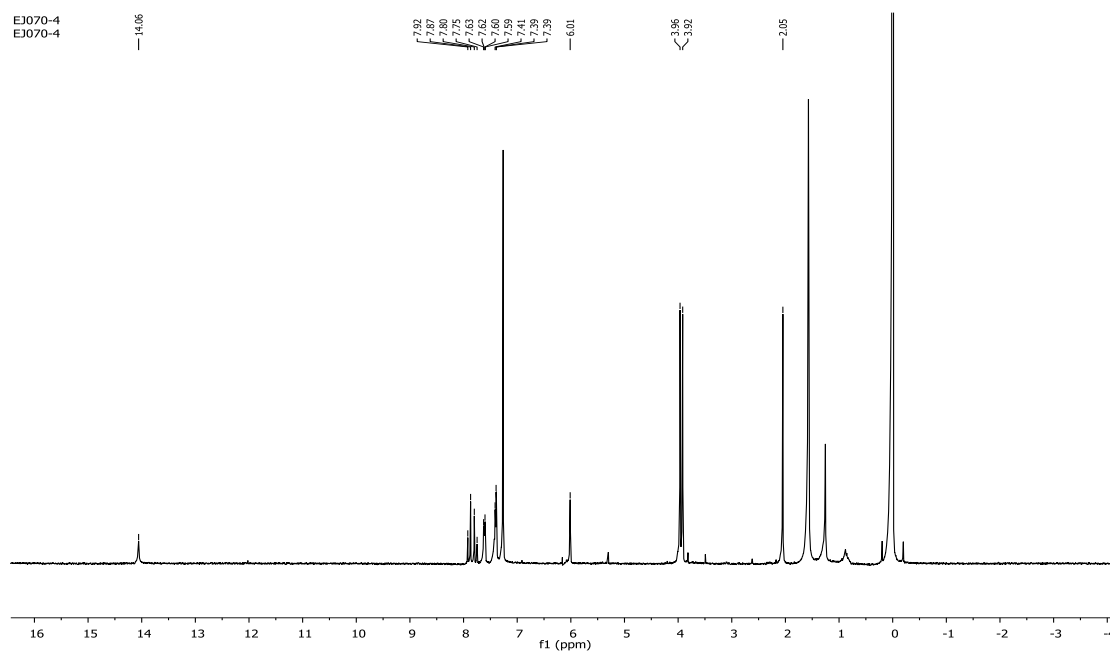


Figure S-3.7 The ^1H NMR (CDCl_3) spectrum of aurentiacin (**8**)

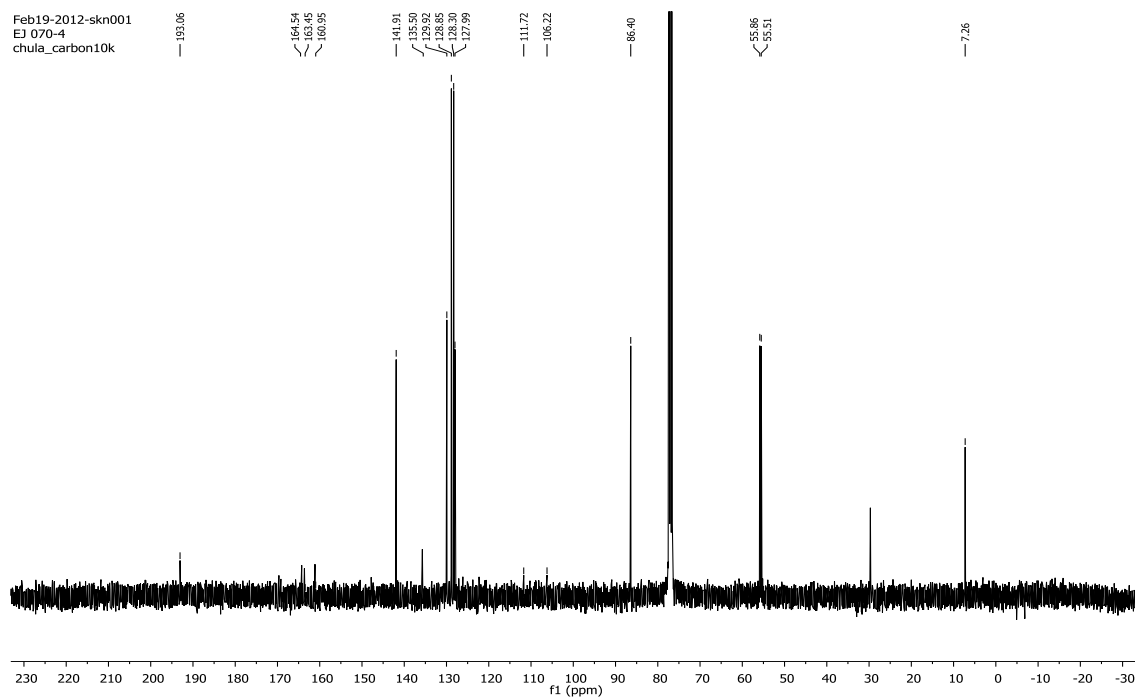


Figure S-3.8 The ^{13}C NMR (CDCl_3) spectrum of aurentiacin (**8**)

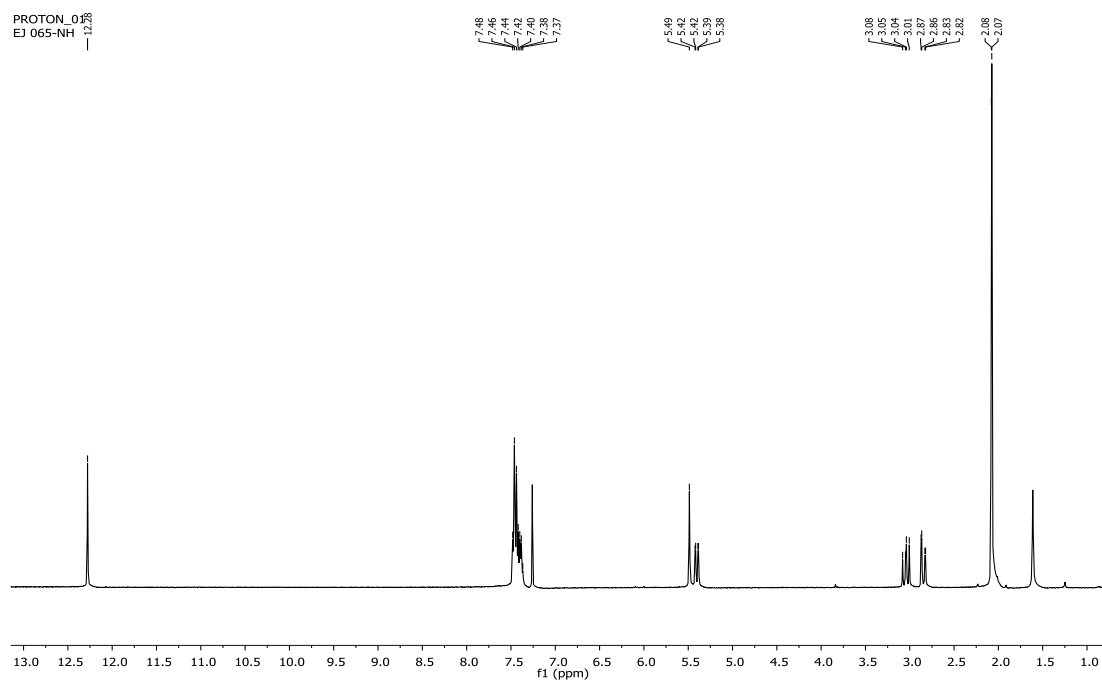


Figure S-3.9 The ^1H NMR (CDCl_3) spectrum of demethoxymatteucinol (**9**)

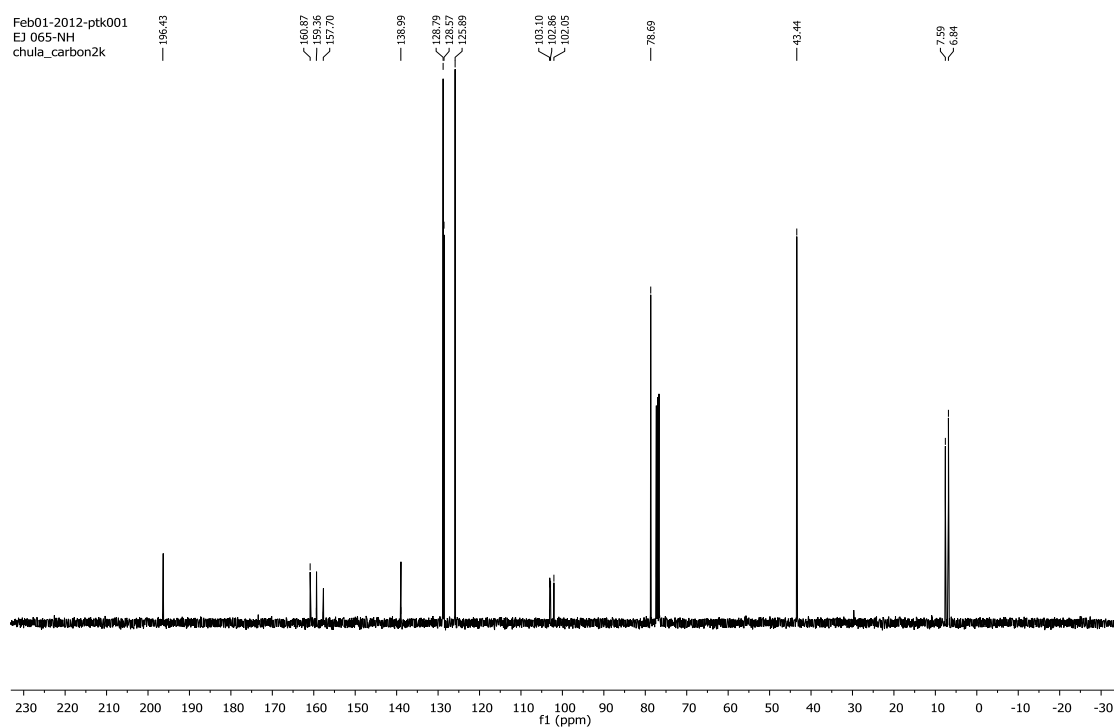


Figure S-3.10 The ^{13}C NMR (CDCl_3) spectrum of demethoxymatteucinol (**9**)

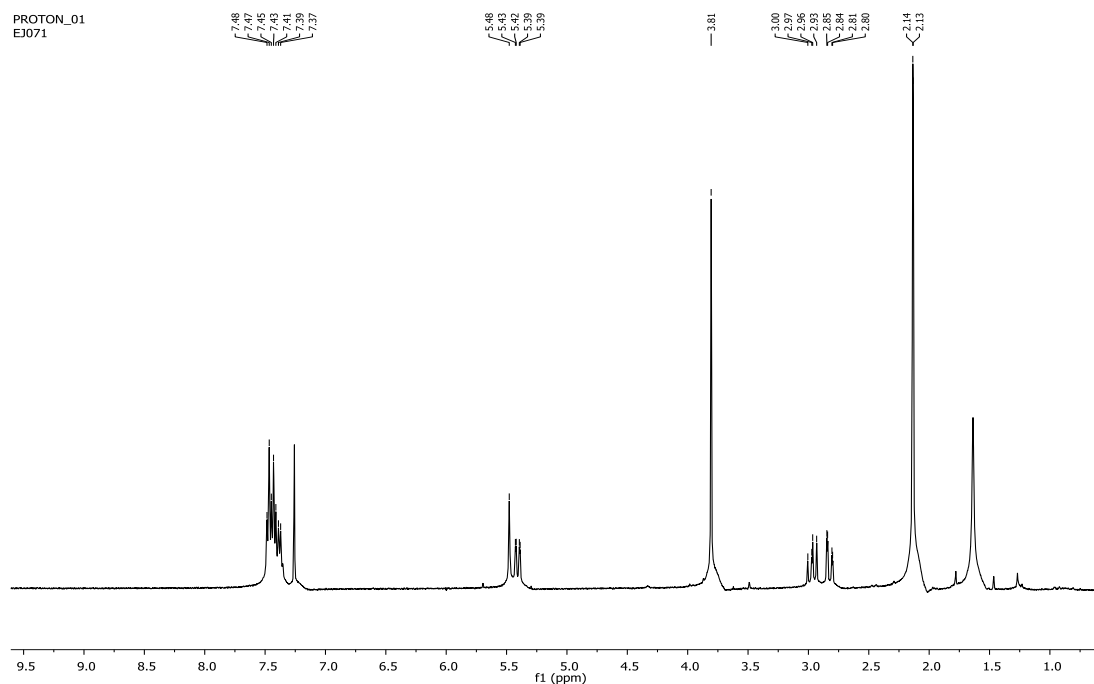


Figure S-3.11 The ^1H NMR (CDCl_3) spectrum of 7-hydroxy-5-methoxy-6, 8-dimethyl flavanone (**10**)

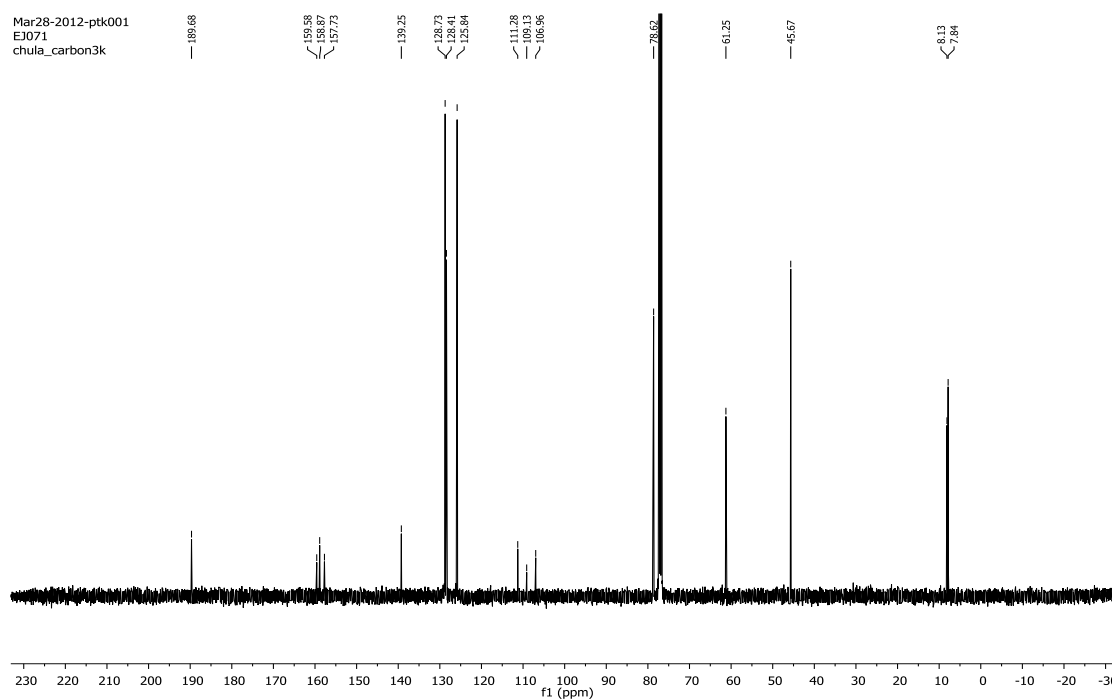


Figure S-3.12 The ^{13}C NMR (CDCl_3) spectrum of 7-hydroxy-5-methoxy-6, 8-dimethyl flavanone (**10**)

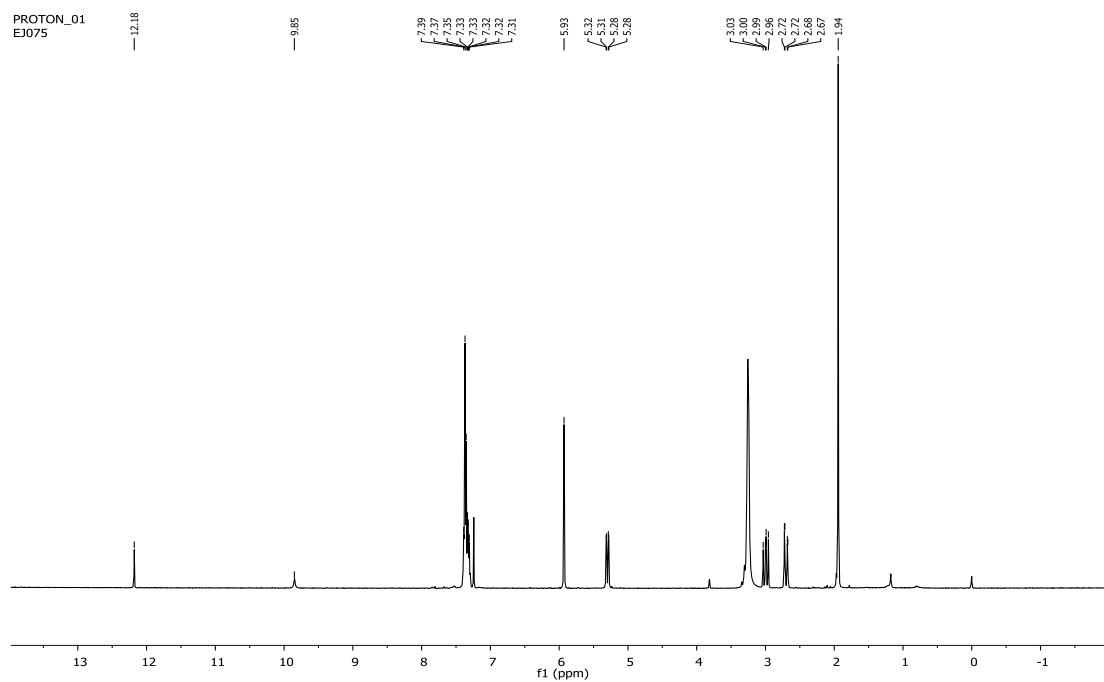


Figure S-3.13 The ^1H NMR (CDCl_3) spectrum of strobopinin (**11**)

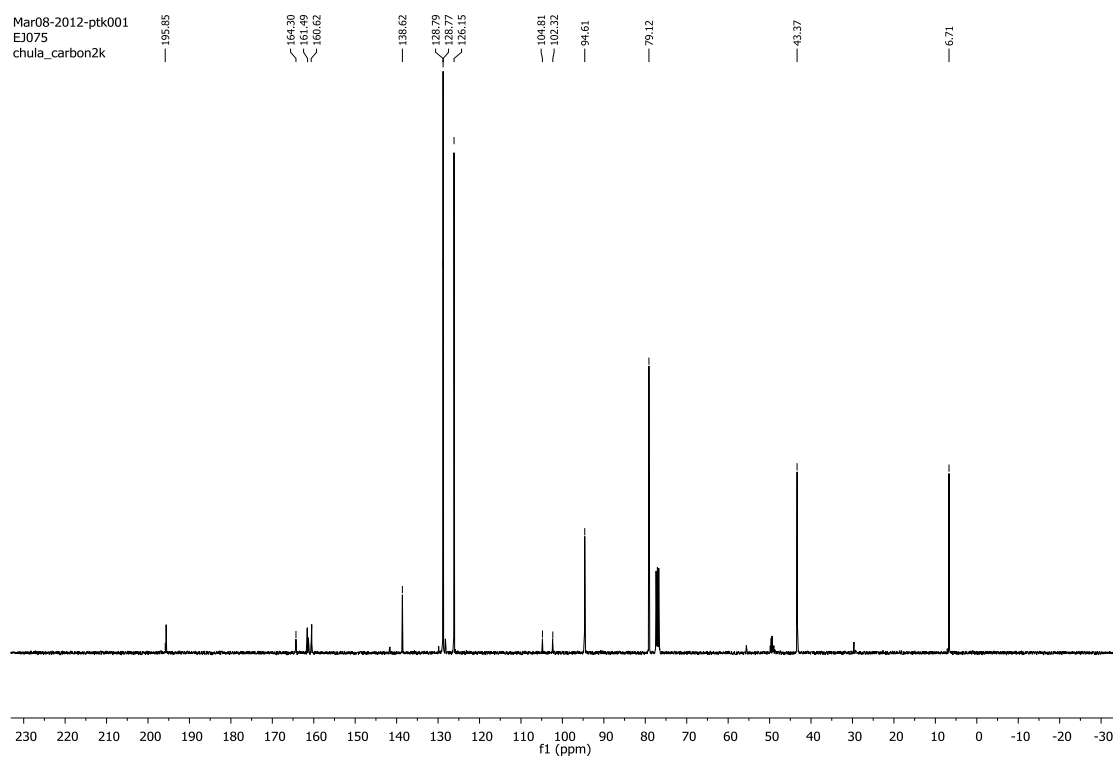


Figure S-3.14 The ^{13}C NMR (CDCl_3) spectrum of strobopinin (**11**)

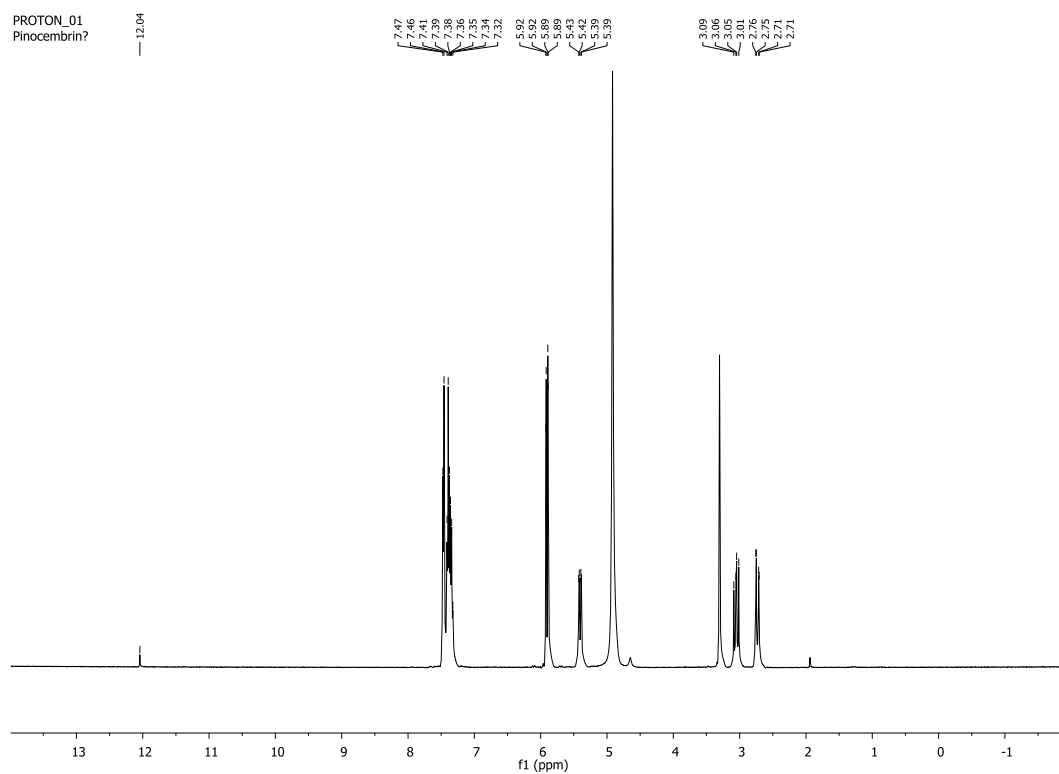


Figure S-3.15 The ^1H NMR (CD_3OD) spectrum of pinocembrin (**12**)

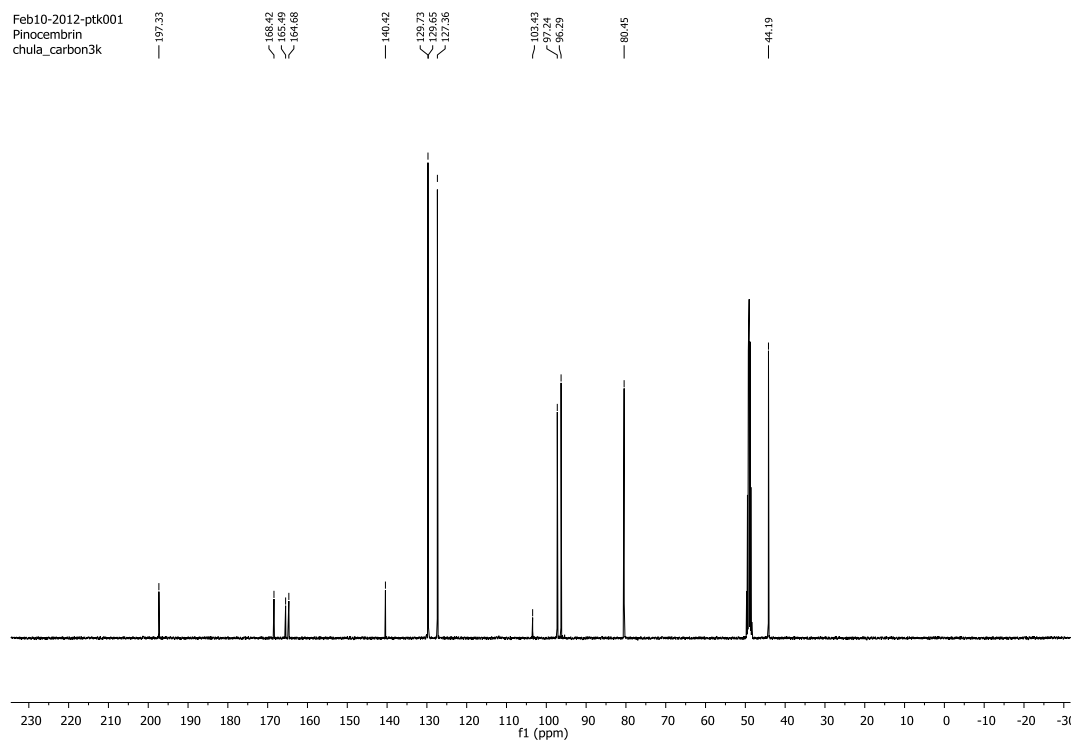


Figure S-3.16 The ^{13}C NMR (CD_3OD) spectrum of pinocembrin (**12**)

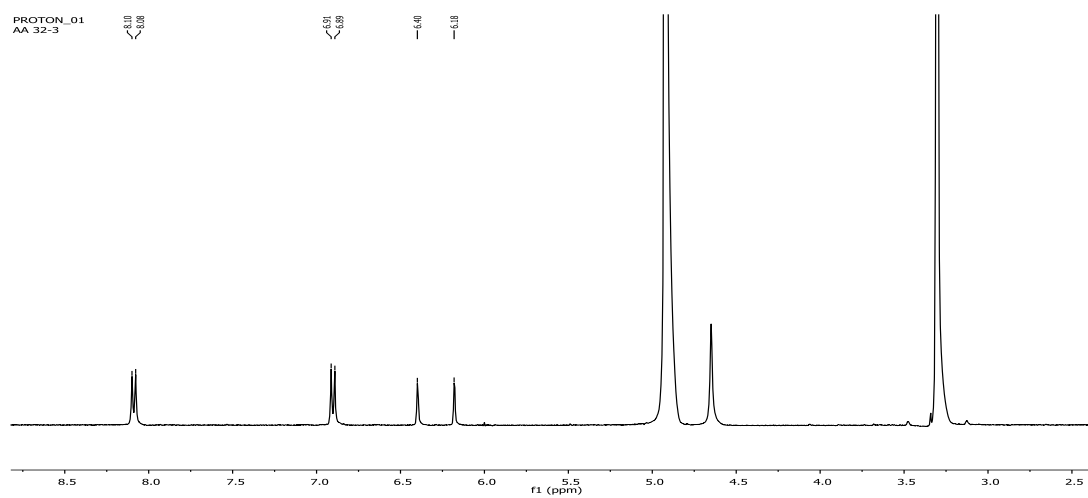


Figure S-3.17 The ¹H NMR (CD₃OD) spectrum of kaempferol (**2**)

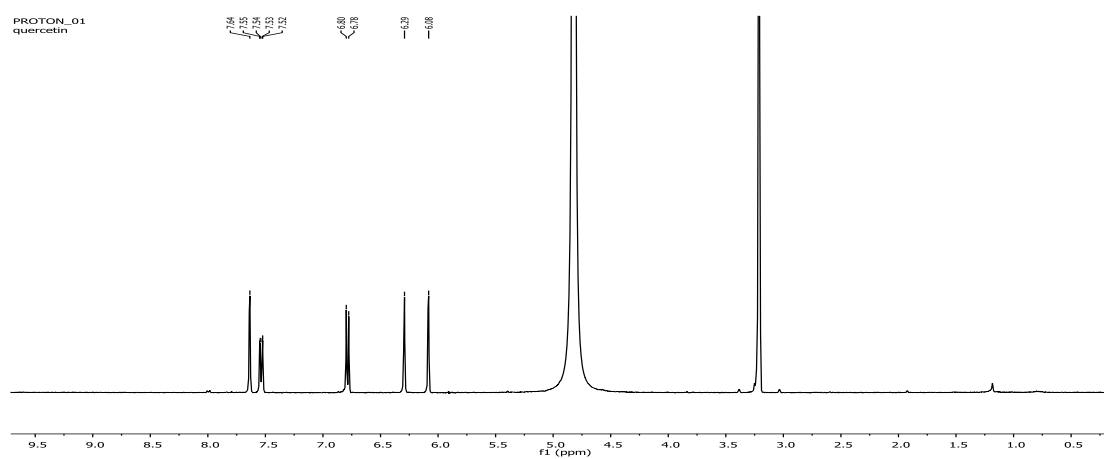


Figure S-3.18 The ¹H NMR (CD₃OD) spectrum of quercetin (**13**)

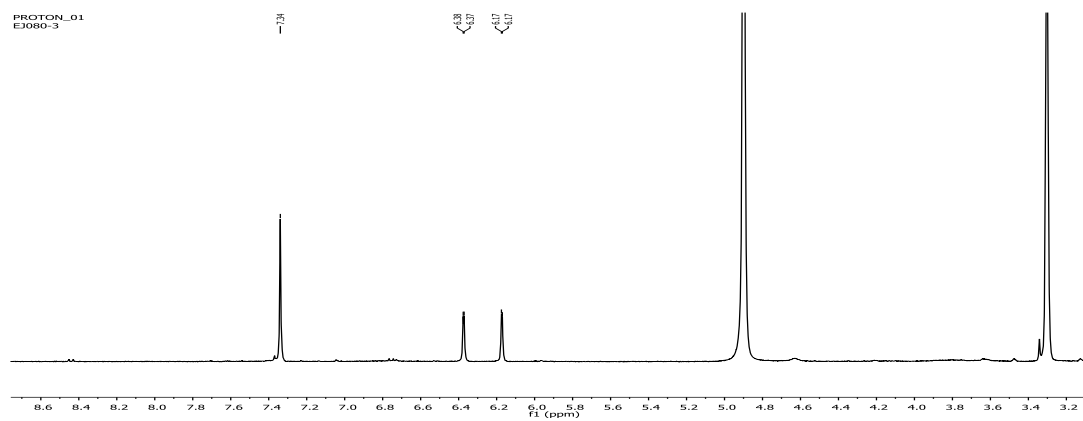


Figure S-3.19 The ¹H NMR (CD₃OD) spectrum of myricetin (**14**)

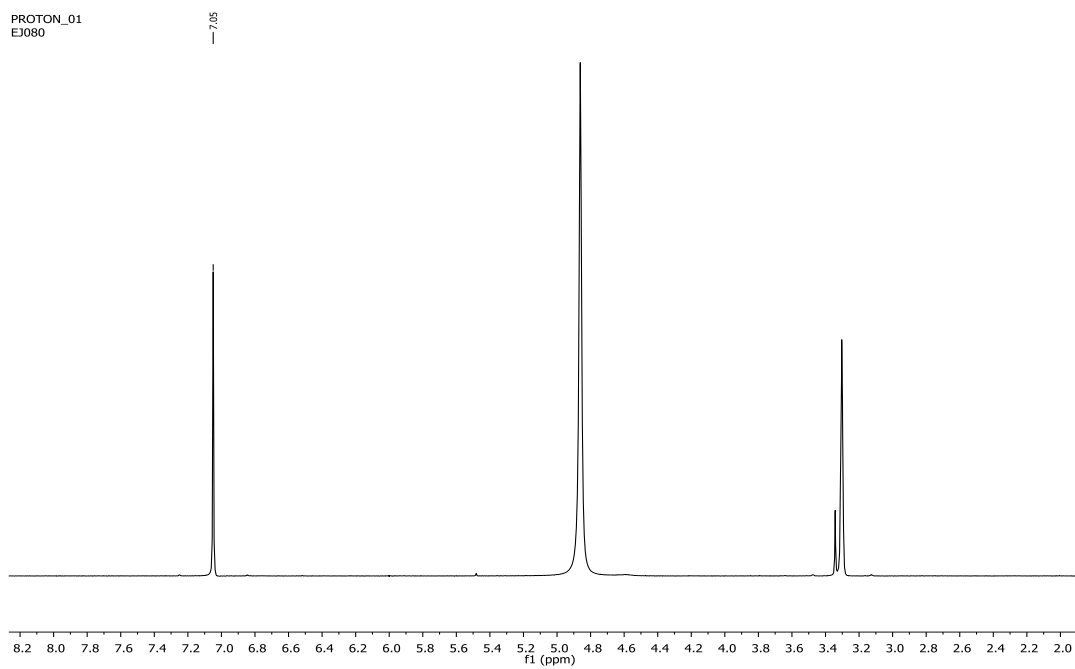


Figure S-3.20 The ^1H NMR (CD_3OD) spectrum of gallic acid (**15**)

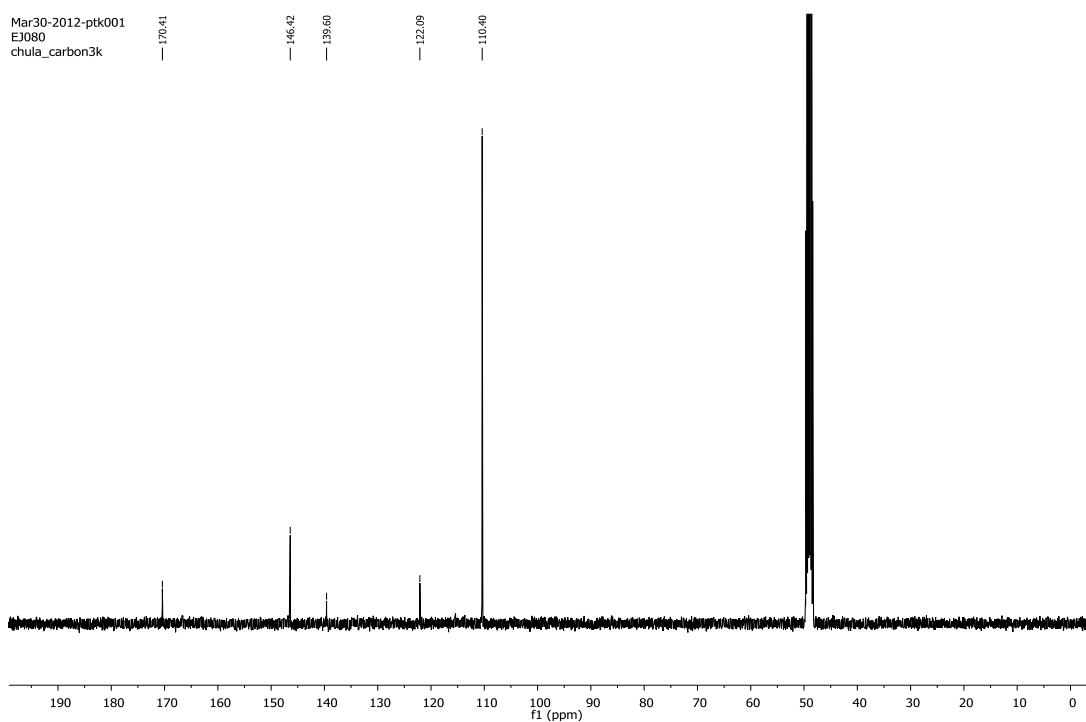


Figure S-3.21 The ^{13}C NMR (CD_3OD) spectrum of gallic acid (**15**)

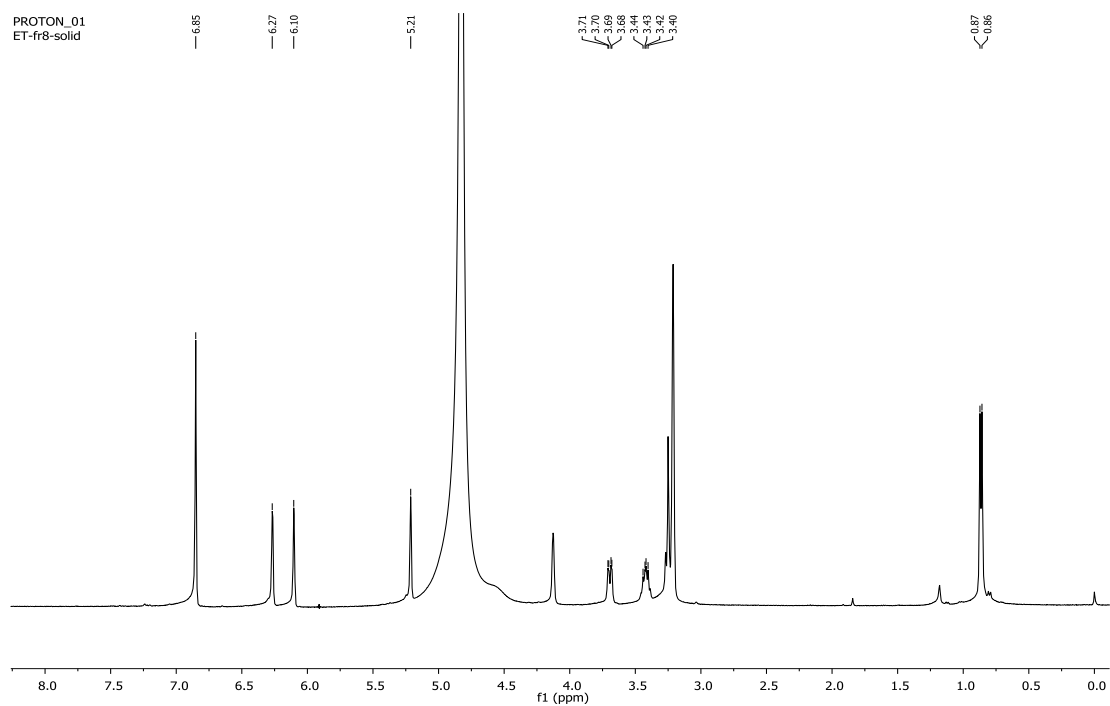


Figure S-3.22 The ^1H NMR (CD_3OD) spectrum of myricitrin (**16**)

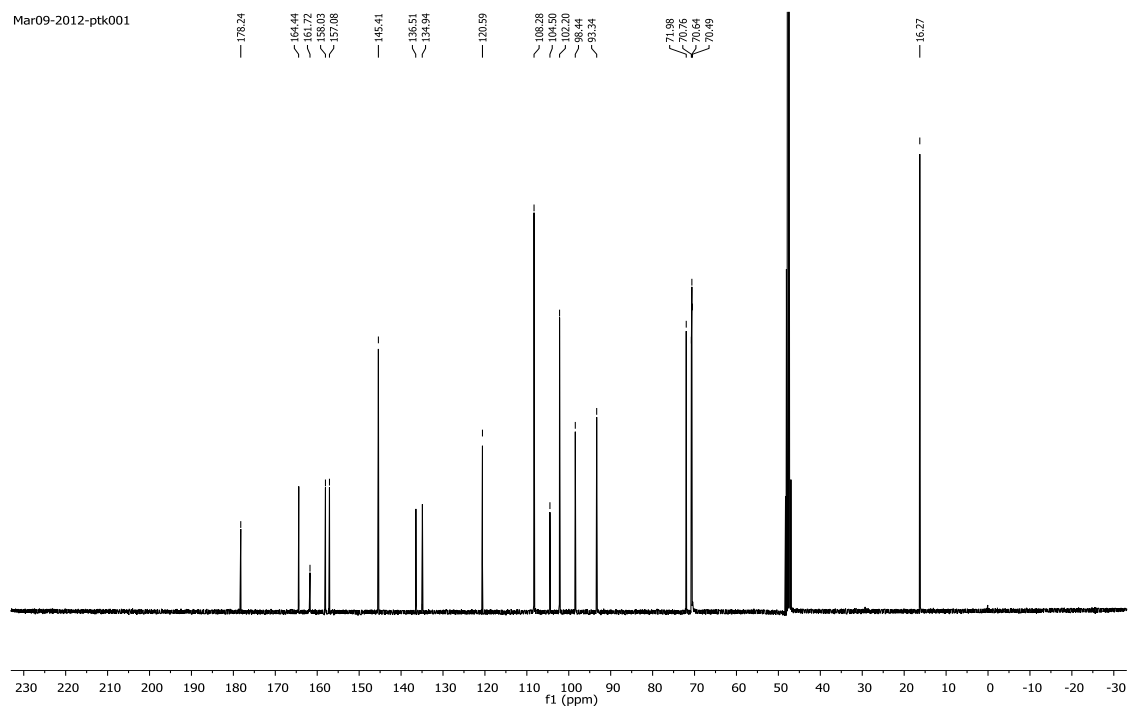
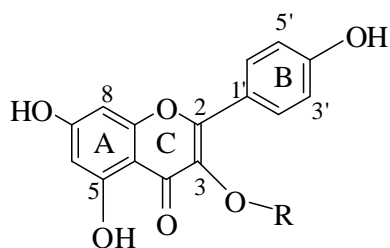


Figure S-3.23 The ^{13}C NMR (CD_3OD) spectrum of myricitrin (**16**)

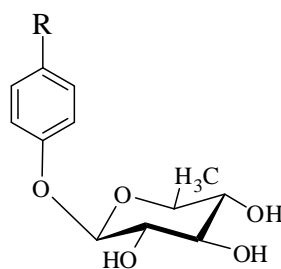
CHAPTER IV

CONCLUSION

The α -glucosidase inhibitors from *Moringa oleifera* and *Syzygium samarangense* leaves were identified. Two 1, 4-disubstituted aromatic named *p*-hydroxybenzaldehyde-*O*- α -L-rhamnopyranoside (**1**) and 1-*O*-(4-hydroxymethylphenyl)- α -L-rhamnopyranoside (**4**) together with two flavanoids named keampferal (**2**) and kaempferol-3-*O*- β -glucopyranoside (**3**) were isolated from methanol extract of *M.oleifera* leaves. 1, 4-disubstituted aromatic rhamnoside exhibited inhibitory effect against α -glucosidase less than 50% inhibition whereas two flavonoids showed inhibitory activity against α -glucosidases from baker's yeast and rat intestine that displayed IC₅₀ value. On the other hand, four flavonols named kaempferol (**2**), quercetin (**13**), myricetin (**14**) and myricitrin (**16**); six flavanones named 5-hydroxy-7-methoxy-6-methyl flavanone (**7**), pinostrobin (**8**), demethoxymatteucinol (**9**), 7-hydroxy-5-methoxy-6 (**10**), 8-dimethyl flavanone, strobopinin (**11**) and pinocembrin (**12**); two chalcones named 2', 4'-dihydroxy-6'-methoxy-3', 5'-dimethylchalcone (**5**) and aurentiacin (**8**) along with gallic acid were isolated from ethyl acetate extract of *S. samarangense*. Almost flavonoids and gallic acid broadly inhibited α -glucosidases from baker's yeast and rat intestine whereas flavanones having methoxy group on aromatic inhibitory ring A selectively inhibited α -glucosidase from baker's yeast. In addition, inhibitory mechanisms of 2', 4'-dihydroxy-6'-methoxy-3', 5'-dimethylchalcone (**5**) and strobopinin (**11**) were studied. The kinetic study indicated that both compounds possess mix-type inhibition, in which competitive inhibition was dominant.



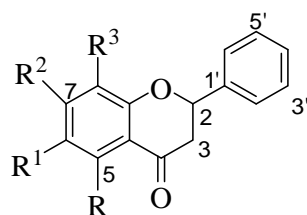
keampferol (**2**); R = H
 keampferol-3-*O*- β -glucopyranoside (**3**); R = Rhamnose



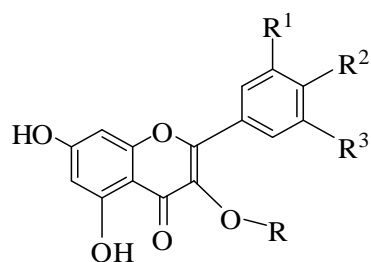
p-hydroxybenzaldehyde-*O*- α -L-rhamnopyranoside (**1**); R = $\text{HC}=\text{O}$

1-*O*-(4-hydroxymethylphenyl)-4- α -L-rhamnopyranoside (**4**); R = CH_2OH

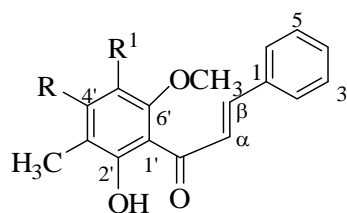
Figure 4.1 The structure of isolated compounds from *M. oleifera*



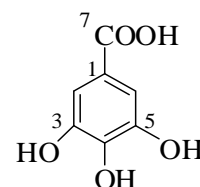
	R	R ¹	R ²	R ³
5-hydroxy-7-methoxy-6-methyl flavanone (6)	OH	CH ₃	OCH ₃	H
pinostrobin (7)	OH	H	OCH ₃	H
demethoxymatteucinol (9)	OH	CH ₃	OH	CH ₃
7-hydroxy-5-methoxy-6, 8-dimethyl flavanone (10)	OCH ₃	CH ₃	OH	CH ₃
strobopinin (11)	OH	CH ₃	OH	H
pinocembrin (12)	OH	H	OH	H



	R	R ¹	R ²	R ³
kaempferol (2)	H	H	OH	H
quercetin (13)	H	OH	OH	H
myricetin (14)	H	OH	OH	OH
myricitrin (16)	Rhamnose	OH	OH	OH



2', 4'-dihydroxy-6'-methoxy-3', 5'-dimethylchalcone (**5**);
 R = OH, R¹ = CH₃
 aurentiacin (**8**); R = OCH₃, R¹ = H



gallic acid (**15**)

Figure 4.2 The structure of isolated compounds from *S. samarangense*

REFERENCES

- Adisakwattana, S., Charoenlertkul, P., and Yibchok-Anun, S. α -Glucosidase inhibitory activity of cyaniding-3-galactoside and synergistic effect with acarbose. Journal of Enzyme Inhibition and Medicinal Chemistry. 24 (2009): 65-69.
- Adityachaudhury, N., Das, A.K., Choudhury, A., and Daskanungo, P.L. Aurentiacin, a new chalcone from Didymocarpus Aurentiaca. Phytochemistry. 15 (1976): 229-230.
- Anwar, F., Latife, S., Ashraf, M., and Gilani, A. H. *Moringa oleifera*: a food plant with multiple medicinal uses. Phytotherapy Research. 21 (2007): 17-25.
- Amor, E.C., Villaseñor, I.M., Nawaz, S.A., Hussain, M.S., and Choudhary, M.I.A dihydrochalcone from *Syzygium samarangense* with anticholinesterase activity. Philippine Journal of Science. 134 (2005): 105-111.
- Bhatnagar, S.S., Santapau, H., Desai, J.D.H., Yellore, S., and Rao, T.N.S. Biological activity of Indian medicinal plants. Part 1. Antibacterial, antitubercular and antifungal action. Indian Journal of Medical Research. 49 (1961): 799-805.
- Bhattacharya, S.B., Das, A.K., and Banerji, N. Chemical investigations on the gum exudates from Sonja (*Moringa oleifera*). Carbohydrate Research. 102 (1982): 253-262.
- Bhattarai, N.K. Folk medicinal use of plants for respiratory complaints in central Nepal. Fitoterapia. 64 (1993): 163-169.
- Chattopadhyay, E.D., Sinha, B.K., and Vaid, L.K. Antibacterial activity of *Syzygium species*. Fitoterapia. 119 (1998): 365-367.
- Chen, H., Feng, R., Guo, Y., Sun, L., and Jiang, J. Hypoglycemic effect of aqueous extracts of *Rhizoma polygonati odorati* in mice and rats. Journal of Ethnopharmacology. 74 (2001): 225-229.
- Dahot, M.U. Vitamin contents of flowers and seeds of *Moringa oleifera*. Pakistan Journal of Biochemistry. 21 (1988): 1-24.
- Dolly, J., Prashant, K.R., Amit, K., Shikha, M., and Geeta, W. Effect of *Moringa oleifera* Lam. leaves aqueous extract therapy on hyperglycemic rats. Journal of Ethnopharmacology. 123 (2009): 392-396.

- Eduardo, B.D.M., Adriane, D.S.G., and Ivone, C. α - and β -Glucosidase inhibitors: chemical structure and biological activity. Tetrahedron. 62 (2006): 10277-10302.
- Eldahshan, O.A. Isolation and structure elucidation of phenolic compounds of Carob leaves grown in Egypt. Current Research Journal of Biological Sciences. 3 (2011): 52-55.
- Escandón-Rivera, S., González-Andrade, M., Bye, R., Linares, E., Navarrete, A., and Mata, R. α -Glucosidase inhibitors from *Brickellia cavanillesii*. Journal of Natural Products. 75 (2012): 968-974.
- Faizi, S., Siddiqui, B.S., Saleem, R., Aftab, K., Shaheen, F., and Gilani, A. H. Hypotensive constituents from the pods of *Moringa oleifera*. Planta Medica. 64 (1998): 225-228.
- Gershell, L. Type 2 diabetes market. Nature Reviews Drug Discovery. 4 (2005): 367-368.
- Ghayur, M.N., and *et al.* Presence of calcium antagonist activity explains the use of *Syzygium samarangense* in diarrhoea. Phytotherapy Research, 20 (2006): 49–52.
- Grond, S., Papastavrou, I., and Zeeck, A. Novel α -L-Rhamnopyranosides from a Single Strain of *Streptomyces* by Supplement-Induced Biosynthetic Steps. Journal of Organic Chemistry. 1 (2002): 3237-3242.
- Grover, J.K., Yadav, S., and Vats, V. Medicinal plants of India with antidiabetic potential. Journal of Ethnopharmacology. 81 (2002): 81-100.
- Guk Hwang, I., and *et al.* Isolation and characterisation of an α -glucosidase inhibitory substance from fructose–tyrosine Maillard reaction products. Food Chemistry. 127 (2011): 122-126.
- Heng, X. Inhibition kinetics of flavonoids on yeast α -glucosidase merged with docking simulations. Protein and Peptide Letters. 17 (2010): 1270-1279.
- Hung, H.Y., Qian, K.Q., Morris-Natschke, S.L., Hsu, C.S., and Lee, K.H. Recent discovery of plant-derived anti-diabetic natural products. Natural Product Reports. 29 (2012): 580-606.
- Han, A.R., Kang, Y.J., Windono, T., Lee, S.K., and Seo, E.K. Prenylated flavonoids from the heartwood of *Artocarpus communis* with inhibitory activity on

- lipopolysaccharide-induced nitric oxide production. Journal of Natural Products. 69 (2006), 719–721.
- Harborne, J.B. The flavonoids: advances in research since 1986. London SE1 8HN, UK: Chapman & Hall, 1986.
- Hufford, C.D., and Oguntimein, B.O. New dihydrochalcones and flavanones from *Uvaria Angolensis*. Journal of Natural Products. 45 (1982): 337-342.
- Jaiswal, D., Rai, P.K., Kumar, A., Mehta, S., and Watal, G. Effect of *Moringa oleifera* Lam. leaves aqueous extract therapy on hyperglycemic rats. Journal of Ethnopharmacology. 123 (2009): 392-396.
- Kandra, L., Zajacz, A., Remenyik, J., and Gyemant, G. Kinetic investigation of a new inhibitor for human salivary α -amylase. Biochemical and Biophysical Research Communications. 334 (2005): 824-828.
- Kenjiro, T., Yuji, M., Kouta, T., and Tomoko, M. Inhibition of α -Glucosidase and α -Amylase by Flavonoids. Journal of Nutrition Sciences Vitaminol. 52 (2006): 149-153.
- Kiat, T.S., Phippen, R., Yusof, R., Ibrahim, H., Khalid, N., and Rahman, N.A. Inhibitory activity of cyclohexenyl chalcone derivatives and flavonoids of Fingerroot, *Boesenbergia rotunda* (L.), towards dengue-2 virus ns3 protease. Bioorganic and Medicinal Chemistry Letters, 16 (2006): 3337–3340.
- Kuo, Y.C., Yang, L.M., and Lin, L.C. Isolation and immunomodulatory effect of flavonoids from *Syzygium samarangense*. Planta Medica. (2004): 1237-1239.
- Lalas, S., and Tsaknis, J. Extraction and identification of natural antioxidants from the seeds of *Moringa oleifera* tree variety of Malawi. Journal of the American Oil Chemists' Society. 79 (2002): 677-683.
- Lee, S.S., Lin, H.C., and Chen, C.K. Acylated flavonol monorhamnosides, α -glucosidase inhibitors from *Machilus philippinensis*. Phytochemistry. 69 (2008): 2347-2353.
- Lespagnol, A., Lespagnol, C., Lesieur, D., Cazin, J.C., Cazin, M., and Beerens, H. Analgesic, anti-inflammatory and antimicrobial activities of chalcones and dihydrochalcones derived from salicylic acid. Chimica Therapeutica. 7 (1972): 365–369.

- Li, W.L., Zheng, H.C., Bukuru, J., and De Kimpe, N. Natural medicines used in the Traditional Chinese medicinal system of therapy of diabetes mellitus. Journal of Ethnopharmacology. 92 (2004): 1-21.
- Lin, H-Y., Kuo, Y-H., Lin, Y-L., and Chiang, W. Journal of Agricultural and Food Chemistry. 57 (2009): 6623-6629.
- Lineweaver, H., and Burk, D. The determination of enzyme dissociation constants. Journal of the American Chemical Society. 580 (1934): 658-666.
- Liu, X., Zhou, H.J., and Rohdewald, P. French maritime pine bark extract Pycnogenol dose-dependently lowers glucose in type 2 diabetic patients. Journal of Diabetic Care. 27 (2004): 839.
- Loutfi, M., Mulvihill, N.T., Boccalatte, M., Farah, B., Fajadet, J., and Marco, J. Impact of restenosis and disease progression on clinical outcome after multivesselstenting in diabetic patients. Catheterization and Cardiovascular Interventions. 58 (2003): 451-454.
- Makonnen, E., Hunde, A., and Damecha, G. Hypoglycaemic effect of *Moringa stenopetala* aqueous extract in rabbits. Phytotherapy Research. 11 (1997): 147-148.
- Mehta, L.K., Balaraman, R., Amin, A.H., Bafna, P.A., and Gulati, O.D. Effect of fruit of *Moringa oleifera* on the lipid profile of normal and hypercholesterolemia rabbits. Journal of Ethnopharmacology. 86 (2003): 191-195.
- Mishra, G., and *et al.* Traditional uses, phytochemistry and pharmacological properties of *Moringa oleifera* plant: An overview. Der Phamacia Lettre. 3(2000): 141-164.
- Morton, J.F. The horseradish tree, *Moringa pterigosperma*(Moringaceae). A boon to arid lands. Economic Botany. 45 (1991): 318–333.
- Mustafa, K.A., Kjaergaard, H.G., Perry, N.B., and Weavers, R.T. Hydrogen-bonded rotamers of 2', 4', 6'-trihydroxy-3'-formyldihydrochalcone, an intermediate in

- the synthesis of a dihydrochalcone from *Leptospermum recurvum*. Tetrahedron. 59 (2003): 6113-6120.
- Mustafa, K.A., Kjaergaard, H.G., Perry, N.B., and Weavers, R.T. Lipophilic C-methylflavonoids with no B-ring oxygenation in *Metrosideros* species (Myrtaceae). Biochemical Systematics and Ecology. 33 (2005): 1049-1059.
- Nadkarni, A.K. Popular Prakashan: Bombay. Indian Materia Medica. 1 (1976): 810–816.
- Nonaka, G., Aiko, Y., Aritake, K., and Nishioka, I. Tannins and related compounds. CXIX. Samarangenins a and b, novel proanthocyanidins with doubly bonded structures, from *Syzygium samarangense* and *S. aqueum*. Chemical and Pharmaceutical Bulletin. 40 (1992), 2671–2673.
- Palada, M.C., and Changl, L.C. Suggested cultural practices for *Moringa*. International Cooperators' Guide AVRDC [Online]. 2003. Available from : <http://www.avrdc.org> [2011, Oct 2]
- Qaiser, M. Moringaceae. In Flora of West Pakistan. vol. 38, University of Karachi Press: Karachi. (1973): 1–4.
- Rhabasa-Lhoret, R., and Chiasson, J. Alpha-glucosidase inhibitors. 3rd ed., International Textbook of diabetes mellitus, vol 1. UK: John Wiley, 2004.
- Ramachandran, D., Peter, K.V., and Gopalakrishnan. P.K. Drumstick (*Moringa oleifera*): A multipurpose Indian vegetable. Economic Botany. 34 (1980): 276-283.
- Ruckmani, K., Kavimani, S., Anandan, R., and Jaykar B. Effect of *Moringa oleifera* Lam on paracetamol-induced hepatotoxicity. Indian Journal of Pharmacology Sciences. 60 (1998): 33–35.
- Resurreccion-Magno, M.H.C., Villaseñor, I.M., Harada, N., and Monde, K. Antihyperglycaemic flavonoids from *Syzygium samarangense* (Blume) Merr. and Perry. Phytotherapy Research. 19 (2005): 246-251.
- Sabale, V., Patel, V., Paranjape, A., Arya, C., Sakarkar, S.N., and Sabale, P.M. *Moringa oleifera* (Drumstick): An Overview. Pharmacological Reviews. 2 (2008): 7-13.
- Samreen, R. Diabetes mellitus. Scientific Research and Essay. 4 (2009): 367-373.

- Shimizu, R., Shimabayashi, H., and Moriwaki, M. Enzymatic production of highly soluble myricitrin glycosides using β -galactosidase. Bioscience, Biotechnology and Biochemistry. 70 (2006): 940-948.
- Shrestha, I., and Joshi, N. Medicinal plants of the Lete village of Lalitpur district. Nepal International Journal of Pharmaceutical. 31 (1993): 130-134.
- Siddhuraju, P., and Becker, K. Antioxidant properties of various solvent extracts of total phenolic constituents from three different agro-climatic origins of drumstick tree (*Moringa oleifera* Lam.). Journal of Agricultural and Food Chemistry. 15 (2003): 2144–2155.
- Simirgiotis, M.J., Adachi, S., and Reynertson, K.A. Cytotoxic chalcones and antioxidants from the fruits of *Syzygium samarangense* (Wax Jambu). Food Chemistry. 107 (2008): 813-819.
- Solladié, G., Gehrold, N., and Maignan, J. Synthesis of (+)-(R)-5-hydroxy-6-hydroxymethyl-7-methoxy-8-methylflavanone. Tetrahedron: Asymmetry. 10 (1999): 2739-2747.
- Srivastava, R., Shaw, A.K., and Kulshreshtha, D.K. Triterpenoids and chalcone from *Syzygium samarangense*. Phytochemistry. 38 (1995), 687–689.
- Sukari, M.A., Ching, A.Y.L., Lian, G.E.C., Rahmani, M., and Khalid, K. Cytotoxic constituents from *Boesenbergia pandurata* (Roxb.) Schltr. Natural Product Sciences. 13 (2007): 110-113.
- Svetaz, L., Tapia, A., Lopez, S.N., Furlan, R.L.E., Petenatti, E., and Pioli, R. Antifungal chalcones and new caffeic acid esters from *Zuccagnia punctata* acting against soybean infecting fungi. Journal of Agricultural and Food Chemistry. 52 (2004), 3297–3300.
- Tende, J.A., Ezekiel, I., Dikko, A.A.U., and Goji, A.D.T. Effect of ethanolic leaves extract of *Moringa oleifera* on blood glucose levels of streptozocin-induced diabetics and normoglycemic wistar rats. British Journal of Pharmacology and Toxicology. 2 (2011): 1-4.
- Wong, K.C., and Lai, F.Y. Volatile constituents from the fruits of four *Syzygium* species grown in Malaysia. Flavour and Fragrance Journal, 11 (1996): 61–66.
- Wutythamawech, W. Encyclopedia of Thai Herbs. Bangkok: OS Printing, 1997

VITA

Miss. Patrawadee Toprangkobsin was born on October 21, 1986 in Lopburi Province, Thailand. She graduated with Bachelor's Degree of Engineering, major in Petrochemicals and polymeric materials from Faculty of Science, SilpakornUniversity, in 2009. She then continued her graduate degree at the Department of Chemistry, Chulalongkorn University. During the time she was studying in the Master of Science program at the Department of Chemistry.